

LINEAR LIBRARY  
C01 0068 2081



OBSERVATIONS OF GALAXIES IN A COSMOLOGICAL CONTEXT

by

A.W. Sievers

A thesis submitted in fulfilment of the  
requirements of the Degree of Master of Science

University of Cape Town

June 1982

UNIVERSITY OF CAPE TOWN  
LIBRARY  
SERIALS ACQUISITION  
ROSEBUD DRIVE  
CAPE TOWN 7700

The copyright of this thesis vests in the author. No quotation from it or information derived from it is to be published without full acknowledgement of the source. The thesis is to be used for private study or non-commercial research purposes only.

Published by the University of Cape Town (UCT) in terms of the non-exclusive license granted to UCT by the author.

## Acknowledgements

The author would like to thank his supervisor Prof. George Ellis for much patient help in producing this thesis. Many discussions with Judith Perry and Tony Fairall help<sup>ed</sup> a lot to clarify the subject.

The financial support of the Council for Scientific and Industrial Research and the University of Cape Town is gratefully acknowledged. The computing facilities at U.C.T. have been essential for the numerical work shown in this thesis.

## Declaration

No portion of this thesis has been previously submitted in support of an application for any other degree or qualification in this or any other University.

## Abstract

The basic theory of observations of galaxies in a cosmological context is reviewed and extended to include e.g. the point-spread effect of the atmosphere. From this the relation between the sources (objects) and the images of these sources is derived (the observational map). A program is developed to calculate this map and some results are given.

## Table of contents

1. Introduction	1-1
2. Theory: The Observational Map	2-1
2.1. Summary	2-1
2.2. The Radiation Field	2-6
2.2.1. Basic Concepts	2-6
2.2.2. Spherical Symmetric Radiation Field	2-8
2.2.3. The measured intensity of radiation	2-12
2.2.4. The Flux and Luminosity for "nearby" Galaxies	2-19
2.3. The Magnitude Scales	2-21
2.3.1. Definitions	2-21
2.3.2. Bolometric Absolute Magnitudes	2-22
2.3.3. Absolute Colour Magnitude	2-24
2.3.4. Apparent Colour Magnitude	2-25
2.4. The Observational Map	2-30
2.4.1. The Defining Equations	2-30
2.4.2. Forward Map	2-31
2.4.3. Inverse Map	2-32
2.5. A Specialised Form of the Map	2-34
2.5.1. Brightness Profiles for Elliptical Galaxies	2-34
2.5.2. Intergalactic Absorbtion	2-38
2.5.3. The Magnitude Correction	2-39
2.5.4. The Observer Area Distance	2-41
3. Numerical Methods	3-1
3.1. The Problem	3-1
3.2. The Integration Procedure	3-2
3.3. The Integration Routines	3-5
3.4. Root Solving Routines	3-8
3.5. Fitting a Polynominal	3-9
4. Application of the Program	4-1
5. Conclusion	5-1
6. Appendix	6-1
7. References	7-1

## 1. Introduction

There are many different models of the universe in the large, proposed by cosmologists. In principle it is possible to use distant astronomical objects as beacons in space-time and so decide between different cosmological models [see e.g. Ellis 1980 or Sandage 1961]. The goal of observational cosmology is to use astronomical observations in order to select among this multitude. The difficulties in measuring faint astronomical objects and interpreting these observations are severe. We can only hope to be successful if we can make a clear statement of the observational method used and the resulting observational limits. Following the paper "Towards a 'correctionless' observational cosmology" [G.F.R.Ellis and J.J.Perry (1979)], a clear analysis of astronomical observations is possible without the introduction of "corrections". This thesis can be considered as a step towards this aim. It develops and presents both the details and some extensions to an observational method outlined by G.F.R.Ellis in "Limits to verification in cosmology" [Ellis 1980].

Consider a class of similar objects that can be specified by two parameters, take e.g. the class of elliptical galaxies of EO type. This class of objects define an OBJECT PLANE, whose axes are the object's intrinsic magnitude and its scaling radius (which is proportional to the diameter) [see Arp 1965]. Then, at any distance or redshift  $z$ , the observational method used results in an OBSERVATIONAL MAP from the object-plane to an IMAGE PLANE, whose axes are the apparent magnitude and apparent angle of the resulting images (in a Friedmann universe the distance can be characterized by  $z$ , the cosmological redshift of an astronomical object) [see Fig.1 and 2]. The corrections necessary to obtain the

absolute properties of astronomical sources, e.g. to invert the map, are contained in the theory, and the assumptions made can be stated explicitly.

By having a clear division between the object- and image-plane, it is evident that OBSERVATIONAL LIMITS are to be placed in the image-plane [see section 4]. It turns out that a limit on apparent magnitude  $m_{op}$  may be of only secondary importance. The limits shown in Fig.13 were drawn for the Anglo Australian Sky Survey and it can be shown that a limit of  $m_{op} = 23$  is not the critical feature, but rather that the most important limit is the angular limit (limit of resolution; distinguishing galaxies from stars) and the limit on the apparent surface brightness. The resolution and detection limits expected for space telescope observations are also shown. It can be seen clearly how the expected increase in resolution by a factor of 10 increases the number of objects that can be observed in different sections of the object-plane [see Fig.12].

Light-rays from stars and galaxies are smeared out by the atmosphere ('seeing') and by the detecting instrument (e.g. diffraction). This POINT-SPREAD EFFECT may be represented by a point-spread function. For ground-based telescopes, seeing dominates and a good approximation to the point-spread function is a Gaussian distribution. The same point-spread function also represents, to an first approximation, the central diffraction image of a point-source (e.g. a star) and may be a reasonable approximation to the point-spread function of the space telescope [see J.Stock and A.D.Williams 1962]. Near the limit of resolution the point-spread effect dominates [see Fig.4] and may not be ignored in any realistic calculation. Particularly striking is the large drop in central surface brightness of galaxies due to

this effect [see Fig.15], which implies that many objects "detectable" without point-spread, fall below detection and are lost for observation.

In section 2 the basic theory of the observational map and its inverse is given and then applied to a particular simplified case used for numerical calculations (the relevant computer program is given in the appendix). In section 3 the numerical methods and their application in the program are detailed, and some results obtained by use of the program are shown in section 4. Finally, some suggestions for generalization of the observational map and how to apply it to a wider class of objects, are given in section 5. One of the most important applications of the observational map will be an investigation of the statistics of number-counts. The appropriate analysis and numerical methods are presently under development.

## 2. Theory: The Observational Map

### 2.1. Summary

The "Observational" map from the object- to the image-plane and its inverse is derived: Firstly only fairly general assumptions are made, and secondly, a more specific, simplified form is derived to be used in calculations.

The assumptions that have been made in the derivation are:

1) The source (e.g. galaxy) is spherically symmetric (or circular, lying perpendicular to the line of sight) with a surface brightness  $B_\nu$  (at the object) at the metric radius  $r$  given by

$$B_\nu(r, z) = B(r, z) \mathcal{J}(\nu, r, z) ; \int_0^\infty \mathcal{J}(\nu, r, z) d\nu = 1 ,$$

where  $\mathcal{J}(\nu, r, z)$  is the spectral function defined by the above relations. Here the dependence on  $z$ , the redshift of the source, indicates a possible source evolution.

[The notation used here follows Ellis and Perry 1979.]

2) The observations are made in directions in which the images remain undistorted. This condition is satisfied in any Friedmann Universe in all directions. A metric radius  $r$  then subtends an angle  $\alpha$  at the observer given by the relation

$$\alpha = r / r_o(z) ,$$

where  $r_o$ , the OBSERVER AREA DISTANCE, is only a function of  $z$ . The measured specific intensity,  $I_\nu$ , is given by:

$$I_{\nu}(\alpha, z) = \frac{B(r, z)}{(1+z)^3} g[\nu(1+z), r, z],$$

assuming no emission or absorption, extinction or scattering into or out of the beam along the line of sight [see Ellis 1971, 1980; Ellis and Perry 1979].

3) The SPECTRUM of the emitted radiation does not change across the source, i.e.

$$g[\nu, r, z] = g[\nu, z]$$

and the radial variation of brightness is the product of an amplitude  $B_0(z)$  and a normalized radial function  $f(\beta)$  whose functional form does not evolve. Thus

$$B(r, z) = B_0(z) f(\beta), \quad f(0) = 1,$$

here  $\beta = r/a(z)$  and  $a(z)$  is the scaling radius. Again dependence on  $z$  indicates source evolution; the spectrum, central brightness and the radius of a galaxy may evolve (the radius of a galaxy is proportional to  $a(z)$ ).

4) We represent the combined effects of the optical imaging system (e.g. diffraction, seeing and instrumental scattering) by a POINT-SPREAD FUNCTION (p.s.f.) in the focal plane. This p.s.f. is here taken to be a Gaussian with dispersion  $\tilde{\sigma}$ , i.e. to have the form:

$$S(\rho, \nu) = \frac{1}{2\pi \tilde{\sigma}^2} e^{-\rho^2/2\tilde{\sigma}^2}.$$

It is circularly symmetric and thus implies circularly symmetric images. In general,  $\tilde{\sigma} = \tilde{\sigma}(\nu)$  but for simplicity we shall initially take  $\tilde{\sigma}$  to be constant with frequency  $\nu$ .

In the first section the fundamental concepts of the theory of the radiation field is outlined. Then it is shown that the point-spread effect can be represented by a radial function  $\tilde{f}$  (the "new" brightness profile) given by a convolution of the profile  $f$ :

$$\tilde{f}(\beta) = \tilde{f}(R, A) = \frac{1}{\pi} \int_0^{\infty} dy \int_0^{\pi} d\theta y e^{-\left(\frac{y^2}{2} + \frac{R^2}{2} - yR \cos\theta\right)} f(Ay)$$

such that the specific intensity is given by

$$\tilde{I}(\alpha, \nu, z) = \frac{B_0(z)}{(1+z)^3} g[\nu(1+z), z] \tilde{f}(\beta).$$

Here  $R = r/w$  and  $A = W/a(z)$  where we have defined  $W = r_0(z) \sigma$ .  $\sigma = \frac{r_0}{d}$  is the dispersion in radians ( $d$  represents the focal length of the camera) and thus  $W$  is the radius of the disc (at the observed galaxy) corresponding to the angle  $\sigma$ .

Using the assumptions 1-3 the equations for the emitted radiation flux and luminosity for galaxies are derived. The LUMINOSITY is given by

$$L_\nu(z) = 4\pi B_0(z) g(\nu, z) a^2(z) g(\beta_m)$$

and the RADIATION FLUX at distance  $R > a(z) \cdot \beta_m$

$$F_\nu(z) = \frac{L_\nu(z)}{4\pi R^2} = \frac{B_0(z) g(\nu, z) a^2(z) g(\beta_m)}{R^2},$$

where  $g(\beta_m) = 2\pi \int_0^{\beta_m} \beta f(\beta) d\beta$ .

Using these equations, the fundamental definitions for the absolute and apparent magnitude and assumption 4, the APPARENT MAGNITUDE  $m_\nu(A_{op})$  is derived.  $2A_{op}$  is the apparent diameter of

the observed galaxy given by a DETECTION LIMIT  $S_L(\nu) = I_\nu(A_{op}, z)$

on the measured intensity. The equations are

$$S_L(\nu) = \frac{B_0(z)}{(1+z)^3} \int [\nu(1+z), z] e^{-p(\nu, z)} \tilde{f}(\beta_{op}), \quad \text{--- A}$$

$$A_{op} = \frac{r_{op}(1+z)^{p_1}}{r_0(z) \cdot 10^3} = \frac{r_{op}}{a} \frac{a}{r_0(z) \cdot 10^3} (1+z)^{p_1} = \beta_{op} \frac{a}{r_0(z) \cdot 10^3} (1+z)^{p_1}, \quad \text{--- B}$$

$$m_\nu(A_{op}) = M_{bol} + \Delta M - 2.5 \log_{10}(1+z) - 2.5 \log_{10} \frac{\tilde{g}(\beta_{op})}{g_\infty} \quad \text{--- C}$$

$$+ 5 \log_{10} \frac{r_0(z)(1+z)^2}{D_M} - (2.5 p_2 + 5 p_1) \log_{10}(1+z) + 25.$$

Where  $p(\nu, z)$  is the optical depth up to  $z$ ,

$$a(z) = a(1+z)^{p_1} \quad \text{gives the radial evolution,}$$

$$B_0(z) = B_0(1+z)^{p_2} \quad \text{gives the brightness evolution,}$$

$$\Delta M - 2.5 \log_{10}(1+z) \quad \text{is the bolometric and K-correction and}$$

$$-2.5 \log_{10} \frac{\tilde{g}(\beta_{op})}{g_\infty} \quad \text{is the aperture correction.}$$

As above:  $\tilde{g}(\beta_{op}) = 2\pi \int_0^{\beta_{op}} \beta \tilde{F}(\beta) d\beta$

and  $g_\infty = \mathcal{L}_{\beta \rightarrow \infty} g(\beta) = \mathcal{L}_{\beta \rightarrow \infty} \tilde{g}(\beta).$

Finally  $M_{bol}$  is the bolometric absolute magnitude and  $D_M = 10^6$  pc a scaling distance.

NOTE:  $r_0$  is given in Mpc,  $a$  and  $r$  in kpc.

$$1 \text{ pc or 1 parsec} = 3.262 \text{ light years} = 3.086 \cdot 10^{13} \text{ km}$$

The equations A, B and C determine the map from the object plane ( $a, M_{bol}$ ) to the image plane ( $A_{op}, m_{op}$ ) and its inverse. Further

assumptions are made in section 2.5; simple brightness profiles are chosen, a FRW cosmology is assumed and simple expressions for intergalactic absorption and the magnitude correction are derived, giving a more specialised form of the map, which is used for numerical calculations shown in subsequent sections.

## 2.2. The Radiation Field

The basic definitions and concepts of radiation theory are reviewed and then applied to a spherically symmetric radiation field. The specific intensity of radiation (received), valid for all redshifts, is stated and the effects of intergalactic absorption, point-spread and spectral sensitivity of the detector are shown and the resultant intensity derived. Finally, by making several simplifying assumptions about the spectral and radial form of the radiation emitted by galaxies, specific expressions for the radiation flux and the luminosity are given. The basic concepts can be found in references 1 to 6 or in any textbook on Astrophysics.

### 2.2.1. Basic Concepts

A. Specific Intensity: It is convenient to describe a radiation field by the specific intensity. In order to define this quantity consider a point P in a radiation field, an infinitesimal surface  $d\sigma$  with normal  $\underline{d\sigma}$  ( $d\sigma = |\underline{d\sigma}|$ ) at point P and a unit vector  $\underline{n}$  in direction  $(\theta, \phi)$  [see fig. 2-1]. Then let

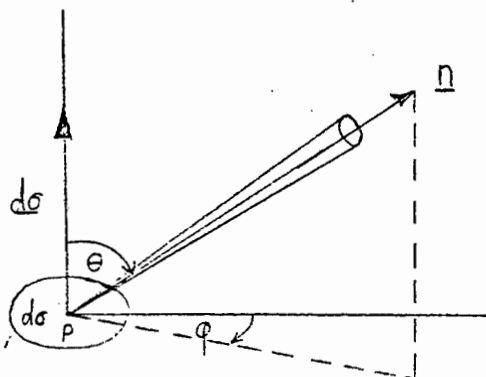
$dE_\nu(\theta, \phi)$  = amount of radiation (energy) in the frequency interval  $[\nu, \nu + d\nu]$ , in the time interval  $[t, t + dt]$  passing through  $d\sigma$  in element of solid angle  $d\omega$  about  $\underline{n}$  [erg].

Define the specific intensity by

$$I_\nu(\theta, \phi) = \frac{dE_\nu(\theta, \phi)}{d\nu d\omega (d\sigma \cdot \underline{n}) dt} \quad [\text{erg} \cdot \text{Hz}^{-1} \cdot \text{ster}^{-1} \cdot \text{cm}^{-2} \cdot \text{sec}^{-1}]$$

if this <sup>angular</sup> limit exists.

Figure 2-1.



i.e. The specific intensity = energy travelling per unit time, per unit frequency, per unit surface ~~perpendicular to~~<sup>in</sup> the direction  $\underline{n}$ , in a unit solid angle.

The total intensity or integrated intensity is given by

$$I(\theta, \varphi) = \int_0^{\infty} I_\nu(\theta, \varphi) d\nu .$$

**B. Radiation Flux and Luminosity:** The radiation flux is defined to be the radiant energy crossing the surface  $d\sigma$  in all directions per unit frequency, per unit time and per unit area. Thus

$$F_\nu \equiv \int_0^{4\pi} d\omega I_\nu(\theta, \varphi) \cos \theta = \int_0^{2\pi} d\varphi \int_0^\pi d\theta I_\nu(\theta, \varphi) \cos \theta \sin \theta , \quad (1 a)$$

where the element of solid angle  $d\omega = \sin \theta d\varphi d\theta$  .

Often the flux  $F_\nu^+$  in the "upper half space" defined as:

$$F_\nu^+ \equiv \int_0^{2\pi} d\varphi \int_0^{\pi/2} d\theta I_\nu(\theta, \varphi) \cos \theta \sin \theta \quad (1 b)$$

$$[F_\nu^+] : \text{erg} - \text{Hz}^{-1} - \text{cm}^{-2} - \text{sec}^{-1}$$

is used. The mean intensity  $\bar{I}_\nu^+$  (i.e. the mean over all directions

for the "outgoing" radiation) is defined by:

$$\bar{I}_\nu^+ \equiv \frac{\int_0^{2\pi} d\varphi \int_0^{\pi/2} d\theta I_\nu(\theta, \varphi) \cos\theta \sin\theta}{\int_0^{2\pi} d\varphi \int_0^{\pi/2} d\theta \cos\theta \sin\theta} = \frac{F_\nu^+}{\pi}$$

so that

$$F_\nu^+ = \pi \bar{I}_\nu^+ . \quad (1 c)$$

The luminosity  $L_\nu$  of a radiating body is the total energy emitted into exterior space by that body per unit frequency and per unit time. It is:

$$L_\nu = \int_\Sigma d\sigma F_\nu^+ \quad [\text{erg} - \text{Hz}^{-1} - \text{sec}^{-1}] , \quad (2)$$

where  $\Sigma$  is a closed surface enclosing the radiating body. The quantities above are monochromatic quantities. Define the integrated flux and integrated or total luminosity by:

$$F = \int_0^\infty F_\nu d\nu \quad \text{and} \quad L = \int_0^\infty L_\nu d\nu \quad \text{respectively.}$$

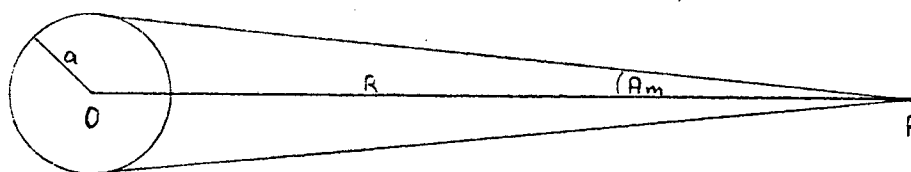
Note: In some textbooks the flux  $F$  is defined as  $F = \frac{L}{4\pi R^2}$

### 2.2.2. Spherically Symmetric Radiation Field

Consider a spherical radiating body with radius  $a$ , center  $O$  at distance  $R$  from an observer at  $P$ . Choose polar coordinates whose origin is at the center of symmetry  $O$ , then

$$I_\nu(\theta, \varphi) = I_\nu(\theta).$$

Figure 2-2.



For any  $R > a$ , the flux  $F_{\nu}^{+}$  is constant over the surface of the sphere with radius  $R$ , thus from eq 2:

$$L_{\nu} = \int d\sigma F_{\nu}^{+} = 4\pi R^2 F_{\nu}^{+}, \text{ and we can write}$$

$$F_{\nu}^{+} = \frac{L_{\nu}}{4\pi R^2}$$

and

$$\bar{I}_{\nu}^{+} = \frac{L_{\nu}}{4\pi^2 R^2}. \quad (3)$$

Consider the case where  $R \gg a$  but  $R$  (and  $a$ ) small enough such that  $z \approx 0$

From eq. 1 b :

$$F_{\nu}^{+} = \int_0^{2\pi} d\varphi \int_0^{A_m} d\theta I_{\nu}(\theta) \cos\theta \sin\theta,$$

where  $A_m$  is the angle subtended by  $a$  at the observer at  $P$ .

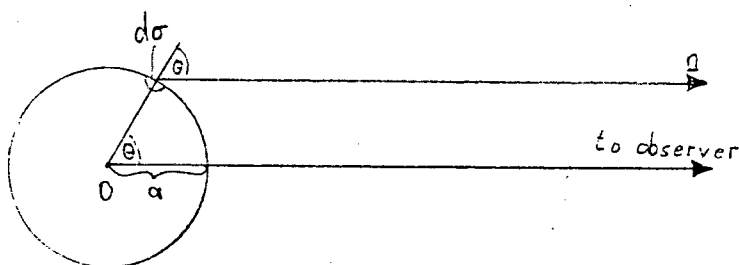
Now for  $A_m \ll 1$ :  $\cos\theta \doteq 1$  and  $\sin\theta \doteq \theta$ , thus

$$F_{\nu}^{+} \doteq 2\pi \int_0^{A_m} I_{\nu}(\theta) \theta d\theta. \quad (4)$$

The radiation in direction of the observer at  $P$  (direction  $\underline{n}$  say) may be assumed to be plane parallel. A surface element on the sphere is given by [see Fig. 2-3]

$$d\sigma = a^2 \sin\theta d\theta d\varphi.$$

Figure 2-3.



Hence the mean intensity  $\bar{I}_{\nu, n}$  over the disc with radius  $a$  in direction  $\underline{n}$  is given by

$$\bar{I}_{\nu, n} = \frac{\int_0^{2\pi} d\varphi \int_0^{\pi/2} d\theta I_{\nu}(\theta) \cos \theta \sin \theta a^2}{\pi a^2}$$

$$= \frac{F_{\nu}^+}{\pi}$$

by eq. 1b and the assumption of spherical symmetry.

Thus  $\bar{I}_{\nu}^+ = \bar{I}_{\nu, n} = F_{\nu}^+ / \pi$ , and the mean at one point over all directions is equal to the mean at all points in one direction.

So for a spherically symmetric radiator subtending an angle  $2Am$  with  $Am \ll 1$  we may project the angular variation in intensity into a radial variation across an effective object-plane and write:

$$I_{\nu}(\theta, \varphi) \doteq B_{\nu}(r, z) = B(r, z) \mathcal{G}(\nu, r, z) : \int_0^{\infty} \mathcal{G}(\nu, r, z) d\nu = 1 \quad (5a)$$

This is the emitted specific intensity or surface brightness. The dependence on  $z$  reflects the possibility of brightness and

spectral evolution;  $r$  is the distance measured at the source (e.g. galaxy) from its center.  $r$  is called the metric or projected radius for galaxies. Equation 5a also defines the spectral function  $g$ . Note that  $B_p(r, z)$  is not limited by this definition.

At the observer ( $z=0$ ) the specific intensity of radiation, due to a source at redshift  $z$  with surface brightness given by eq.5a, is given by:

$$I_{\nu}(\alpha, z) = \frac{B(r, z)}{(1+z)^3} g[\nu(1+z), r, z], \quad (5b)$$

where  $\alpha$  is the angle measured at the observer corresponding to a metric radius  $r$ . Here we exclude any emission or absorption, extinction or scattering into or out of the beam along the line of sight. (see Ellis and Perry 1979)

In an "ideal" cosmological model (null geodesics are distortion free) the metric radius  $r$  can be given by:

$$r = \alpha r_0(z). \quad (6)$$

Here  $r_0(z)$  is the observer area distance (see e.g. Ellis 1971).

In an Friedmann Universe the observer area distance is given by

$$r_0(z) = \frac{c}{H_0 q_0^2 (1+z)^2} \left\{ q_0 z + (q_0 - 1) \left( \sqrt{2q_0 z + 1} - 1 \right) \right\} [Mpc], \quad (7)$$

where  $c$  = speed of light in km/sec

$H_0$  = Hubble constant in km/sec/Mpc

and  $q_0$  = the deceleration parameter

Two assumptions are usually made to describe galaxies: [see Ellis and Perry 1979]

1) The frequency dependence of the emitted radiation does not vary across the face of the galaxy. Thus  $g(\nu, r, z) \doteq g(\nu, z)$ .

2) The radial variation of brightness is characterised by an amplitude which may evolve with  $z$ ,  $B_0(z)$ , and a normalized radial function whose functional form does not evolve,  $f(\beta)$ .  $\beta = r/a$  and  $a$  is a scaling radius which may evolve i.e.  $a=a(z)$ . Thus

$$B_\nu(r, z) = B_0(z) g(\nu, z) f(r/a(z)) \quad (8a)$$

and

$$I_\nu(\alpha, z) = \frac{B_0(z)}{(1+z)^3} g[\nu(1+z), z] f(r/a(z)) \quad (8b)$$

### 2.2.3. The measured intensity of radiation

We consider the effect of intergalactic absorption, point-spread and detector spectral sensitivity in turn

#### A Intergalactic Absorption

Allowing for absorption by intervening matter we can rewrite eq.5b as:

$$I_\nu(\alpha, z) = \frac{B(r, z)}{(1+z)^3} g[\nu(1+z), r, z] e^{-p(\nu, z)}, \quad (9)$$

where  $p(\nu, z)$  is the optical depth up to redshift  $z$  given by:

$$p(\nu, z) = \int_0^z n_a(z') \sigma_a(z', \nu(1+z')) \frac{dl}{dz'} dz'$$

$n_a$  is the number density of absorbers with interaction cross-section  $\sigma_a$  along the light ray and  $dl$  is a proper length interval. Usually  $n_a$  is given in  $\text{cm}^{-3}$  and  $\sigma_a$  in  $\text{cm}^2$ .

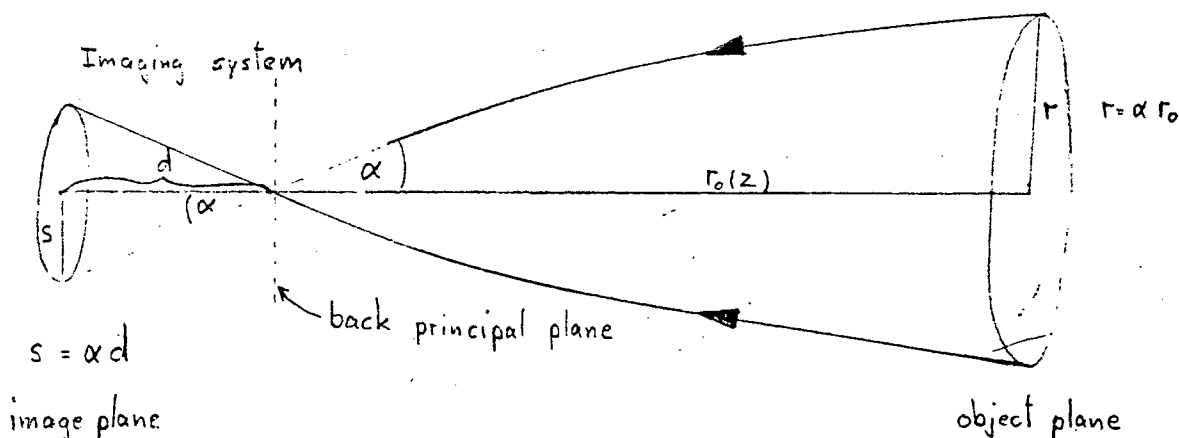
[see section 6'6.4 of Ellis 1971]

## B Point-spread Effect

The image of a galaxy can be thought of as made up by a very large number of light rays. Each ray is slightly blurred by seeing, diffraction, scattering etc. i.e. the image of a galaxy has to be convolved with a point-spread function. At any point in the image all "point-spread" light rays contribute to the measured specific intensity, which is then represented as a sum (integral) of all these contributions.

The source-detector relation for the ideal imaging system can be represented as follows:

Figure 2-4.

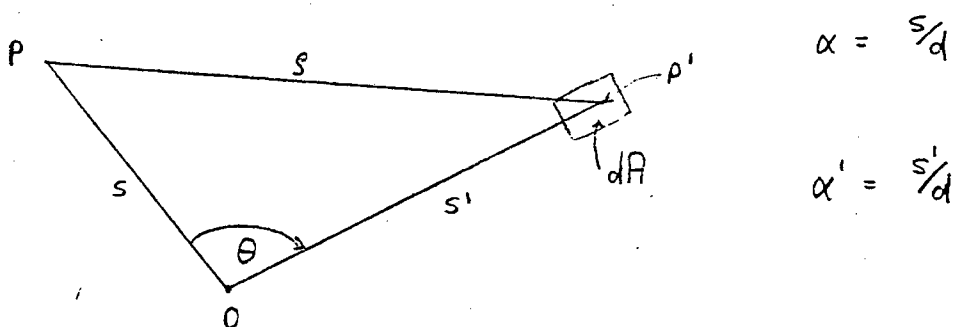


$d$  is the distance from the back principal plane of the detector to the image plane. If the angle subtended by the object is  $\alpha$ , then the angle subtended by the image from the back principal plane is also  $\alpha$  and  $s = \alpha d$ .

Consider the image-plane: The center of the image is at  $O$  [see Fig.2-5]. We want to determine the intensity at the point  $P$ . Assume a spherically symmetric point-spread function  $\mathcal{S}(s, \nu)$ , where  $s$  is the distance between point  $P$  and point  $P'$  of integration. Then the intensity  $dI$  at  $P$  due to the radiation incident on point  $P$  will be:

$$dI = I_\nu(\alpha', z) \mathcal{S}(s, \nu) dA .$$

Figure 2-5.



Here  $\alpha' = s'/d$  and  $dA$  is an infinitesimal area-element at  $P'$ . Then the intensity  $\tilde{I}$  will be:

$$\tilde{I}_\nu(\alpha, z) = \iint_{\text{plate}} I_\nu(\alpha', z) \mathcal{S}(s, \nu) dA, \quad \text{where } \alpha = s/d$$

i.e.  $\tilde{I}_\nu$  is a convolution of  $I_\nu$  with a point-spread function  $\mathcal{S}$ .

When the atmosphere dominates, the most important part of the pointspread function has a Gaussian form [King 1971; Kormendy 1973; Schweizer 1979]. Then

$$\mathcal{S}(s, \nu) = \frac{1}{\pi \tilde{\sigma}^2} e^{-s^2/2\tilde{\sigma}^2}, \quad \tilde{\sigma} = \tilde{\sigma}(\nu). \quad (10)$$

Where  $\tilde{\sigma}$  is called the dispersion, it is the value for  $s$  where  $\mathcal{S}$  has dropped to  $e^{-1/2}$  of its maximum value.

The Gaussian point-spread function also represents, to a first approximation, the central diffraction image of a focal stellar image. [see Stock and Williams 1962 pg 393]

The factor  $1/2\pi\sigma^2$  normalises  $\mathcal{P}$  since

$$\frac{1}{2\pi\sigma^2} \int_{-\infty}^{\infty} dx \int_{-\infty}^{\infty} dy e^{-(x^2+y^2)/2\sigma^2} = \frac{1}{2\pi\sigma^2} \int_0^{\infty} dr 2 \int_0^{\pi} d\theta e^{-r^2/2\sigma^2} = 1.$$

The specific intensity at  $\alpha$  is given by

$$\tilde{I}_\nu(\alpha, z) = 2 \int_0^{\infty} ds' \int_0^{\pi} d\theta I_\nu(\alpha', z) \frac{s'}{2\pi\sigma^2} e^{-(s^2 + s'^2 - 2ss'\cos\theta)/2\sigma^2}$$

[Choosing polar coordinates  $(s, \theta)$  with origin  $O$  and reference line  $OP$ ,  $dA = s' ds' d\theta$  and  $s^2 = s^2 + (s')^2 - 2s s' \cos \theta$ ]

Changing variables to  $y = s/\sigma$ , and further put  $R = s'/\sigma$ , we have

$$\tilde{I}_\nu(\alpha, z) = \frac{1}{\pi} \int_0^{\infty} dy \int_0^{\pi} d\theta I_\nu(y \frac{\sigma}{\alpha}, z) y e^{-(y^2 + R^2 - Ry \cos \theta)}$$

By eq. 8b and putting  $A = \frac{\sigma}{\alpha} \frac{r_0(z)}{\alpha(z)}$  we obtain

$$\tilde{I}_\nu(\alpha, z) = \frac{B_0(z)}{(1+z)^2} \mathcal{G}[\nu(1+z), z] \frac{1}{\pi} \int_0^{\infty} dy \int_0^{\pi} d\theta y e^{-(y^2 + R^2 - Ry \cos \theta)} f(Ay) \quad (11)$$

Note that  $R = s'/\sigma = \frac{s}{\alpha} \frac{d}{\sigma} = \alpha \frac{d}{\sigma} = \frac{r}{r_0} \frac{d}{\sigma}$  so that  $r = \frac{\sigma}{\alpha} r_0 R$ .

We define  $\sigma = \frac{\sigma}{\alpha}$ , the dispersion in radians and  $W = r_0 \sigma$ .  $W$  is the metric radius at the galaxy corresponding to the angle  $\sigma$  subtended by the point-spread function. Now  $R = r/W$  and  $A = W/\alpha$  so that  $A \cdot R = \frac{r}{\alpha} = \beta$ .

By comparison of eq 8b and eq 11 we can define a point-spread profile  $\tilde{f}$  as:

$$\tilde{f}(\beta) = \tilde{f}(R, A) = \frac{1}{\pi} \int_0^{\infty} dy \int_0^{\pi} d\theta y e^{-(y^2 + R^2 - Ry \cos \theta)} f(Ay) \quad (12)$$

It is easy to show that in the limit as  $\sigma \rightarrow 0$ ,  $\tilde{f} \rightarrow f$  and  $\tilde{I} \rightarrow I$ . If we write eq 11 in the form

$$\tilde{I}_\nu(\alpha, z) = \frac{B_0(z)}{(1+z)^3} g[\nu(1+z), z] \int_{-\infty}^{\infty} dx \int_{-\infty}^{\infty} dy I(\alpha', z) \frac{1}{2\pi\sigma^2} e^{-\frac{(x^2+y^2)}{2\sigma^2}},$$

where cartesian coordinates  $(x, y)$  with origin P are chosen. By theorem I [see pg.2-17] with  $\frac{1}{2\sigma^2} = n$  we have

$$\lim_{\sigma \rightarrow 0} \tilde{I}_\nu(\alpha, z) = I_\nu(\alpha, z). \quad (\text{at } x=y=0, \alpha' = \alpha)$$

DEFINITION: A good function is one which is everywhere differentiable any number of times and such that it and all its derivatives are  $O(|x|^N)$  as  $x \rightarrow \infty$  for all  $N$ .

THEOREM I

The sequence equivalent to  $e^{-n(x^2+y^2)} \left(\frac{n}{\pi}\right)$  defines a generalised function  $\delta(x,y)$  such that

$$\int_{-\infty}^{\infty} dx \int_{-\infty}^{\infty} dy \delta(x,y) F(x,y) = F(0,0)$$

if  $F$  is a good function.

This theorem is proved in Lighthill (1960) pg 17 for one dimension. It is here rewritten for two dimensions.

Proof: Let  $I = \left| \int_{-\infty}^{\infty} dx \int_{-\infty}^{\infty} dy e^{-n(x^2+y^2)} \left(\frac{n}{\pi}\right) F(x,y) - F(0,0) \right|$ , then

$$\begin{aligned} I &\leq \int_{-\infty}^{\infty} dx \int_{-\infty}^{\infty} dy e^{-n(x^2+y^2)} \left(\frac{n}{\pi}\right) |F(x,y) - F(0,0)| \\ &\leq \int_{-\infty}^{\infty} dx \int_{-\infty}^{\infty} dy e^{-n(x^2+y^2)} \left(\frac{n}{\pi}\right) \max \left\{ \left| \frac{\partial F}{\partial x} \right|; \left| \frac{\partial F}{\partial y} \right| \right\} |(x-0) + (y-0)| \\ &\leq \max \left\{ \left| \frac{\partial F}{\partial x} \right|; \left| \frac{\partial F}{\partial y} \right| \right\} \int_{-\infty}^{\infty} dx \int_{-\infty}^{\infty} dy e^{-n(x^2+y^2)} \left(\frac{n}{\pi}\right) (|x| + |y|). \end{aligned}$$

$$\text{Now } \int_{-\infty}^{\infty} e^{-nx^2} \sqrt{\frac{n}{\pi}} |x| dx = \frac{1}{\sqrt{n\pi}}$$

$$\text{and } \int_{-\infty}^{\infty} e^{-nx^2} \sqrt{\frac{n}{\pi}} dx = \sqrt{\frac{n}{\pi}} \sqrt{\frac{\pi}{n}} = 1 \text{ so that}$$

$$I \leq \max \left\{ \left| \frac{\partial F}{\partial x} \right|; \left| \frac{\partial F}{\partial y} \right| \right\} \frac{2}{\sqrt{n\pi}} \rightarrow 0 \text{ as } n \rightarrow \infty,$$

as the derivatives of  $F$  are bound ( $F$  is a good function)

### C Detector Response

Given an image intensity  $\tilde{I}_v(\alpha, z)$  at the focal plane, some detector will be used to measure this intensity. The measurement will depend on the instrument used and on the conditions under which it is used (e.g. for a photographic plate ~~it is~~<sup>they are</sup> the exposure time, the development time and temperature, sensitivation procedure etc.) Denote the total of these conditions relevant to the observation by C.

The final detector output depends basically on two factors:

#### 1) The detector spectral sensitivity:

Under conditions C only certain frequency ranges can effect the detector output. This can be described by a function  $\phi$ , the spectral sensitivity [see e.g. Weaver 1962] such that the effective total or integrated intensity  $I_0$  is given by

$$I_0(\alpha, z) = \int_0^{\infty} \tilde{I}_v(\alpha, z) \phi(\nu, C) d\nu. \quad (13)$$

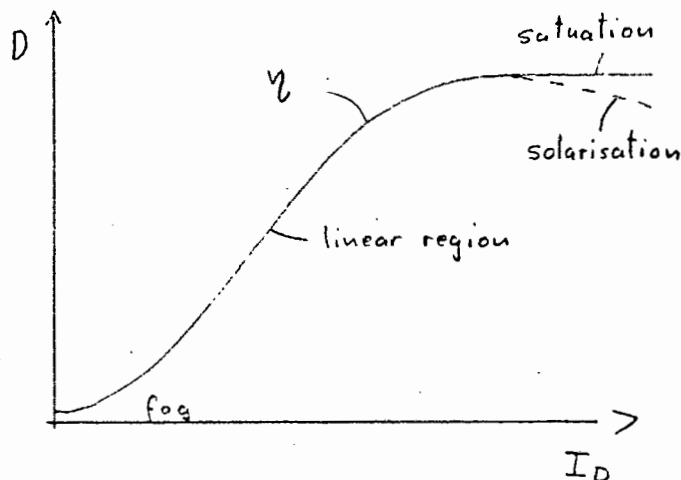
#### 2) The detector characteristic curve:

This gives the total detector response D (also called darkening) to the image plane radiant energy distribution  $I_0$  [see Stock and Williams (1962)] Write

$$D(\alpha, z) = \eta(I_0, C),$$

where  $\eta$  is the detector response to  $I_0$  under conditions C. In general, this curve will have a form like that shown (Fig 2.6), for any specific C. It may turn over for large  $I_0$ , if the detector has a region of solarisation. [see Weaver 1962]

Figure 2-6.



In derivations that follow we do not consider the detector response function or night sky subtraction. We assume that the observational data are corrected for both effects and our starting point is eq.13.

#### 2.2.4. The Flux and Luminosity for "nearby" Galaxies

Some "absolute" properties of the galaxy model are given here, assuming Euclidean space. Assume a galaxy at distance  $R$  with redshift  $z \ll 1$ , the metric radius  $r$  will correspond to an angle  $\theta = r/R$  and  $A_m = r_m/R$ , where  $r_m$  is that value of  $r$  which includes "all" of the galaxy (the theoretical profile has to be truncated). Assuming further that  $A_m \ll 1$ , then eq.4 holds and from eq.5a

$$F_\nu = 2\pi \int_0^{A_m} B_\nu \theta d\theta,$$

then from eq. 8a

$$\begin{aligned} F_\nu &= 2\pi \int_0^{r_m} B_\nu(r, z) \frac{r}{R} \frac{dr}{R} \\ &= 2\pi \frac{B_0(z) \mathcal{J}(\nu, z)}{R^2} \int_0^{r_m} f\left(\frac{r}{a(z)}\right) r dr. \end{aligned}$$

$$\text{Put } \frac{r}{a(z)} = \beta \quad \Rightarrow \quad \beta_m = \frac{r_m}{a(z)},$$

then

$$F_{\nu} = \frac{B_0(z) \mathcal{J}(\nu, z) a^2(z)}{R^2} \int_0^{\beta_m} 2\pi f(\beta) \beta d\beta ;$$

define  $g(\beta_m) = \int_0^{\beta_m} 2\pi \beta f(\beta) d\beta ,$

then  $F_{\nu}(z) = \frac{B_0(z) \mathcal{J}(\nu, z) a^2(z)}{R^2} g(\beta_m) .$

(14)

The luminosity  $L_{\nu}$  is given by eq 3, i.e.

$$L_{\nu}(z) = 4\pi B_0(z) \mathcal{J}(\nu, z) a^2(z) g(\beta_m)$$

and

$$L(z) = 4\pi B_0(z) a^2(z) g(\beta_m),$$

(15)

since  $\int_0^{\infty} \mathcal{J}(\nu, z) d\nu = 1 .$

In later applications we replace  $g(\beta_m)$  with  $g_{\infty} \equiv \int_{\beta \rightarrow \infty} g(\beta)$ . It is not obvious that this is physically meaningful [see King 1978], but De Vaucouleurs gives for the De Vaucouleurs profile a range for  $\beta$  of  $0.003 < \beta < 15$  and  $\frac{g(15)}{g_{\infty}} = 0.98$ . It seems thus reasonable to approximate  $g(\beta_m)$  by  $g_{\infty}$ . [see De Vaucouleurs 1959]

NOTE: It is assumed in this derivation that the flux at optical wavelengths is much larger than the X-ray or radio flux.

### 2.3. The Magnitude Scales

We first summarize the basic definitions for the absolute and apparent magnitudes together with the correct magnitude scales (taken from "Astrophysical Quantities" by C.W.Allen 3rd edition). [Allen 1973] We then give the absolute and apparent colour magnitudes for galaxies in terms of the flux and luminosity expressions of section 2.2. The detection limit on the received specific intensity is incorporated in these expressions. In order to compare our equations with those of the "standard" literature, the K-correction, aperture correction and bolometric correction are defined. Finally source evolution is introduced and we are in the position to write down the observational map.

#### 2.3.1. Definitions

M = absolute magnitude    D = 10pc

m = apparent magnitude    D = 1kpc

d = luminosity distance    D = 1Mpc

$r_o$  = observer area distance

$f_\lambda$  = actual smoothed flux of radiation  
near effective wavelength

L = luminosity

1pc =  $3.086 \cdot 10^{18}$  cm

and we have that  $d = r_o(1+z)^2$  [Weinberg 1972]

The basic equations are

$$M - m - 5 \log_{10} \frac{d}{D} = m - 5 \log \frac{r_0 (1+z)^2}{D_M} - 25, \quad (16a)$$

$$M = M_0 - 2.5 \log_{10} (L/L_0), \quad (16b)$$

$$m_1 - m_2 = -2.5 \log_{10} (f_1/f_2). \quad (16c)$$

The above definitions assume measurement within an aperture  $A > A_m$  and proper sky subtraction. Actual measurements are based on the use of "standard stars" of known magnitude.

Note: Write log for  $\log_{10}$

### 2.3.2. Bolometric Absolute Magnitudes

Define the bolometric absolute magnitude  $M_b$  as:

$$M_b = M_\odot^b - 2.5 \log(L/L_\odot); \quad M_\odot^b = 4.75$$

$$L_\odot = 3.826(8) \times 10^{33} \text{ erg/sec.}$$

The sun is a spherically symmetric radiator with mean surface brightness  $B_\odot$  (say), then from eq. 3

$$L_\odot = 4\pi R_\odot^2 B_\odot; \quad R_\odot \text{ the sun's radius}$$

"Near" a galaxy we have from eq 15

$$L(z) = 4\pi B_\odot(z) \alpha(z) g_\infty.$$

Then

$$M_b = M_0^b - 2.5 \log \left[ \frac{B_0(z) a^2(z) g_\infty}{B_0 R_0^2 \pi} \right]$$

$$= M_0^b - 2.5 \log \left[ \frac{B_0(z)}{B_0} \left( \frac{a}{D} \right)^2 \frac{g_\infty}{\pi} \right] + 5 \log \frac{R_0}{D}.$$

$$\Rightarrow M_b = -2.5 \log \left[ \frac{B_0(z)}{B_0} \left( \frac{a}{D} \right)^2 \frac{g_\infty}{\pi} \right] - 38.48 \quad (17)$$

and  $B_0 = 2.04 \cdot 10^{10} \text{ erg-cm}^{-1}\text{-sec}^{-1}\text{-ster}^{-1}$ .

### Physical Units:

Definitions: We use units where

$$m_{bol} \equiv -2.5 \log f/f_0; f_0 \equiv 2.48 \cdot 10^{-5} \text{ erg-sec}^{-1}\text{-cm}^{-2}$$

It follows that for the absolute magnitude

$$M_{bol} = -2.5 \log (L/L_0); L_0 = 2.97 \cdot 10^{35} \text{ erg-sec}^{-1},$$

and, to measure the surface brightness in magnitudes per square arc-sec define

$$M_{bol} \equiv -2.5 \log (S/S_0); S_0 = 2.48 \cdot 10^{-5} \text{ erg-sec}^{-1}\text{-cm}^{-2}\text{-(arc sec)}^{-2}$$

$$\text{or } S_0 = 1.055 \cdot 10^6 \text{ erg-sec}^{-1}\text{-cm}^{-2}\text{-ster}^{-1}.$$

$$L_e \equiv 4\pi D_k^2 S_0 \pi = 3.966 \cdot 10^{50} \text{ erg-sec}^{-1}.$$

Then

$$M_{bol} = -2.5 \log \left( \frac{L}{L_e} \frac{L_e}{L_0} \right)$$

$$= -2.5 \log \frac{L_e}{L_0} - 2.5 \log \left[ \frac{4\pi a^2 B_0 g_\infty}{4\pi D_k^2 S_0 \pi} \right].$$

$$\therefore M_{bol} = -37.82 - 2.5 \log \left[ \frac{B_0(z)}{S_0} \left( \frac{a}{D_k} \right)^2 \frac{g_\infty}{\pi} \right] \quad (18a)$$

Note: There is a shift in scale between  $M_b$  and  $M_{bol}$  of .025. This shift in scale is not present if values from Allen 2nd edition are used.

### 2.3.3. Absolute Colour Magnitude

Definition

$$M_V = M_V^{\circ} - 2.5 \log \frac{L_V(z)}{L_V^{\circ}} ; d_V = L_V \Delta V$$

where  $L_V \Delta V$  is the energy emitted per sec in  $\Delta V = \nu_2 - \nu_1$ ,

more correctly  $L_V = \int_{\nu_1}^{\nu_2} L_V d\nu$  [erg-sec<sup>-1</sup>].

From eq.15

$$L_V(z) = 4\pi B_0(z) a^2(z) g_{\infty} \int(\nu, z) \Delta V$$

and for the Sun

$$L_V^{\circ} = 4\pi^2 B_0 R_0^2 g_0(\nu) \Delta V$$

from the definition

$$\begin{aligned} M_V &= M_V^{\circ} - 2.5 \log \left[ \frac{B_0(z) a^2(z) \int(\nu, z) \Delta V g_{\infty}}{B_0 R_0^2 g_0(\nu) \Delta V \pi} \right] \\ &= M_V^{\circ} - 2.5 \log \left[ \frac{B_0(z)}{B_0} \left( \frac{a}{R_0} \right)^2 \frac{\int(\nu, z)}{g_0(\nu)} \frac{g_{\infty}}{\pi} \right] - 2.5 \log \left[ \frac{B_0}{B_0} \left( \frac{R_0}{R_0} \right)^2 \right] \end{aligned}$$

Now from eq.18a with  $B_0 = B_0$ ;  $a = R_0$  and for a spherical radiator we have  $g_{\infty} = \pi$ , thus:

$$\begin{aligned} -2.5 \log \left[ \frac{B_0}{B_0} \left( \frac{R_0}{R_0} \right)^2 \right] &= -2.5 \log \left[ \frac{B_0}{B_0} \left( \frac{R_0}{R_0} \right)^2 \frac{\pi}{\pi} \right] \\ &= -M_{bol}^{\circ} - 37.82 \end{aligned}$$

$$\therefore M_V = -37.82 - 2.5 \log \left[ \frac{B_0(z)}{B_0} \left( \frac{a}{R_0} \right)^2 \frac{\int(\nu, z)}{g_0(\nu)} \frac{g_{\infty}}{\pi} \right] + M_V^{\circ} - M_{bol}^{\circ}$$

The bolometric correction for the sun is given by

$$M_V^{\circ} - M_{bol}^{\circ} = m_V^{\circ} - m_{bol}^{\circ}$$

and since

$$m_v^0 - m_{bol}^0 = -2.5 \log \frac{f_v^0}{f_{bol}^0} = -2.5 \log \frac{\int_0^{\infty} g_0(v) \Delta v}{\int_0^{\infty} g_0(v) dv}$$

$$= -2.5 \log \int_0^{\infty} g_0(v) \Delta v$$

we have

$$M_v = -2.5 \log \left[ \frac{\beta_0(z)}{\beta_0} \left( \frac{a(z)}{D_k} \right)^2 \frac{g_{\infty}}{\pi} \int_0^{\infty} g(v, z) \Delta v \right] - 37.82 \quad (19a)$$

If the frequency band is not small enough for 19a to be accurate we write

$$M_v = -2.5 \log \left[ \frac{\beta_0(z)}{\beta_0} \left( \frac{a(z)}{D_k} \right)^2 \frac{g_{\infty}}{\pi} \int_{\nu_1}^{\nu_2} g(v, z) dv \right] - 37.82 \quad (19b)$$

#### 2.3.4. Apparent Colour Magnitude

We measure the flux up to a detection limit  $\mathcal{I}_L(v)$  in specific intensity corresponding to an aperture  $A_{ap}$ . Thus from eq. 9

$$\mathcal{I}_L(v) = I_v(A_{ap}, z) = \frac{B(A_{ap}, r_0(z), z)}{(1+z)^3} \mathcal{I}[v(1+z), A_{ap}, r_0(z), z] e^{-p(v, z)}$$

and from eq's 11 and 12

$$\mathcal{I}_L(v) = \frac{\beta_0(z)}{(1+z)^3} \mathcal{I}[v(1+z), z] e^{-p(v, z)} \tilde{f}(\beta_{ap}) \quad \text{where } \beta_{ap} = \frac{A_{ap} r_0(z)}{a(z)} \quad (20a)$$

Note: Since the spectral distribution of the night sky is not the same <sup>as</sup> than that of any particular galaxy, the apparent angle  $A_{ap}$  depends on the measured frequency:  $A_{ap} = A_{ap}(v)$ , therefore  $\beta = \beta(v)$ .

We assume that this effect is not important in the derivation

that follows, restricting its validity (possibly) to narrow bandwidth filters.

$$\text{Also } \tilde{A}_{ap}(z) = \frac{a(z)}{r_0(z)} \left( \tilde{f}^{-1} \left( \frac{B_L (1+z)^3}{B_0(z) g[v(1+z), z]} \right) \right).$$

We measure the flux in an aperture  $\tilde{A}_{ap}$  at frequency  $\nu$ . From eq's. 4, 11 and 12 we have that

$$\begin{aligned} \tilde{F}_\nu(\tilde{A}_{ap}) &= \int_0^{\tilde{H}_{ap}} \tilde{I}_\nu(\alpha, z) 2\pi \alpha d\alpha \\ &= \frac{B_0(z)}{(1+z)^3} g[v(1+z), z] e^{-p(\nu, z)} \int_0^{\tilde{H}_{ap}} \tilde{f} \left( \frac{\alpha r_0(z)}{a(z)} \right) 2\pi \alpha d\alpha. \end{aligned}$$

$$\text{put } \frac{\alpha r_0}{a} = \beta \quad \text{and} \quad \tilde{\beta}_{ap} = \frac{\tilde{H}_{ap} r_0}{a}$$

$$\therefore \tilde{F}_\nu(\tilde{A}_{ap}) = \frac{B_0}{(1+z)^3} g[v(1+z), z] e^{-p(\nu, z)} \left( \frac{a}{r_0} \right)^2 \int_0^{\tilde{\beta}_{ap}} \tilde{f}(\beta) 2\pi \beta d\beta.$$

Define  $\tilde{g}(\beta) = \int_0^\beta \tilde{f}(x) 2\pi x dx$  and then

$$\tilde{F}_\nu(\tilde{A}_{ap}) = \frac{B_0}{(1+z)^3} g[v(1+z), z] e^{-p(\nu, z)} \left( \frac{a(z)}{r_0(z)} \right)^2 \tilde{g}(\tilde{\beta}_{ap}). \quad (20b)$$

Over the frequency band  $\Delta\nu_i = [\nu_1, \nu_2]$  of the  $i$ -th filter (with spectral sensitivity  $\phi_i(\nu, C)$ ) the flux  $F_{\Delta\nu_i}$  is given by

$$\tilde{F}_{\Delta\nu_i}(\tilde{A}_{ap}) = \int_{\nu_1}^{\nu_2} \tilde{F}_\nu(\tilde{A}_{ap}) \phi_i(\nu, C) d\nu.$$

Here  $C$  denotes the the conditions of observation [see section 2.2.3]. Now

$$\tilde{F}_{\Delta\nu_i}(\tilde{A}_{ap}) = \frac{B_0(z)}{(1+z)^3} \left( \frac{a}{r_0} \right)^2 \int_{\nu_1}^{\nu_2} \phi_i(\nu, C) g[v(1+z), z] e^{-p(\nu, z)} \tilde{g}(\tilde{\beta}_{ap}) d\nu.$$

and if we make the additional assumption, that  $\sigma \neq \sigma(v)$ , we have

$$\tilde{F}_{\Delta v_i}(\tilde{A}_{\Delta v_i}) = \frac{B_0(z)}{(1+z)^3} \left( \frac{a(z)}{r_0(z)} \right)^2 \tilde{g}(\tilde{\beta}_{\Delta v_i}) \tilde{\Phi}_i(z),$$

where

$$\tilde{\Phi}_i(z) \equiv \int_{v_1}^{v_2} \phi_i(v, z) g[v(1+z), z] e^{-p(v, z)} dv.$$

(20c)

We measure

$$M_{\Delta v_i} - M_{\Delta v_i}^0 = -2.5 \log \left( \frac{F_{\Delta v_i}}{F_{\Delta v_i}^0} \right)$$

$$= -2.5 \log \left[ \frac{B_0(z)}{(1+z)^3} \left( \frac{a}{r_0} \right)^2 \tilde{g}(\tilde{\beta}_{\Delta v_i}) \tilde{\Phi}_i(z) / \frac{\pi R_0^2 B_0}{d_0^2} \int_{v_1}^{v_2} g_0(v) dv \right].$$

Since for the sun  $L_0 = 4\pi R_0^2 B_0$ , the flux at distance  $d_0$  is given by  $F_0 = L_0 / 4\pi d_0^2 = \pi R_0^2 B_0 / d_0^2$  at a particular wavelength.

Rewrite this as

$$M_{\Delta v_i} - M_{\Delta v_i}^0 = -2.5 \log \left[ \frac{B_0(z)}{B_0} \tilde{\Phi}_i(z) \left( \frac{a}{D_k} \right)^2 \frac{g_\infty}{\pi} \right] - 2.5 \log \left[ \frac{d_0}{B_0} \left( \frac{D_k}{R_0} \right)^2 \right]$$

$$+ 5 \log \left[ \frac{r_0(z)(1+z)^{v_2}}{D} \right] - 5 \log \frac{d_0}{D} + 2.5 \log \int_{v_1}^{v_2} g_0(v) dv - 2.5 \log \frac{\tilde{g}(\tilde{\beta}_{\Delta v_i})}{g_\infty}.$$

From section 2.3.3:

$$-2.5 \log \left[ \frac{d_0}{B_0} \left( \frac{D_k}{R_0} \right)^2 \right] = -M_{bol}^0 - 37.82,$$

further from eq.16a

$$M_{\Delta v_i} - 5 \log \frac{d_0}{D} = M_{\Delta v_i}^0$$

and the bolometric correction is

$$2.5 \log \int_{v_1}^{v_2} g_0(v) dv = -(M_{\Delta v_i}^0 - M_{bol}^0)$$

so that

$$m_{\Delta v_i}(\tilde{A}_{\Delta v_i}) = -2.5 \log \left[ \frac{B_0(z)}{B_0} \left( \frac{a(z)}{D_k} \right)^2 \frac{g_\infty}{\pi} \int_{v_1}^{v_2} g(v, z) dv \right] - 2.5 \log \left[ \frac{\tilde{\Phi}_i(z)}{\int_{v_1}^{v_2} g(v, z) dv} \right]$$

$$+ 5 \log \left[ \frac{r_0(z)(1+z)^2}{10^{-5} \text{ cm}} \right] - 2.5 \log \left[ \frac{\tilde{g}(\tilde{\beta}_{\Delta v_i})}{g_\infty} \right] - 37.82.$$

Finally from eq.19b

$$m_{\Delta v_i}(\tilde{A}_{ap}) = M_{\Delta v_i} - 2.5 \log \left[ \frac{\Phi_i(z)}{\int_{v_1}^{v_2} \mathcal{G}(v, z) dv} \right] + 5 \log \left[ \frac{r_0(z) (1+z)^{3/2}}{D_M} \right] - 2.5 \log \frac{\tilde{g}(\tilde{\beta}_{ap})}{g_\infty} + 25 \quad (21a)$$

which, in terms of the bolometric magnitude, is

$$m_{\Delta v_i}(\tilde{A}_{ap}) = M_{bol} - 2.5 \log \Phi_i(z) + 5 \log \left[ \frac{r_0(z) (1+z)^{3/2}}{D_M} \right] - 2.5 \log \frac{\tilde{g}(\tilde{\beta}_{ap})}{g_\infty} + 25 \quad (21b)$$

We can rewrite eq.21b as follows (for comparison with the literature)

$$\begin{aligned} m_{\Delta v_i}(\tilde{A}_{ap}) &= M_{bol} - 2.5 \log (1+z) - 2.5 \log \frac{\int_{v_1}^{v_2} \Phi_i(v, C) \mathcal{G}[v(1+z), z] dv}{\int_{v_1}^{v_2} \Phi_i(v, C) \mathcal{G}[v, z] dv} \\ &\quad - 2.5 \log \left[ \int_{v_1}^{v_2} \Phi_i(v, C) \mathcal{G}(v, z) dv \right] - 2.5 \log \frac{\tilde{g}(\tilde{\beta}_{ap})}{g_\infty} \\ &\quad + 5 \log \left[ \frac{r_0(z)}{D_M} (1+z)^2 \right] + 25 \\ &= M_{bol} + 5 \log \left[ \frac{r_0(z)}{D_M} (1+z)^2 \right] + 25 + K_i(z) + \Delta m_{bol_i} + A^{\sigma}(\tilde{\beta}_{ap}), \end{aligned}$$

where  $K_i(z) = K$ -correction as given by [Oke and Sandage 1968 or De Vaucouleurs 1977]

$$= -2.5 \log (1+z) - 2.5 \log \left[ \frac{\int_{v_1}^{v_2} \Phi_i(v, C) \mathcal{G}[v(1+z), z] dv}{\int_{v_1}^{v_2} \Phi_i(v, C) \mathcal{G}[v, z] dv} \right],$$

$\Delta m_{bol_i}$  = Bolometric correction

$$= -2.5 \log \left[ \int_{v_1}^{v_2} \Phi_i(v, C) \mathcal{G}(v, z) dv \right]$$

and  $A^{\sigma}(\tilde{\beta}_{ap})$  = Aperture correction

$$= -2.5 \log \frac{\tilde{g}(\tilde{\beta}_{ap})}{g_\infty}.$$

Source Evolution:

Define evolution parameters  $p_1$  and  $p_2$  as

$$a(z) = a_0 (1+z)^{p_1}$$

(22)

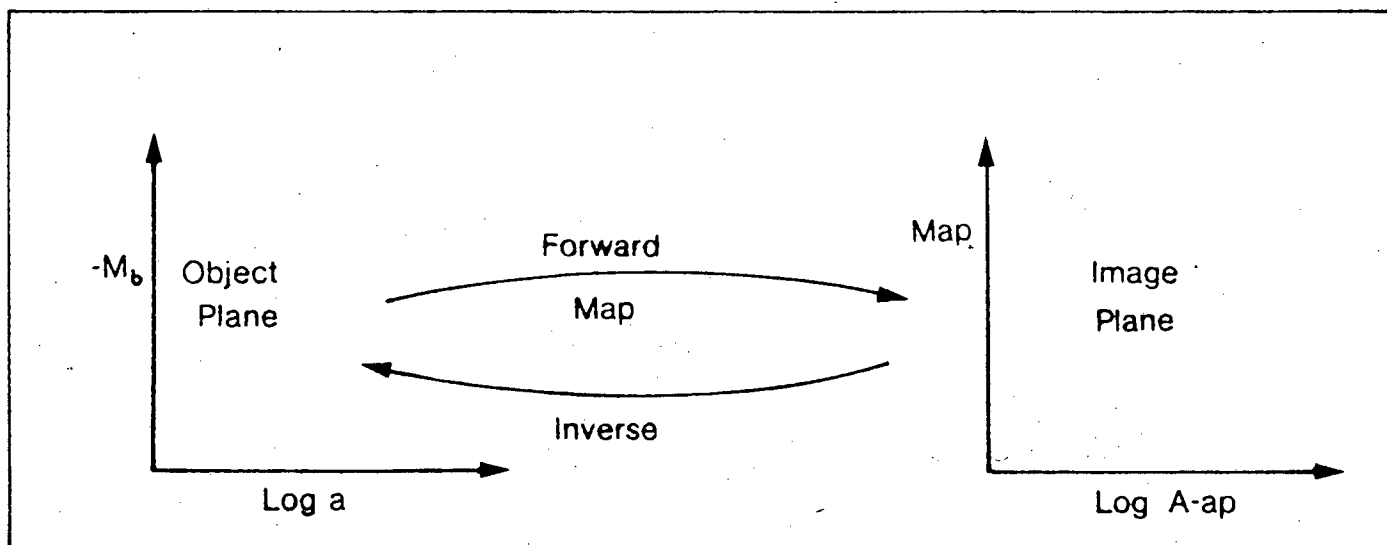
$$L_0(z) = L_0 (1+z)^{p_2}$$

thus replace  $M_{bol}$  by  $M_{bol} - 2.5 \log(1+z)^{p_1} - 5 \log(1+z)^{p_2}$  and  $a(z)$  in the equations derived above.  $p_1$  is the radial evolution index and  $p_2$  the luminosity evolution index.

## 2.4. The Observational Map

The map from the object to the image plane and its inverse is derived. The map is not defined on the whole of the object plane and the condition for its existence is given. Likewise for the inverse map.

Figure 2-7.



## 2.4.1. The Defining Equations

a) Define the detection limit  $S_L$  in magnitudes as

$$\begin{aligned}
 S_L &= -2.5 \log \left[ \frac{\int_0^{v_k} \phi_i(v, z) S_L(v) dv}{S_0} \right] \text{ and from eq. 20a and 22} \\
 &= -2.5 \log \left[ \frac{B_0 (1+z)^{P_2}}{S_0} \frac{1}{(1+z)^3} \int_0^{v_k} \phi(v, z) \mathcal{G}[v(1+z), z] e^{-p(v, z)} \tilde{f}(\beta_{ap}) dv \right] \\
 &= -2.5 \log \left[ \frac{B_0 (1+z)^{P_2}}{S_0} \left( \frac{a(1+z)^{P_1}}{D_k} \right)^2 \frac{g_\infty}{\pi} \right] + 5 \log \frac{a(1+z)^{P_1}}{D_k} + 2.5 \log \frac{g_\infty}{\pi} \\
 &\quad + 5 \log (1+z)^{3/2} - 2.5 \log \tilde{\Phi}_i(z) - 2.5 \log \tilde{f}(\beta_{ap}).
 \end{aligned}$$

$$\begin{aligned}
 \therefore S_L &= M_{b01} + 4 M_i + 5 \log \left( \frac{a}{D_k} \right) + 5 \log (1+z)^{3/2} - 2.5 \log \tilde{f}(\beta_{ap}) \\
 &\quad + 2.5 \log \frac{g_\infty}{\pi} - 2.5 \log (1+z)^{P_2} + 37.82
 \end{aligned}$$

(22 a)

where  $\Delta M_i \equiv -2.5 \log \tilde{F}_i(z) = -2.5 \log \left[ \int_{\nu_1}^{\nu_2} \phi_i(\nu, c) \mathcal{J}[\nu(1+z), z] e^{-p(\nu z)} d\nu \right]$

b) The apparent colour magnitude is given by

$$M_{\Delta\nu_i}(A_{ap}) = M_{bol} + \Delta M_i + 5 \log \frac{r_0(z) (1+z)^{3/2}}{D_M} - 2.5 \log \frac{\tilde{g}(\beta_{ap})}{g_\infty} - (2.5 p_2 + 5 p_1) \log(1+z) + 25. \quad (22b)$$

c) The apparent angle in terms of the scaling radius is given by:

$$\log A_{ap} = \log \frac{a(1+z)^{p_1}}{r_0(z)} \beta_{ap}, \quad \text{or}$$

$$\log A_{ap} = \log \frac{a}{D_k} - \log \frac{r_0(z)}{D_M} - 3 + \log \beta_{ap} + p_1 \log(1+z). \quad (22c)$$

#### 2.4.2. Forward Map

$$\left( \log \frac{a}{D_k}; M_{bol} \right) \rightarrow \left( \log A_{ap}; m_{\Delta\nu}(A_{ap}) \right)$$

For each point in the object plane  $(\log A_{ap}, M_{bol})$  at redshift  $z$  there is a one-to-one map to the image plane provided, that

$$I_\nu^s(0, z) > S_L(\nu)$$

i.e.

$$\begin{aligned} -2.5 \log \tilde{F}(0) < S_L - (M_{bol} + \Delta M_i + 37.82) - 2.5 \log \frac{g_\infty}{\pi} \\ - 5 \log \left( \frac{a}{D_k} (1+z)^{3/2} \right) + 2.5 p_2 \log(1+z) \end{aligned}$$

Solve for  $\beta_{ap}$  from eq. 22a

$$\begin{aligned} -2.5 \log \tilde{F}(\beta_{ap}) = S_L - (M_{bol} + \Delta M_i + 37.82) - 2.5 \log \frac{g_\infty}{\pi} - 5 \log \left( \frac{a}{D_k} (1+z)^{3/2} \right) \\ + 2.5 p_2 \log(1+z) \end{aligned}$$

$$\begin{aligned}
 \text{then } \log A_{ap} &= \log \frac{a}{D_k} - \left( \log \left( \frac{r_0(z)}{D_M} \right) + 3 \right) + \log \beta_{ap} + p_1 \log (1+z) \\
 \text{and } m_{av_i}(A_{ap}) &= M_{bol} + \Delta M_i - 2.5 \log \frac{\tilde{g}(\beta_{ap})}{g_\infty} + 5 \log \frac{r_0(z)(1+z)^{3/2}}{D_M} + 25 \\
 &\quad - (2.5 p_2 + 5 p_1) \log (1+z) .
 \end{aligned} \tag{23}$$

### 2.4.3. Inverse Map

$$(\log A_{ap} ; m_{av_i}(A_{ap})) \rightarrow \left( \log \frac{a}{D_k} ; M_{bol} \right)$$

The inverse map exists only when

$$5 \log A_{ap} + m_{av_i}(A_{ap}) < S_L - 27.82 \quad [\text{see pg.2-33}].$$

Substitute for  $M_{bol}$  and  $\log \frac{a}{D_k}$  in eq.22a from eq's 22b and 22c and regroup, then

$$-2.5 \log \left\{ \frac{\beta_{ap}^2 \tilde{f}(\beta_{ap})}{\tilde{g}(\beta_{ap})/g_\infty} \right\} = S_L - m_{av_i}(A_{ap}) - 5 \log A_{ap} - (27.82 + 2.5 \log \frac{g_\infty}{g}). \tag{24a}$$

For any assumed profile  $\beta^2 f(\beta)/g(\beta)$  is a well defined function which is constant along lines of constant surface brightness. Now solve for  $\beta_{ap}$  from eq.24a, the map is then defined by:

$$\log \frac{a}{D_k} = \log A_{ap} + \log \frac{r_0(z)}{D_M} + 3 - \log \beta_{ap} - \log (1+z)^{p_1} \tag{24b}$$

and

$$\begin{aligned}
 M_{bol} &= m_{av_i}(A_{ap}) - \Delta M_i + 2.5 \log \frac{\tilde{g}(\beta_{ap})}{g_\infty} - 5 \log \frac{r_0(z)(1+z)^{3/2}}{D_M} \\
 &\quad + (2.5 p_2 + 5 p_1) \log (1+z) - 25 .
 \end{aligned} \tag{24c}$$

The limit of  $\frac{\beta^2 f(\beta)}{g(\beta)}$  for  $\beta \rightarrow 0$

This limit is indeterminate, thus use L'Hospital's rules

$$\begin{aligned} \therefore \lim_{\beta \rightarrow 0} \frac{\beta^2 f(\beta)}{g(\beta)} &= \lim_{\beta \rightarrow 0} \frac{2\beta f(\beta) + \beta^2 f'(\beta)}{2\pi\beta f(\beta)} \quad \text{as } g(\beta) = 2\pi \int_0^\beta x f(x) dx \\ &= \lim_{\beta \rightarrow 0} \frac{2f(\beta) + 2\beta f'(\beta) + 2\beta f'(\beta) + \beta^2 f''(\beta)}{2\pi f(\beta) + 2\pi\beta f'(\beta)}, \quad f'(\beta) = \frac{df}{d\beta} \\ &= \frac{1}{\pi} \quad \text{if } \beta f'(\beta) \text{ and } \beta^2 f''(\beta) \rightarrow 0 \text{ as } \beta \rightarrow 0 \end{aligned}$$

define  $G(\beta) \equiv -2.5 \log \frac{\beta^2 f(\beta)}{g(\beta)/g_\infty}$  then  $\lim_{\beta \rightarrow 0} G(\beta) = -2.5 \log \frac{g_\infty}{\pi}$ .

Note that for any finite value for  $\beta$

$$\int_0^\beta x f(x) dx < \beta^2 f(\beta) \quad \text{for small enough } \beta$$

and the limit  $\lim_{\beta \rightarrow 0} \frac{\beta^2 f(\beta)}{g(\beta)} = \frac{1}{\pi}$  is approached from below. Thus  $G(\beta)$  has a minimum at  $\beta=0$  and by eq.24a we must have

$$G(0) < S_L - m_{av}(A_{ap}) - 5 \log A_{ap} - (27.82 + 2.5 \log \frac{g_\infty}{\pi})$$

and as  $G(0) = \lim_{\beta \rightarrow 0} G(\beta) = -2.5 \log \frac{g_\infty}{\pi}$  we have

$$m_{av}(A_{ap}) + 5 \log A_{ap} < S_L - 27.82$$

## 2.5. A Specialised Form of the Map

In order to compute the observational map, the following approximations have been made

### 2.5.1. Brightness Profiles for Elliptical Galaxies

#### A) de Vaucouleurs $r^{1/4}$ -law [de Vaucouleurs 1959 or 1977]

Define B as the surface brightness at metric radius r, and let  $B_{0v}$  be the central surface brightness (i.e.  $r=0$ ), then

$$B/B_{0v} = f(\beta) = e^{-[(\beta)^{1/4}]^4} \quad \text{where } \beta = \frac{r}{a_{0v}}, a_{0v} \text{ a scaling radius} \quad (25a)$$

The inverse profile  $f^{-1}$  is given by

$$f^{-1}(x) = (-\ln x)^4$$

From eq.14  $g(\beta)$  is given by

$$g_v(\beta) = 2\pi \int_0^\beta x f(x) dx = 2\pi \int_0^\beta x e^{-(x)^{1/4}} dx$$

put  $z = x^{1/4}$  and integrate by parts

$$g_v(u) = 8! \pi \left\{ 1 - e^{-u} \left[ 1 + u + \frac{u^2}{2!} + \dots + \frac{u^7}{7!} \right] \right\}$$

where  $u = \beta^{1/4}$  and  $g_{v\infty} = 8! \pi$  so that

$$\frac{g_v(u)}{g_{v\infty}} = 1 - e^{-u} \left[ 1 + u + \frac{u^2}{2!} + \dots + \frac{u^7}{7!} \right] \quad (25b)$$

Note: In computing  $g_v/g_{v\infty}$  eq.25b is numerically unstable for small values of u. Making use of the fact that

$$e^x = \underbrace{\left( 1 + x + \frac{x^2}{2!} + \frac{x^3}{3!} + \dots + \frac{x^7}{7!} \right)}_{A(x)} + \underbrace{\left( \frac{x^8}{8!} + \frac{x^9}{9!} + \dots \right)}_{B(x)}$$

we may write  $\frac{g_v(u)}{g_{v\infty}} = 1 - \frac{A(u)}{A(u)+B(u)} = \frac{B(u)}{A(u)+B(u)}$ .

For  $u < 0.8$  approximate  $B(u)$  by

$$B(u) = \left\{ \frac{u^8}{8!} + \frac{u^9}{9!} + \frac{u^{10}}{10!} + \frac{u^{11}}{11!} \right\} = \frac{u^8}{8!} \left( 1 + \frac{u}{9} \left( 1 + \frac{u}{10} \left( 1 + \frac{u}{11} \right) \right) \right).$$

$$\therefore \frac{g_v(u)}{g_{v\infty}} = e^{-u} \left\{ \frac{u^8}{40320} \left( 1 + \frac{u}{9} \left( 1 + \frac{u}{10} \left( 1 + \frac{u}{11} \right) \right) \right) \right\} \text{ for } u < 0.8,$$

$$= 1 - e^{-u} \left\{ 1 + u \left( 1 + \frac{u}{2} \left( 1 + \frac{u}{3} \left( 1 + \frac{u}{4} \left( 1 + \frac{u}{5} \left( 1 + \frac{u}{6} \left( 1 + \frac{u}{7} \right) \right) \right) \right) \right) \right) \right\}.$$

for  $u \geq 0.8$

### An alternative form of the de Vaucouleurs law

Define an "effective" scaling radius  $r_e$  such that  $g_v(1) = \frac{1}{2} g_{v\infty}$  i.e. 1/2 of the total light of the galaxy is contained within a metric radius  $r_e$ . Solve the implicit equation  $g(\frac{1}{2} a_v) = \frac{1}{2} g_{v\infty}$  to find

$$r_e = 3459 a_v.$$

$$\text{Now } \frac{B}{B_{0v}} = e^{-\left(\frac{r}{r_e}\right)^{1/4}} \left(\frac{r_e/a_v}{r_e}\right)^{1/4} = e^{-7.669 \left(\frac{r}{r_e}\right)^{1/4}},$$

Now

$$\text{or } \log \frac{B}{B_{0v}} = -3.331 \left(\frac{r}{r_e}\right)^{1/4}.$$

Define the surface brightness at  $r=r_e$  as  $B_e = B(r_e)$ . Then

$$\log \frac{B}{B_e} = -3.331 \left\{ \left(\frac{r}{r_e}\right)^{1/4} - 1 \right\}$$

and in magnitude units  $\mu = -2.5 \log B$

$$-2.5 \log \frac{B}{B_e} = \mu - \mu_e = 8.326 \left\{ \left(\frac{r}{r_e}\right)^{1/4} - 1 \right\}. \quad (25c)$$

Note: This form of the de Vaucouleurs law has only one free fitting parameter. This is not a serious limitation, as the central surface brightness  $B_0$  is unknown for galaxies beyond the

local group (due to the effect of seeing and limited instrumental resolution the central cores of elliptical galaxies beyond the local group are unresolved [Schweizer 1979, de Vaucouleurs 1979]).

### B) Abell-Mihalas profile [Abell and Mihalas 1966]

Define as for the de Vaucouleurs profile

$$\frac{B}{B_{0R}} = f(\beta) = \begin{cases} (1+\beta)^{-2} & \text{for } \beta \leq 21.4 \\ 22.4(1+\beta)^{-3} & \text{for } \beta > 21.4 \end{cases} \quad (26a)$$

where  $\beta = r/a_R$ ,  $a_R$  a scaling radius. Integrating the profile as before and defining  $\beta_c = 21.4$  we have

$$g_R(\beta) = \begin{cases} 2\pi \left[ \ln(1+\beta) - \frac{\beta}{(1+\beta)} \right] & \text{for } \beta \leq \beta_c \\ 2\pi \left[ \ln(1+\beta_c) + \frac{1}{2(1+\beta_c)} - (1+\beta_c) \left\{ \frac{1}{1+\beta} - \frac{1}{2(1+\beta)^2} \right\} \right] & \text{for } \beta > \beta_c \end{cases} \quad (26b)$$

$$g_R^\infty = 2\pi \left[ \ln(1+\beta_c) + \frac{1}{2(1+\beta_c)} \right] = 19.675.$$

The inverse profile  $f^{-1}$  is given by

$$f^{-1}(x) = \begin{cases} \sqrt{x} - 1 & \text{for } x \geq 1.993 \cdot 10^{-3} \\ \left( \frac{22.4}{x} \right)^{1/3} - 1 & \text{for } 0 < x < 1.993 \cdot 10^{-3} \end{cases}$$

### Fitting the profiles

De Vaucouleurs gives [de Vauc.1959] a very good fit for  $0.03 < r/r_e < 5$ , perhaps even a good fit up to  $r/r_e = 15$ . Abell and Mihalas [Abell and Mihalas 1966] give a good fit for both profiles for  $0.35 < r/a_R < 200$  ( $0.03 < r/r_e < 18; r_e = 11a_R$ ). Kormendy gives the relations  $a_R = 0.093r_e + 0.00$  kpc and  $-2.5 \log B_{0R} = -2.5 \log B_e - 5.27$ , obtained by fitting the brightness profiles to galaxies. [Kormendy 1977]

(Kormendy fits the Hubble profile, but the parameters  $a_R$  and  $B_{0R}$  will have the same values as those for the Abell-Mihalas profile. See eq's A2 and A3 in Kormendy 1977]

Mathematically we can compare the de Vaucouleurs and the Abell-Mihalas profiles as follows. Since the central surface brightness of galaxies is not known and both profiles are physically meaningless at the center (both profiles have a non-zero brightness gradient at  $r=0$ , this corresponds to an infinite space density at the center [King 1978]), assume that the metric radius that contains 1/2 of the light is the same for both profiles, as well as the luminosity  $L$ . From eq.15

$$L = 4\pi B_0 a^2 g_\infty .$$

Now solve  $\frac{g_R(\beta)}{g_{R\infty}} = \frac{1}{2}$  for the Abell-Mihalas profile, obtaining  $\beta = 10.97$ . By definition for the de Vauc. law  $\beta=1$

$$\therefore a_R = \frac{r_e}{10.97} = 0.09119 r_e .$$

Comparing luminosities  $B_{0V} a_V^2 g_{V\infty} = B_{0R} a_R^2 g_{R\infty}$  and by substituting  $a_V = \frac{r_e}{3459}$  and  $a_R = \frac{r_e}{10.97}$  as well as for  $g_{V\infty}$  and  $g_{R\infty}$  we obtain

$$B_{0V} = 15.45 B_{0R} \quad \text{and} \quad -2.5 \log B_{0V} = -2.5 \log B_{0R} - 2.972 .$$

Thus at the center the de Vauc. law is nearly 3 magnitudes brighter. Now  $\log \frac{B_e}{B_{0V}} = -3.331$

$$\therefore -2.5 \log B_{0R} = -2.5 \log B_e - 5.356$$

which differs from the relation found by Kormendy by less than 0.1 magnitude. Alternatively, we can compare the profiles by assuming that the mean surface brightness over a central region  $r_c$  is the same for both profiles.

### 2.5.2. Intergalactic Absorption

From section 2.2.3 the optical depth up to redshift  $z$  is given

by

$$\rho(\nu, z) = \int_0^z n_a(z') \sigma_a(z', \nu(1+z')) \frac{dl}{dz'} dz',$$

where  $n_a(z)$  = number density of absorbers at  $z$

and  $\sigma_a(z, \nu)$  = interaction cross-section of absorbers.

Following Gunn and Peterson [Gunn and Peterson 1965] we specialise to Thomson scattering by free electrons in an ideal cosmological model (FRW).

$$\therefore \sigma_a(z, \nu) = \sigma_e = \text{constant}.$$

The probability of scattering of a photon in a proper length interval  $dl = R(t) du$ , at cosmic time  $t$  and dimensionless parameter distance  $u$  [Sandage 1961], is given by

$$dp = n_e(t) \sigma_e dl,$$

where  $n_e$  and  $\sigma_e$  are the number density and cross-section for electrons respectively. Then the optical depth  $p$  is given by

$$p(z) = \sigma_e \int n_e dl = \sigma_e \int_0^z n_e(z') \frac{dl}{dz'} dz',$$

now for a FRW universe

$$\frac{dl}{dz} = R(t) \frac{du}{dz} = \frac{c H_0^{-1}}{(1+z)^2 (1+2q_0 z)^{1/2}}$$

and

$$n_e(z) = n_e(0) (1+z)^3$$

$$\therefore p(z) = \frac{\sigma_e n_e(0) c}{H_0} \int_0^z \frac{(1+z')}{(1+2q_0 z')^{1/2}} dz'.$$

which can be integrated to give

$$\left. \begin{aligned} p(z) &= \frac{\sigma_e n_e(0) c}{H_0} \frac{1}{3q_0^2} \left\{ (3q_0 + q_0 z - 1)(1 + 2q_0 z)^{1/2} - (3q_0 - 1) \right\} \text{ when } q_0 \neq 0 \\ \text{and} \\ p(z) &= \frac{\sigma_e n_e(0) c}{H_0} \frac{1}{2} (1+z)^2 \dots \dots \dots \text{ when } q_0 = 0. \end{aligned} \right\} \quad (27)$$

Assuming that the universe is composed entirely out of Hydrogen and fully ionised we have for an Einstein-de Sitter universe ( $q_0 = 0.5$ )  $n_e = 10^{-5} \text{ cm}^{-3}$  and for the low-density universe ( $q_0 = 0.01$ )  $n_e = 10^{-7} \text{ cm}^{-3}$ . Taking  $H_0 = 100 \text{ km-sec}^{-1} \text{ Mpc}$ , we have for electrons [Bahcall and Salpeter (1965)]:

$$\frac{\sigma_e n_e(0) c}{H_0} = 6.5 \times 10^3 n_e(0) .$$

The number density for electrons is proportional to  $q_0$  i.e.  $n_e(0) \propto q_0$  [see Sandage 1961 or Bahcall and May 1968] and if  $f_0$  represents the fraction of ionized hydrogen we can write:

$$n_e(0) = 2 \times 10^{-5} f_0 q_0$$

$$\therefore \frac{\sigma_e n_e(0) c}{H_0} = \frac{13 f_0 q_0}{H_0} . \quad (28)$$

### 2.5.3. The Magnitude Correction

A first approximation to the magnitude correction  $\Delta M$  (a combination of the K-correction and bolometric correction see section 2.3.4) is given. A fit to known galaxies showed that the results are approximately correct. The maps are much more sensitive to the value of the detection limit  $S_L$  however than to the value of the magnitude correction.

From section 2.4.1 eq.22a :

$$\Delta M_i = -2.5 \log \bar{\Phi}_i(z)$$

$$= -2.5 \log \left\{ \int_{v_1}^{v_2} \phi_i(v, c) \mathcal{F}[v(1+z), z] e^{-p(v, z)} dv \right\}$$

We make the assumptions:

1) Thompson scattering [see section 2.5.2]

$$p(z) = \frac{\sigma_e n_e(0) c}{H_0} \frac{1}{3q_0^2} \left\{ (3q_0 + q_0 z - 1)(1 + 2q_0 z)^{3/2} - (3q_0 - 1) \right\} ; q_0 \neq 0$$

$$= \frac{\sigma_e n_e(0) c}{H_0} \frac{1}{2} (1+z)^2 ; q_0 = 0$$

2) Power law spectrum  $\mathcal{F}(v, z) = c \left( \frac{v}{v_0} \right)^{-\alpha}$  ;  $\alpha$  = spectral index

3)  $\phi_i$  a stepfunction

$$\phi_i(v, c) = \begin{cases} 0 & v < v_1 \\ 1 & v_1 \leq v \leq v_2 \\ 0 & v > v_2 \end{cases}$$

Consider the integral

$$\int_{v_1}^{v_2} \phi_i(v, c) \mathcal{F}[v(1+z), z] dv = \int_{v_1}^{v_2} c \left( \frac{v(1+z)}{v_0} \right)^{-\alpha} dv$$

$$= (1+z)^{-\alpha} \frac{c}{(1-\alpha)v_0^{-\alpha}} (v_2^{1-\alpha} - v_1^{1-\alpha}), \alpha \neq 1$$

$$\therefore \Delta M_i = -2.5 \log (1+z)^{-\alpha} + \frac{2.5}{\ln 10} p(z) - 2.5 \log \frac{c (v_2^{1-\alpha} - v_1^{1-\alpha})}{(1-\alpha) v_0^{-\alpha}}$$

or

$$\Delta M_i = 2.5 \alpha \log(1+z) + 1.086 p(z) + \Delta M_{in}$$

$$\text{where } \Delta M_{in} = -2.5 \log \frac{c (v_2^{1-\alpha} - v_1^{1-\alpha})}{(1-\alpha) v_0^{-\alpha}}$$

(29)

Monochromatic case: Measure the apparent magnitude in a narrow wavelength interval  $\Delta v$  around  $v$  and make the following approximations:

### 3. Numerical Methods

#### 3.1. The Problem

In the absence of point-spread - the "idealised" map - both the forward and the inverse map can be calculated without any numerical approximation and is straight forward. In the presence of point-spread, the brightness profile is a 2-D convolution of the incident flux with a p.s.f. and has to be approximated numerically. In the forward map with point-spread, an implicit equation (section 2.4 eq.23) of the form

$$-2.5 \log \tilde{F}(\beta_{ap}) - \text{const.} = 0$$

is solved for every mapping.

Here

$$\tilde{F}(\beta_{ap}) = \frac{1}{\pi} \int_0^{\beta_{ap}} dy \int_0^{\pi} d\theta y e^{-(y^2/2 + R_{ap}^2/2 - R_{ap} y \cos\theta)} f(y)$$

where

$$\beta_{ap} = R_{ap} A = \frac{r_{ap}}{W} \frac{W}{a}$$

To complete the map, a triple integral has to be evaluated

$$\tilde{g}(\beta_{ap}) = 2\pi \int_0^{\beta_{ap}} \beta \tilde{F}(\beta) d\beta$$

put  $\beta = RA$  and  $\beta_{ap} = R_{ap}A$ , then

$$\tilde{g}(\beta_{ap}) = 2A^2 \int_0^{R_{ap}} dR \int_0^{\infty} dy \int_0^{\pi} d\theta R y e^{-(y^2/2 + R^2/2 - R y \cos\theta)} f(y)$$

To compute the inverse map, an equation (eq.24a) of the form

$$\tilde{G}(\beta_{ap}) + \text{const.} = 0$$

has to be solved for a given mapping, where

$$\tilde{G}(\beta_{op}) \equiv -2.5 \log \frac{\beta_{op}^2 \tilde{F}(\beta_{op})}{\tilde{g}(\beta_{op})/g_{\infty}}$$

As an first approximation for  $\beta_{op}$ , a fifth order polynomial has been fitted to the inverse of  $\tilde{G}$  for  $\sigma=0$ . A better approximation for  $\beta_{op}$  is then found by an iterative procedure given in section 3.4. This procedure works well for the map with no point-spread ( $\sigma=0$ ), but often fails to converge for  $\sigma>0$ . The program has to be extended to include a better initial approximation for  $\beta_{op}$  to make the inverse map with point-spread reliable.

A double and triple integration routine (section 3.2 and 3.3) as well as a root-solving routine is thus needed to compute the observational map. It was not easy to make the program efficient: To map a single pair of points, often more than ten double integrals have to be evaluated.

### 3.2. The Integration Procedure

The seeing convolved profile is given by

$$\tilde{F}(R, A) = \frac{1}{\pi} \int_0^{\infty} dy \int_0^{\pi} d\theta y e^{-(y^2/2 + R^2/2 - Ry \cos \theta)} f(Ay)$$

It was found empirically that when  $R \geq 15$ , seeing is unimportant (i.e. the image of a galaxy has apparent diameter roughly 15 times the diameter of a star). No such restriction can be put on A, in fact A may become very large ( $\sim 10^6$ ), so that the shape of the integrand can vary considerably over the range of R and A. No satisfactory analytical expression for an upper bound for the integration over y could be found. It was found by calculation that  $R + 5$  is always a sufficiently large upper bound, but for very large values for A this bound could be a thousand

times larger than the least sufficient upper bound. This can result in very inaccurate results. Instead the integral is calculated in two parts; from zero to a suitable chosen, not too large, upper bound  $y_b$  and from  $y_b$  to infinity. The user may subdivide the interval  $[0, y_b]$  at wish into equally spaced intervals (usually a division in two subintervals suffices). On each subinterval a 16-point Legendre-Gauss quadrature is performed. In case  $y_b$  is not a sufficiently large upper bound to give a sufficiently accurate approximation to the integral, a 16 point quadrature is done over the interval  $[y_b, \infty)$ , which is not further subdivided.

The bound  $y_b$  is found in the following way. Define the function

$$I(y, R, A) = y e^{-\left(y^2/2 + R^2/2 - Ry + (Ay)^{1/4}\right)}$$

where we take  $\cos(\theta)=1$  and  $f(\beta) = e^{-|\beta|^{1/4}}$ , the de Vaucouleurs profile for ellipticals. The function  $I$  has a maximum when

$$\frac{\partial I}{\partial y} = 0 \Rightarrow 1 - y^2 + Ry - \frac{1}{4} (Ay)^{1/4} = 0 ;$$

define the function SLOPE by

$$\text{SLOPE}(Y) = 1 - y^2 + Ry - \frac{1}{4} (Ay)^{1/4} ,$$

indicating whether the slope of the tangent to  $I$  in  $y$  is negative, zero or positive.

There are two extreme cases:

A)  $R \gg A$

Approximate  $I$  by  $I(y, R)$  given by

$$I(y, R) = y e^{-\left(y^2/2 + R^2/2 - Ry\right)}$$

with a maximum  $y_1$  for  $y$  satisfying

$$1 - y^2 + yR = 0 .$$

$$\therefore y_1 = R/2 + \sqrt{R^2/4 + 1} .$$

B)  $R \ll A$

Approximate  $I$  by  $I(y, A)$  given by

$$I(y, A) = y e^{-(Ay)^{1/4}}$$

with a maximum  $y_2$  for  $y$  satisfying

$$1 - \frac{1}{4} (yA)^{1/4} = 0 .$$

$$\therefore y_2 = \frac{256}{A} .$$

An upper bound  $y_b$  was chosen in each of both cases such that the integrand drops a factor of  $\sim 100$  from its maximum value

$$\text{In case A : } y_{b_1} = R + 3 .$$

$$\text{In case B : } y_{b_2} = 40\,000/A .$$

The smaller of  $y_{b_1}$  and  $y_{b_2}$  is selected

$$y_m = \min \{ y_{b_1} ; y_{b_2} \}$$

and if  $\text{SLOPE}(Y) < 0$ , this value is chosen as  $y_b$ .

The same procedure is followed for the Abell-Mihalas profile where it is found that

$$y_{b_1} = R + 3 \quad \text{and} \quad y_{b_2} = 400/A .$$

### 3.3. The Integration Routines

The double and triple integration are both done with a Legendre-Gauss Quadrature (16-point). The 16-point quadrature is accurate for all polynomials with order up to 31 ( $2 \times 16 - 1$ ). The results were more accurate by an order of magnitude compared to a 5-point quadrature (used earlier).

The following is taken from [Hildebrand 1974]. Another useful reference is [Conte 1965].

n-point Legendre-Gauss Quadrature

$$\int_{-1}^1 f(x) dx = \sum_{k=1}^n A_k f(x_k) + E,$$

where

$$A_k = \frac{2}{(n+1) P_{n+1}(x_k) P_n'(x_k)} = \frac{2}{n P_{n-1}(x_k) P_n'(x_k)}.$$

$P_n(x)$  is the n-th Legendre polynomial,  $P_n'(x)$  its first derivative and  $x_k$  its k-th root. E is an error term given by

$$E = \frac{2^{2n+1} (n!)^4}{2n+1 [(2n)!]^3} f^{(2n)}(\xi) ; -1 \leq \xi \leq 1.$$

The general case is given by

$$\int_a^b f(x) dx = \frac{b-a}{2} \int_{-1}^1 f\left(y \frac{b-a}{2} + \frac{b+a}{2}\right) dy,$$

if we make the transformation  $x = y \frac{b-a}{2} + \frac{b+a}{2}$ .

$$\text{and } \int_a^{\infty} f(x) dx = \int_{-1}^1 \frac{2}{(1-y)^2} f\left(\frac{2}{1-y} + a-1\right) dy,$$

if we make the transformation  $x = \frac{2}{1-y} + a-1$ .

Note: 
$$\int_a^{\infty} f(x) dx = 2 \sum_{i=1}^n \frac{A_i}{(1-x_i)^2} f\left(\frac{2}{1-x_i} + a - 1\right)$$

$$= 2 \sum_{i=1}^n \frac{A_i}{(1+x_i)^2} f\left(\frac{2}{1+x_i} + a - 1\right),$$

as the roots of  $P_n$  are symmetric with respect to zero i.e.

$$x_i = -x_{n-i+1}.$$

Integrating over two dimensions it follows that:

$$\int_a^b dx \int_c^d dy f(x,y) = \frac{b-a}{2} \frac{d-c}{2} \sum_{i=1}^n \sum_{j=1}^n A_i A_j f\left(\frac{x_i(b-a) + (b+a)}{2}; \frac{x_j(d-c) + (d+c)}{2}\right),$$

and

$$\int_a^b dx \int_d^{\infty} dy f(x,y) = (b-a) \sum_{i=1}^n \sum_{j=1}^n A_i A_j / (1+x_j)^2 f\left(\frac{x_i(b-a) + (b+a)}{2}; \frac{2}{x_j+1} + d - 1\right).$$

And finally in three dimensions, dividing every interval in  $N$  equal subintervals e.g.  $[x_a; x_b]$  is divided into  $NX$  equal subintervals  $[x_{ah}; x_{bh}]$  with length  $\Delta x = x_{bh} - x_{ah}$ .

$$\int_{z_a}^{z_b} dz \int_{y_a}^{y_b} dy \int_{x_a}^{x_b} dx f(x,y,z) = \frac{\Delta x}{2} \frac{\Delta y}{2} \frac{\Delta z}{2} \sum_{h=1}^{NX} \sum_{i=1}^{NY} \sum_{j=1}^{NZ} \sum_{k=1}^n A_k \sum_{l=1}^n A_l \sum_{m=1}^n A_m \times$$

$$f\left[\frac{\Delta x}{2} x_k + \frac{x_{bh} + x_{ah}}{2}; \frac{\Delta y}{2} x_l + \frac{y_{bi} + y_{ai}}{2}; \frac{\Delta z}{2} x_m + \frac{z_b + z_a}{2}\right],$$

and

$$\int_{z_a}^{z_b} dz \int_{y_b}^{\infty} dy \int_{x_a}^{x_b} dx f(x,y,z) = \frac{x_b - x_a}{2} \frac{z_b - z_a}{2} \sum_{k=1}^n A_k \sum_{l=1}^n \frac{2A_l}{(1+x_l)^2} \sum_{m=1}^n A_m \times$$

$$f\left[\frac{x_b - x_a}{2} x_k + \frac{x_b + x_a}{2}; \frac{2}{1+x_l} + y_b - 1; \frac{z_b - z_a}{2} x_m + \frac{z_b + z_a}{2}\right].$$

TABLE: Weights and Abscissas for 16-point QuadratureA<sub>i</sub> ; weighting coefficients

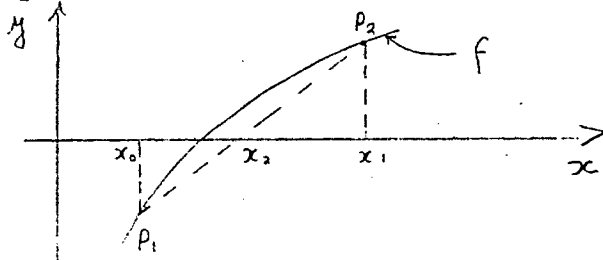
A <sub>1</sub> = A <sub>16</sub>	1.894506105 E-1
A <sub>2</sub> = A <sub>15</sub>	1.826034150 E-1
A <sub>3</sub> = A <sub>14</sub>	1.691565194 E-1
A <sub>4</sub> = A <sub>13</sub>	1.495959888 E-1
A <sub>5</sub> = A <sub>12</sub>	1.246289713 E-1
A <sub>6</sub> = A <sub>11</sub>	9.515851168 E-2
A <sub>7</sub> = A <sub>10</sub>	6.225352394 E-2
A <sub>8</sub> = A <sub>9</sub>	2.715245941 E-2

x<sub>i</sub> ; abscissas

x <sub>1</sub> = -x <sub>16</sub>	9.501250984 E-2
x <sub>2</sub> = -x <sub>15</sub>	2.816035508 E-1
x <sub>3</sub> = -x <sub>14</sub>	4.580167777 E-1
x <sub>4</sub> = -x <sub>13</sub>	6.178762444 E-1
x <sub>5</sub> = -x <sub>12</sub>	7.554044084 E-1
x <sub>6</sub> = -x <sub>11</sub>	8.656312024 E-1
x <sub>7</sub> = -x <sub>10</sub>	9.445750231 E-1
x <sub>8</sub> = -x <sub>9</sub>	9.894009350 E-1

### 3.4. Root Solving Routines

The Secant Method (or "The Rule of False Position") proved to be a reliable and nearly quadratic converging algorithm to solve the implicit equations in the forward and inverse map.



We want to solve  $f(x) = 0$ . The equation of the straight line through  $P_1$  and  $P_2$  is given by

$$y - f(x_1) = \frac{f(x_1) - f(x_0)}{x_1 - x_0} (x - x_1),$$

now if  $y=0$  put  $x=x_2$

$$\therefore x_2 - x_1 = - f(x_1) \frac{x_1 - x_0}{f(x_1) - f(x_0)}$$

or

$$x_2 = x_1 - f(x_1) / \frac{f(x_1) - f(x_0)}{x_1 - x_0}$$

This relation gives the iterative scheme

$$x_{n+1} = x_n - f(x_n) / \frac{f(x_n) - f(x_{n-1})}{x_n - x_{n-1}} \quad \text{for } n=1,2,\dots$$

i.e. given two approximations  $x_{n-1}$  and  $x_n$  to the root of  $f(x) = 0$  a new approximation will be  $x_{n+1}$ .

This method has been implemented as follows:

#### A) Program SECA

A positive solution (root) of  $f(x) = 0$  is required. The program assumes a monotonic increasing function and requires only one initial guess  $x_1$  say.  $x_2$  is then chosen such that the root is

either enclosed by  $x_1$  and  $x_2$ , or  $x_2$  lies closer towards the root than  $x_1$ . The program then starts to iterate. A search for a root is successful if:

- 1) The relative error  $\left( \frac{x_n}{x_{n-1}} - 1 \right) < \epsilon$ .
- 2) The function value  $f(x_n) < 10^{-32}$  for  $n=2,3,4,\dots$

A search is unsuccessful if

- 1) No convergence after 20 iterations .
- 2) If  $f(x_{n+1}) = f(x_n)$  to eight decimal places for  $n=1,2,3,\dots$

In the event that  $x_n < 0$ , then  $x_n = x_{n-1} + x_{n-1}/4$  for  $n=3,4,5,\dots$

#### B) Program SECANT

The same program as in SECA, but a positive root of a monotonic decreasing function is required. In the event that  $x_n < 0$  for any iteration  $n=3,4,5,\dots$ , then  $x_n = x_{n-1}/4$ .

### 3.5. Fitting a Polynomial

A 5th order polynomial has been fitted to the function  $G$  in section 2.4.3 to obtain an first approximation to the inverse map.  $G$  is fitted independently over several intervals.

#### A) De Vaucouleurs profile

Define:

$$\beta_e = \frac{r}{r_e} ; r_e = 3459 a_v \quad (\text{see section 2.5.1})$$

- 1) For  $\beta_e < 0.0005$  an analytical approximation could be used

$$\beta_e(G) = \left( \sqrt{36288 \cdot 10^{0.4G} - 65} - 5 \right)^4$$

2) For  $0.0005 < \beta_e < 0.5$  the polynomial

$$\beta_e(G) = +41.875150 x^5 - 450.97870 x^4 - 873.34070 x^3 + \\ +2816.3958 x^2 + 7315.3342 x + 4282.6471 ,$$

where  $x = G + 10$

3) For  $0.5 < \beta_e < 200$  the polynomial

$$\beta_e(G) = -0.70328080 x^5 + 21.785877 x^4 - 111.20230 x^3 + \\ +3521.4592 x^2 + 7626.6401 x + 4330.0641 .$$

4) For  $\beta_e > 200$  the program returns and prints a message.

B) Abell Mihalas profile

1) For  $0 < \beta < 5$  the polynomial

$$\beta(G) = -28.999653 G^5 - 225.19037 G^4 - 684.14948 G^3 + \\ -1009.9881 G^2 - 715.31806 G - 188.83001 .$$

2) For  $5 < \beta < 895$

$$\beta(G) = -2.6711450 G^5 + 15.395485 G^4 - 9.5759662 G^3 + \\ -14.928260 G^2 + 42.047339 G + 36.346761 .$$

3) For  $\beta > 895$  the program returns and prints a message.

#### 4. Application of the Program

In this section the observational map is calculated for several examples and the results are shown in a series of figures. The computations are done with the program listed in the appendix. The parameters that determine the map are taken from the current literature to make the calculation more realistic. Throughout the calculations a Hubble constant of 50-km-sec-Mpc, a spectral gradient of 0.7 and the De Vaucouleurs brightness law for elliptical galaxies have been used. [see section 2.5]

In figure 1 the object-plane is shown with a grid that is mapped into the image-plane in figures 2 to 7. The x-coordinate is taken to be  $\log r_e$ , where  $r_e$  is the radius in kpc that contains one-half of the light of the De Vaucouleurs brightness model [section 2.5.1]. The y-coordinate is the absolute bolometric magnitude. A typical bright cluster galaxy will have coordinates of  $r_e = 10\text{kpc}$  and  $M_{\text{bol}} = -22$  and is indicated by a dot (e.g. Kormendy gives for M87 in the Virgo cluster  $r_e = 7.3\text{kpc}$  and  $M_{\text{bol}} = -21.64$  [Kormendy 1977]). The crosses mark points that are mapped into the image-plane.

Figure 2 shows the grid from fig.1 at a redshift  $z=0.01$ . The map is taken to be the "ideal" map with no point-spread, no intergalactic absorption and no angular or brightness evolution. A low density FRW-universe is assumed with  $q_0=0.01$  and the detection limit on the surface brightness  $S_L$  is 25 mag per square arc sec. The detection limit  $S_L$  is indicated by a line. The x-coordinate is the  $\log(A_{\text{ap}})$ ,  $A_{\text{ap}}$  the apparent angle in radians. Some values for  $A_{\text{ap}}$  in arc sec are also indicated. The y-coordinate is the apparent magnitude measured through an aperture with an angle of

2Aap. The large distortion of the grid "against" the detection limit is immediately apparent.

In figure 3 the grid is shown at a cosmological redshift  $z=0.2$ . The same parameters are taken for the map as in fig.2. Comparing fig.3 and fig.2 a slight change in shape of the grids can be noted, although the major effect is a displacement of the grid as a whole along the line of constant surface brightness  $S_L$ .

Figure 4 shows the grid mapped with point-spread. all other parameters in the map have the same values ~~than~~<sup>as</sup> in fig.3. Searching the literature [see e.g. R.S.Ellis (1977), King (1978), de Vaucouleurs (1979) or Schweizer (1979)] we found that a seeing disk of diameter 2-3 seconds of arc is fairly common corresponding to a  $\sigma$  of 1 arc sec in the p.s.f. The huge additional distortion can be seen immediately when fig.4 and fig.3 are compared. The general effect is that images are shifted closer to the detection limit  $S_L$ . This shift is large for images with very small or very large  $r_e$  (for a given absolute magnitude). Images ~~with~~ small  $r_e$  are enlarged drastically and the apparent magnitude does not change very much, images with large  $r_e$  are shifted towards and along the line of constant surface brightness  $S_L$  [see fig.7] or fall below the detection limit resulting from the large drop in central surface brightness of the image [see fig.15].

In figure 5 the effect of intergalactic absorption is shown for a FRW universe with  $q_0 = 1.0$ . The cross + marks the grid from fig.1 at redshift  $z=0.2$  for no absorption and the cross x marks it for full absorption  $f=1$  [see section 2.5.2]. Again  $S_L=25$ , no evolution and no pointspread (p.s.) is assumed. For a low density universe with  $q_0=0.01$  the map was nearly identical with and without absorption (this remains true for a redshift of 0.7 !).

In figure 6 the grid in figure 1 is mapped assuming  $S_L=27$  mag

per square arc sec. The remaining parameters of the map are the same as those used in fig.3. Comparing fig.6 and 3 it can be seen that the grid is shifted to the right in fig.6 (as expected). Noteworthy is the change in shape of the grid: images tend to be further away from the brightness limit  $S_L$ , therefore the "distortion" of the grid is less in fig.6 than in fig.3.

In order to show the effect of p.s. more clearly only part of the grid in fig.1 is shown in figure 7 ( $M_{bol}=-21, -23, \text{ and } -25$ ). Triangles mark images mapped without p.s. and circles mark those mapped with p.s. The displacement resulting from p.s. is marked by arrows. All parameters in the map are the same as in fig.3 and 4.

In figures 8 to 10 (redshift, apparent angle) graphs and (redshift, apparent magnitude) graphs are shown for a galaxy with  $r_e=10\text{kpc}$  and  $M_{bol}=-22$ . The detection limit  $S_L$  is assumed to be 25 mag per square arc sec. In figure 8 the effect of galactic evolution is shown. The radial evolution is taken to be  $r_e(z)=r_e(1+z)^{p_1}$  and the central surface brightness is kept constant. The magnitude evolution is taken to be an evolution of the central surface brightness  $B_0(z)=B_0(1+z)^{p_2}$  [see the end of section 2.3.4]. A low density universe with  $q_0=0.01$ , no p.s. and no absorption is assumed.  $\log cz$  is drawn against  $\log A_{ap}$  or  $m_{-ap}$  where  $c$  is the speed of light.

Even more drastic is the change of the limiting redshift (the max redshift for which the galaxy remains detectible) if we introduce p.s. shown in figure 9. As labelled in the fig. the curves are drawn for no p.s. and a point spread of  $\sigma = 1''$ . In both cases the curves for full absorption and for no absorption are shown for a universe with  $q_0=1$ . Notice that the limiting redshift is reached much more suddenly if the map is done with p.s. than without, the curves flatten rather abruptly, as the central region

of the p.s. profile is flat [see fig.15].

In figure 10 curves with different values for  $q_0$  are shown as marked in the fig. ( $q_0=0.02$  and  $1.0$ ). Again the curves are shown with and without p.s. As in fig.9 the p.s. effect is dominant and makes it very difficult to distinguish curves with different values for  $q_0$ . The limiting redshift is the same for curves with different  $q_0$  but no p.s. This is not so if the map is done with p.s., as the limiting redshift is reached much earlier.

In figure 11 the image plane is shown with several observational limits. Firstly the detection limit on the surface brightness  $S_L$  is shown, then the limits  $m-ap=23$  and  $A-ap=1$  arc sec are drawn, being approximately the magnitude limit and the limit of resolution for the Anglo Australian Sky Survey. Finally a magnitude limit of  $A-ap=0.1$  arc sec are taken to represent the observational limits of the Space Telescope [Longair (1979)]. The observable region is in each case the region below the brightness limit  $S_L$ , below the magnitude limit, and to the right of the limit of resolution. These limits are mapped into the object plane in fig's 12, 13 and 14.

Figure 12 shows both, the limit for the sky survey and for the space telescope at a redshift of  $z=0.05$ . No point spread, no evolution and no absorption and  $q_0=0.01$  are assumed. The observational region is above the curves showing the magnitude limit, brightness limit and limit of resolution. Clearly the magnitude limit is not important in both cases, and instead the resolution limit and the surface brightness limit determine the area in the object plane that can be observed. The line parallel to the brightness limit is a line of constant surface brightness of  $14.8$  mag per square arc sec and corresponds to the average central surface brightness for bright elliptical galaxies [Disney

(1976)]. This line may be close to that shown by Halton Arp in fig.3 [Arp (1965)].

In figure 13 the limits are shown again for the sky survey at redshift  $z=0.05$  and  $z=0.2$ . The observable region shifts towards the top of the figure as the redshift increases. The same is done in figure 14 for the limits for the space telescope.

In figure 15 the brightness profiles for a galaxy with  $r_e=10\text{kpc}$  is shown for different redshifts (corresponding to different  $\sigma$  in the p.s.f. as the seeing disk increases relatively to the image of the galaxy). The profiles are drawn for  $z=0.0034, 0.01, 0.05, 0.1, 0.2, 0.4$  and  $0.6$ .

## Figure Captions

Symbols:

$r_e$  = effective radius in de Vaucoulers brightness law

A-AP = apparent angle

M BOL = absolute magnitude

M-AP = apparent magnitude

$z$  = cosmological redshift

$S_L$  = surface brightness limit mag per (arc sec)<sup>2</sup>

$H_0$  = Hubble constant

$q_0$  = deacceleration parameter

$\sigma$  = dispersion in p.s.f. in arc sec

$p_1$  = radial evolution index

$p_2$  = brightness evolution index

$f$  = amount of intergalactic absorbtion

$H_0 = 50 \text{ km-sec}^{-1} \text{-Mpc}^{-1}$ , a spectral gradient of .7 and the De Vaucoulers profile for ellipticals assumed in all calculations.

Figure 1 : Grid in the object-plane.

Figure 2 : Image-plane:  $z = 0.01$ ;  $S_L = 25$ ;  $q_0 = 0.01$ ;  $\sigma = 0$   
 $p_1 = 0$ ,  $p_2 = 0$ ,  $f = 0$ .

Figure 3 : Image-plane:  $z = 0.2$ ;  $S_L = 25$ ;  $q_0 = 0.01$ ;  $\sigma = 0$   
 $p_1 = 0$ ;  $p_2 = 0$ ;  $f = 0$ .

Figure 4 : Image-plane:  $z = 0.2$ ;  $S_L = 25$ ;  $q_0 = 0.01$ ;  $\sigma = 0$  and I"  
 $p_1 = 0$ ;  $p_2 = 0$ ;  $f = 0$ .

Figure 5 : Image-plane:  $z = 0.2$ ;  $S_L = 25$ ;  $q_0 = 1.0$ ;  $\sigma = 0$

$p_1 = 0$ ;  $p_2 = 0$ ;  $f = 0$  and  $1.0$ .

Figure 6 : Image-plane:  $z = 0.2$ ;  $S_L = 27$ ;  $q_0 = 0.01$ ;  $\sigma = 0$

$p_1 = 0$ ;  $p_2 = 0$ ;  $f = 0$ .

Figure 7 : Image-plane:  $z = 0.2$ ;  $S_L = 25$ ;  $q_0 = 0.01$ ;  $\sigma = 0$  and  $1''$

$p_1 = 0$ ;  $p_2 = 0$ ;  $f = 0$ .

Figure 8 : Projection:  $S_L = 25$ ;  $q_0 = 0.01$ ;  $\sigma = 0$

$p_1 = -1, 0, +1$ ;  $p_2 = -1, 0, +1$ ;  $f = 0$ .

Figure 9 : Projection:  $S_L = 25$ ;  $q_0 = 1.0$ ;  $\sigma = 0$  and  $1''$

$p_1 = 0$ ;  $p_2 = 0$ ;  $f = 0$  and  $1.0$ .

Figure 10: Projection:  $S_L = 25$ ;  $q_0 = 0.02$  and  $1.0$ ;  $\sigma = 0$  and  $1''$

$p_1 = 0$ ;  $p_2 = 0$ ;  $f = 0$ .

Figure 11: Image-plane with Observational Limits.

Figure 12: Object-plane, Limits:  $z = 0.05$ ;  $S_L = 25$ ;  $q_0 = 0.01$ ;

$\sigma = 0$ ;  $p_1 = 0$ ;  $p_2 = 0$ ;  $f = 0$ .

Figure 13: Object-plane, Limits:  $z = 0.05$  and  $0.2$  "

Figure 14: Object-plane, Limits:  $z = 0.05$  and  $0.2$  "

Figure 15: Brightness profiles convoluted with a p.s.f

Figure 1

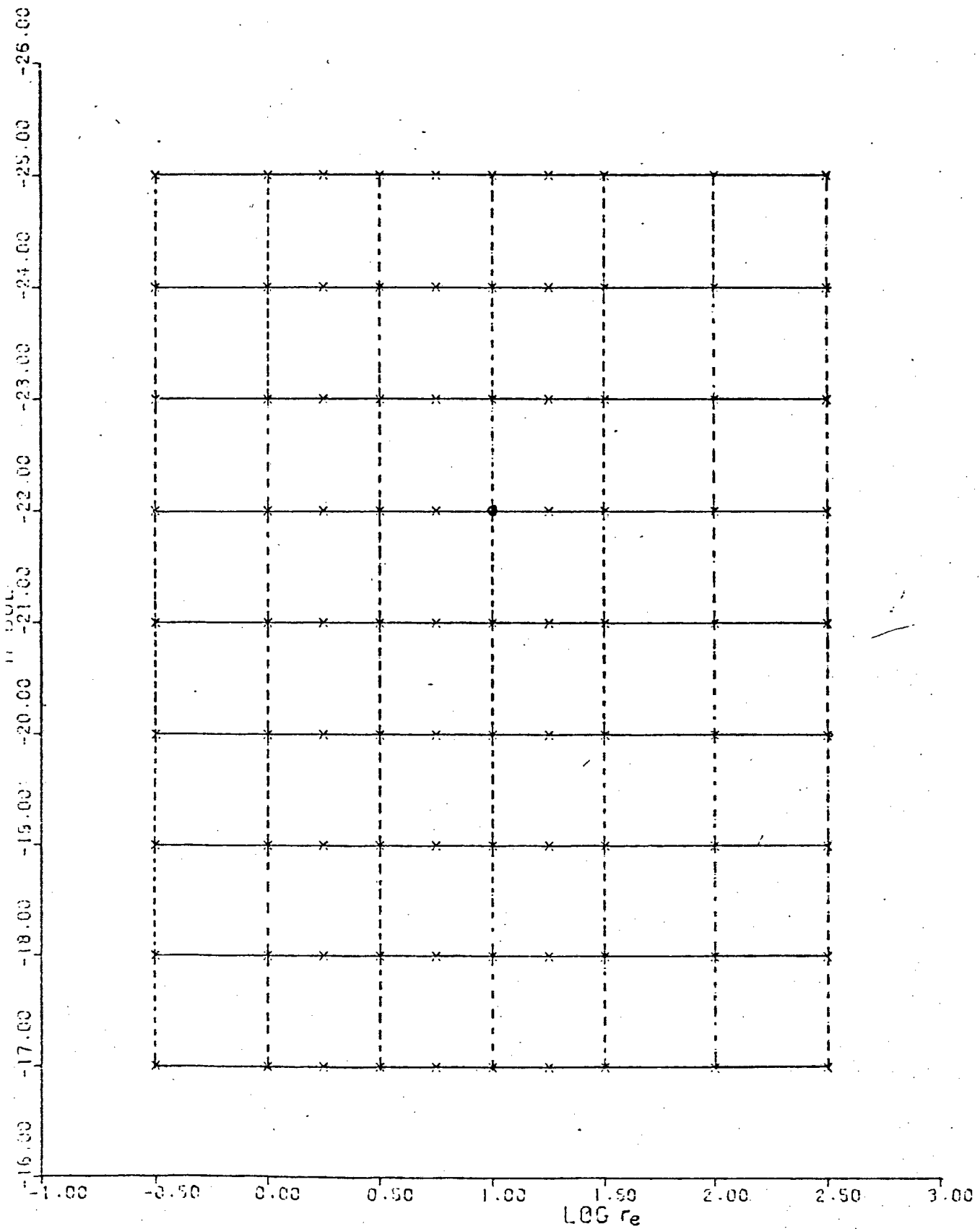


Figure 2

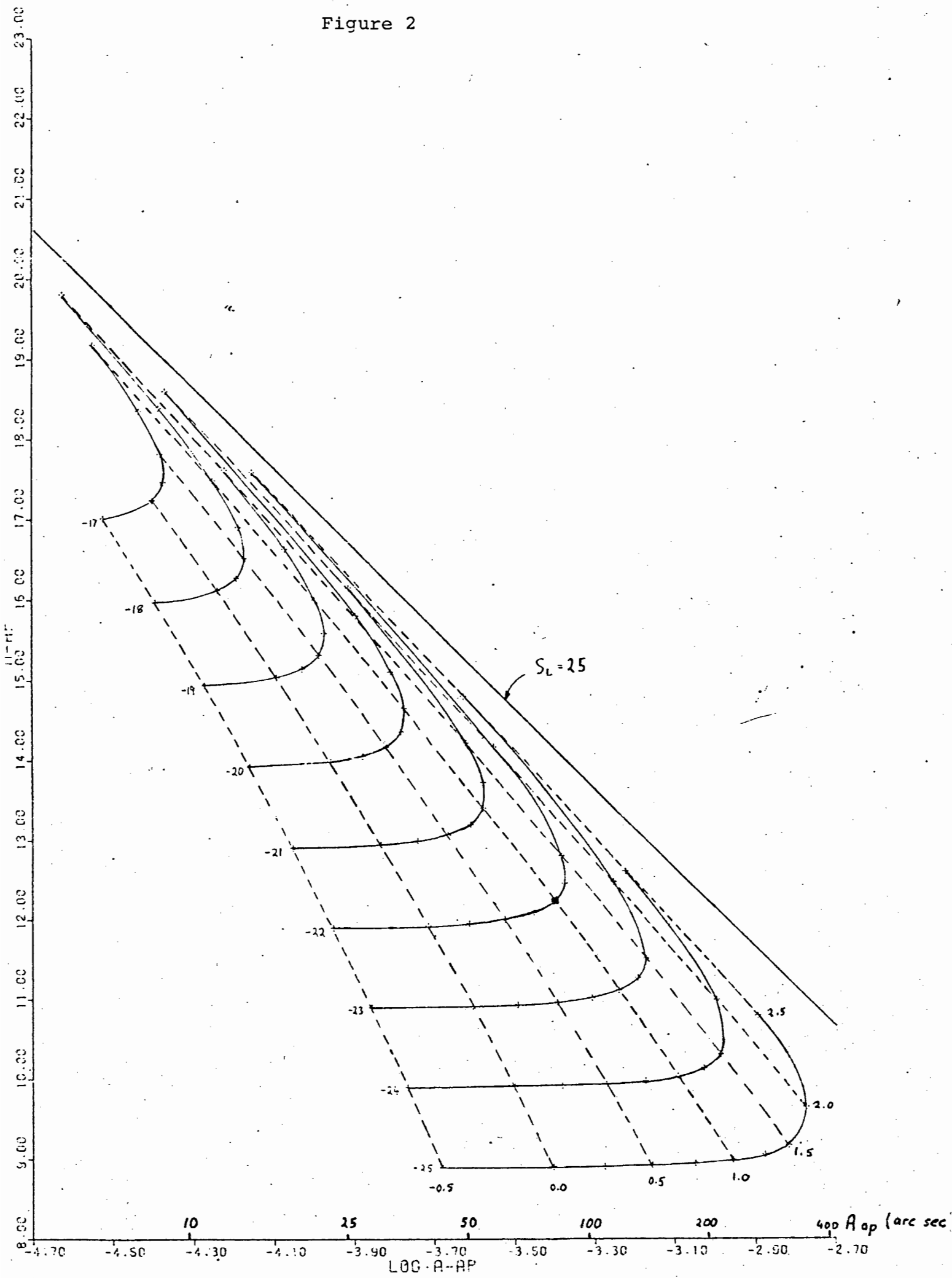


Figure 3

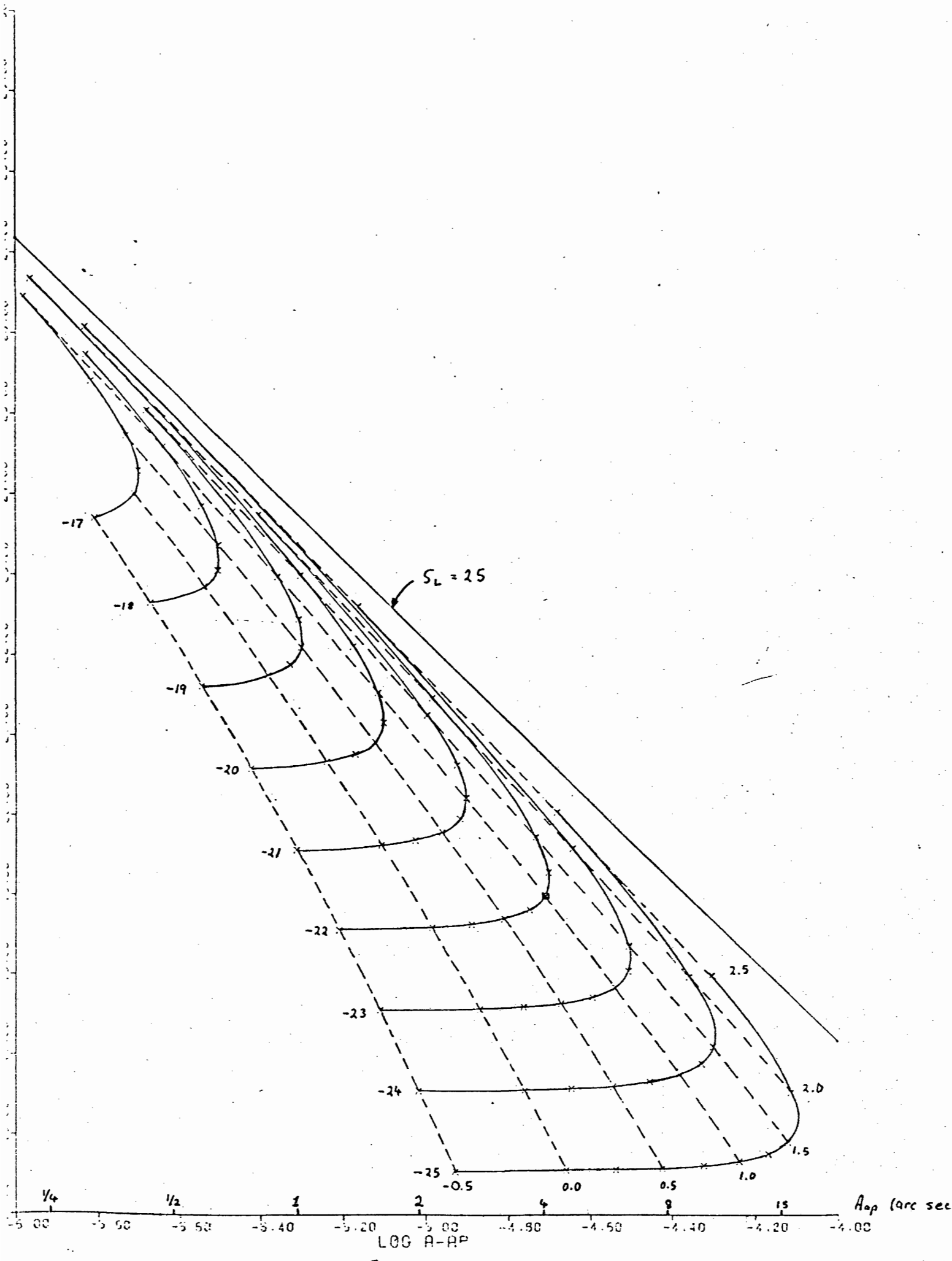


Figure 4

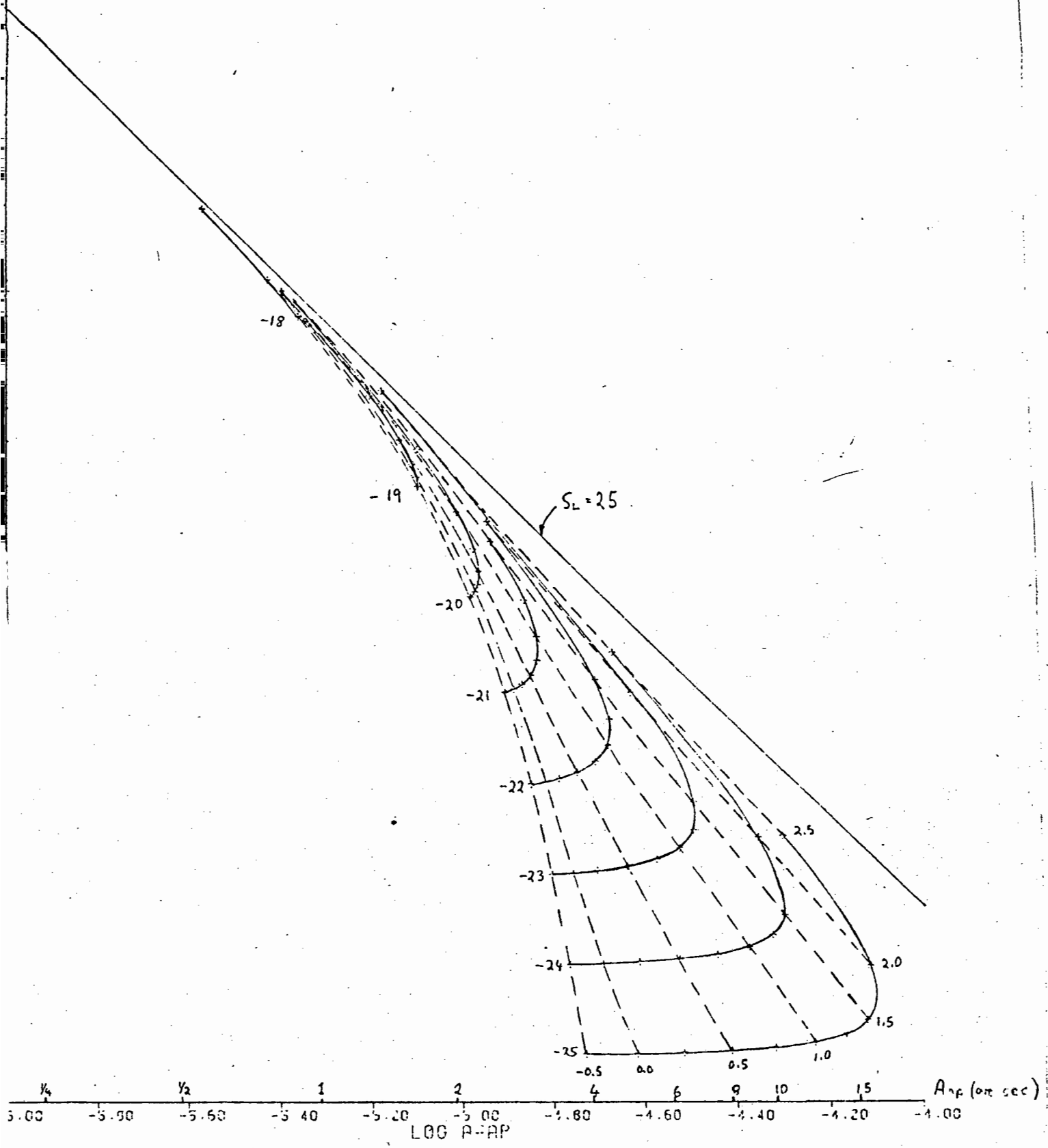


Figure 5

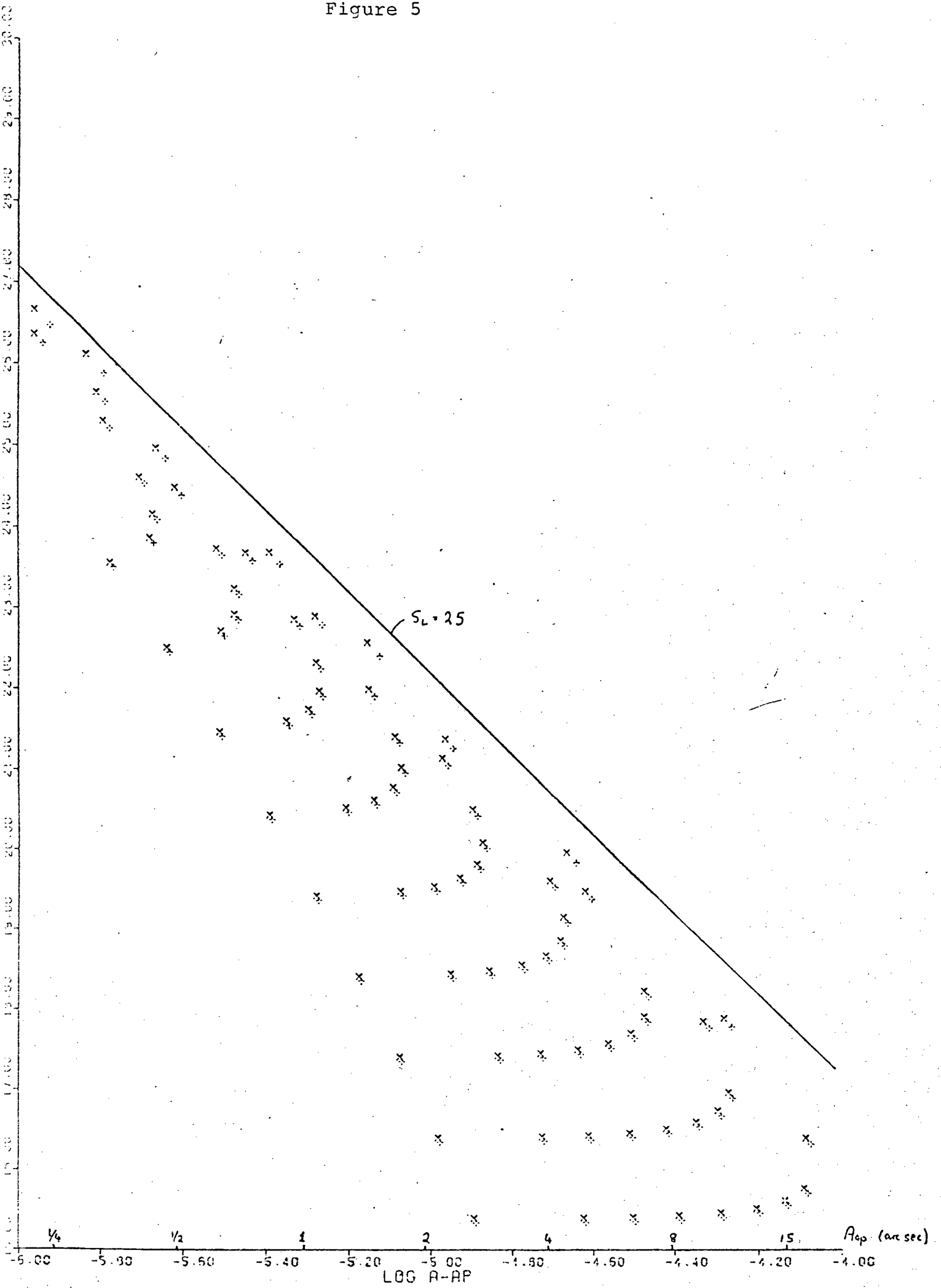


Figure 6

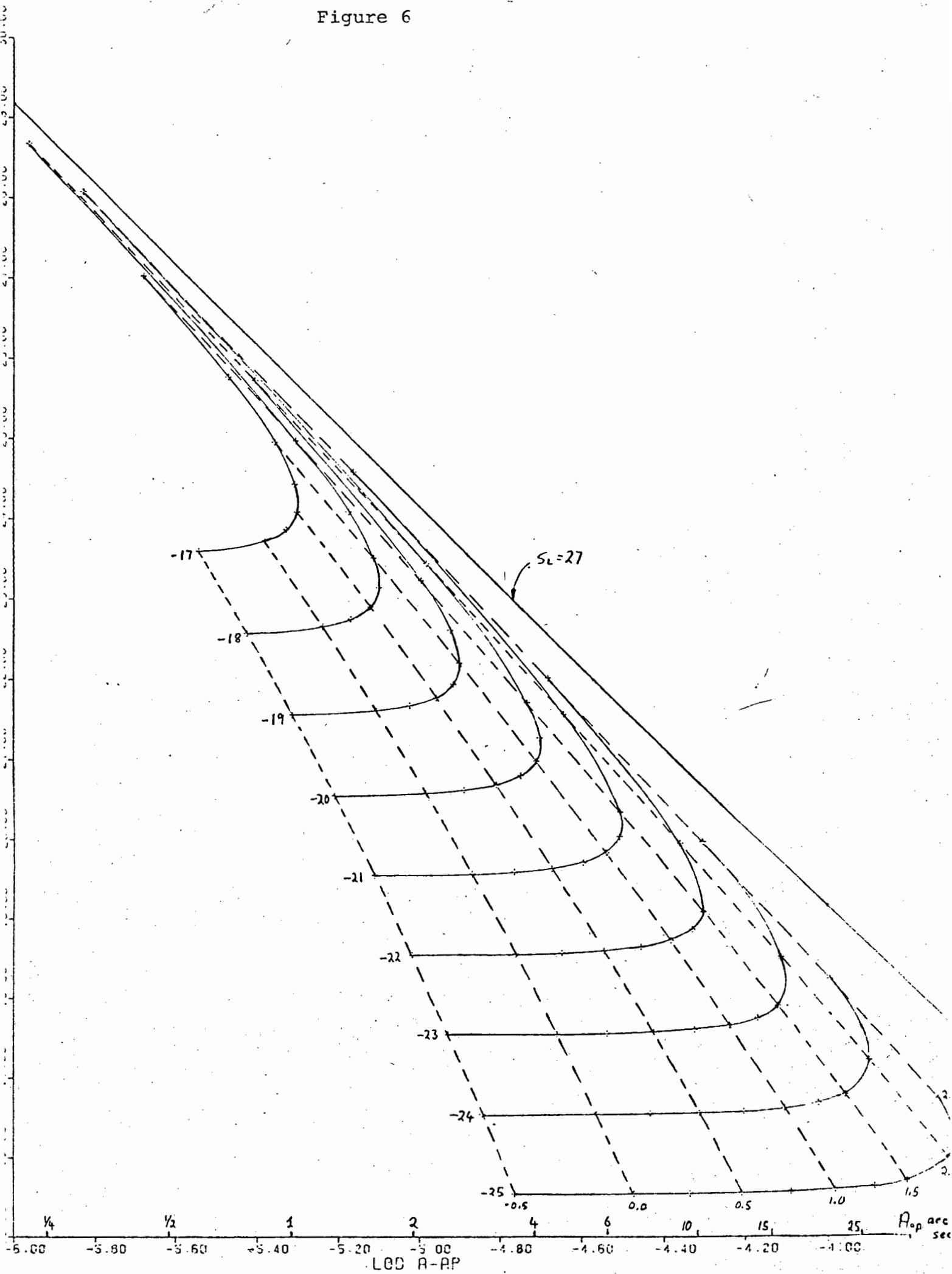


Figure 7

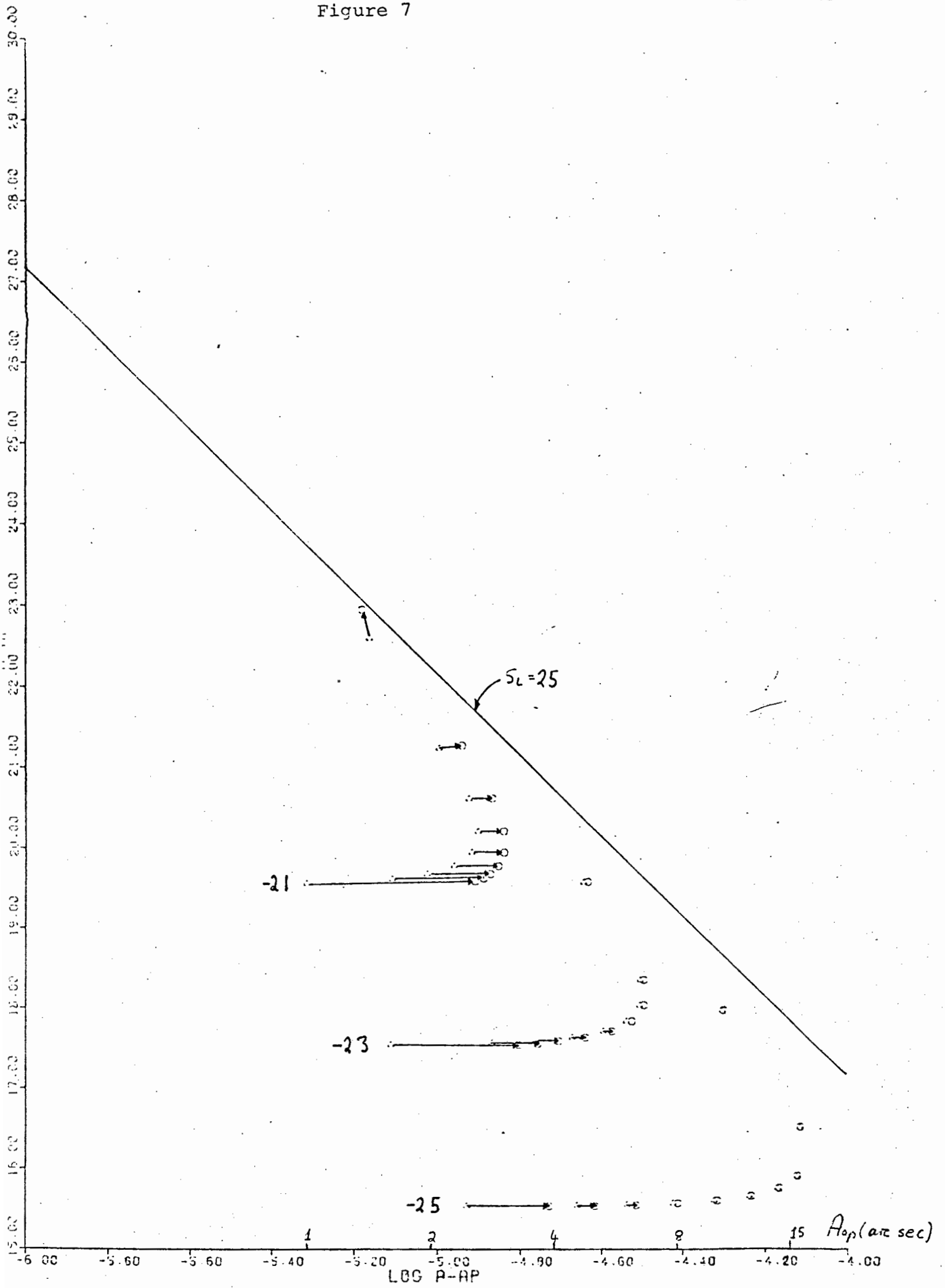


Figure 8

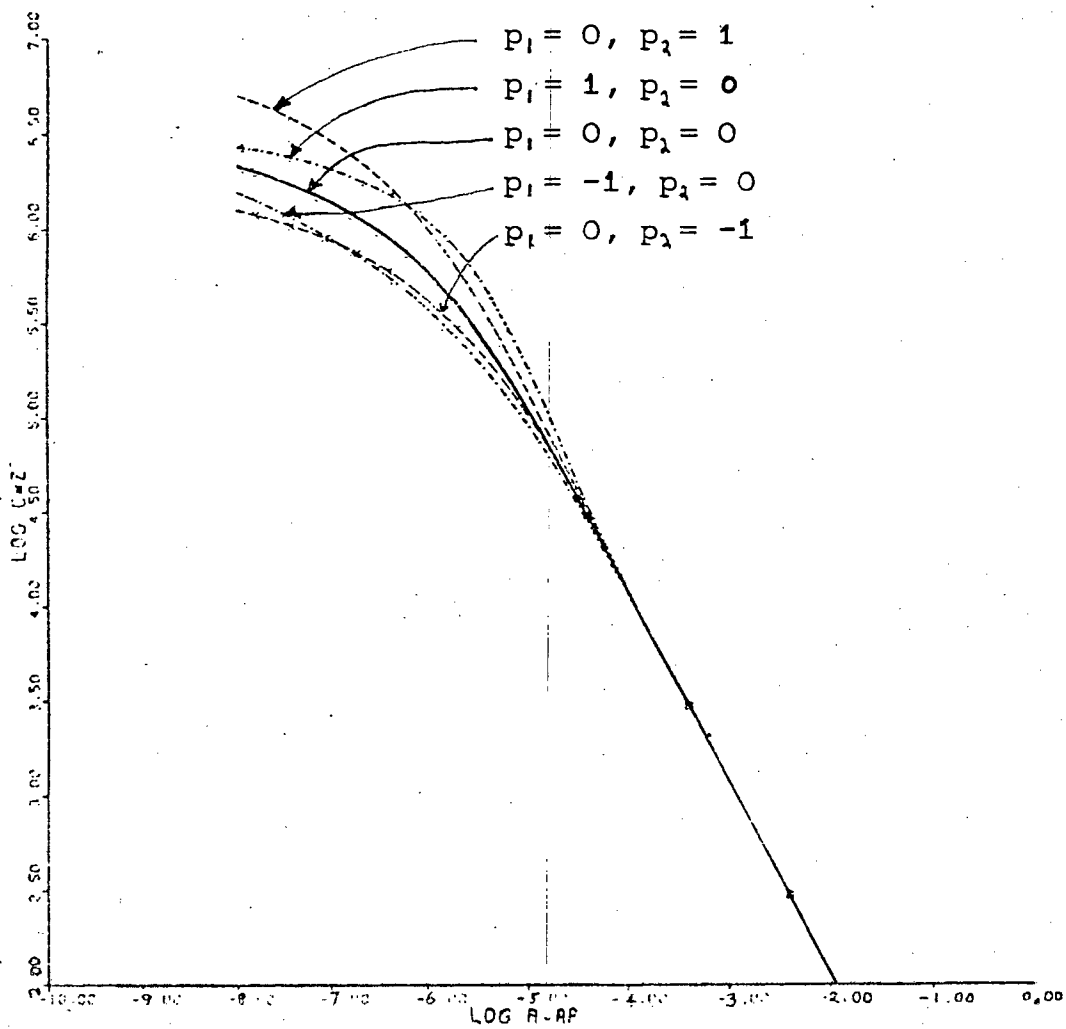
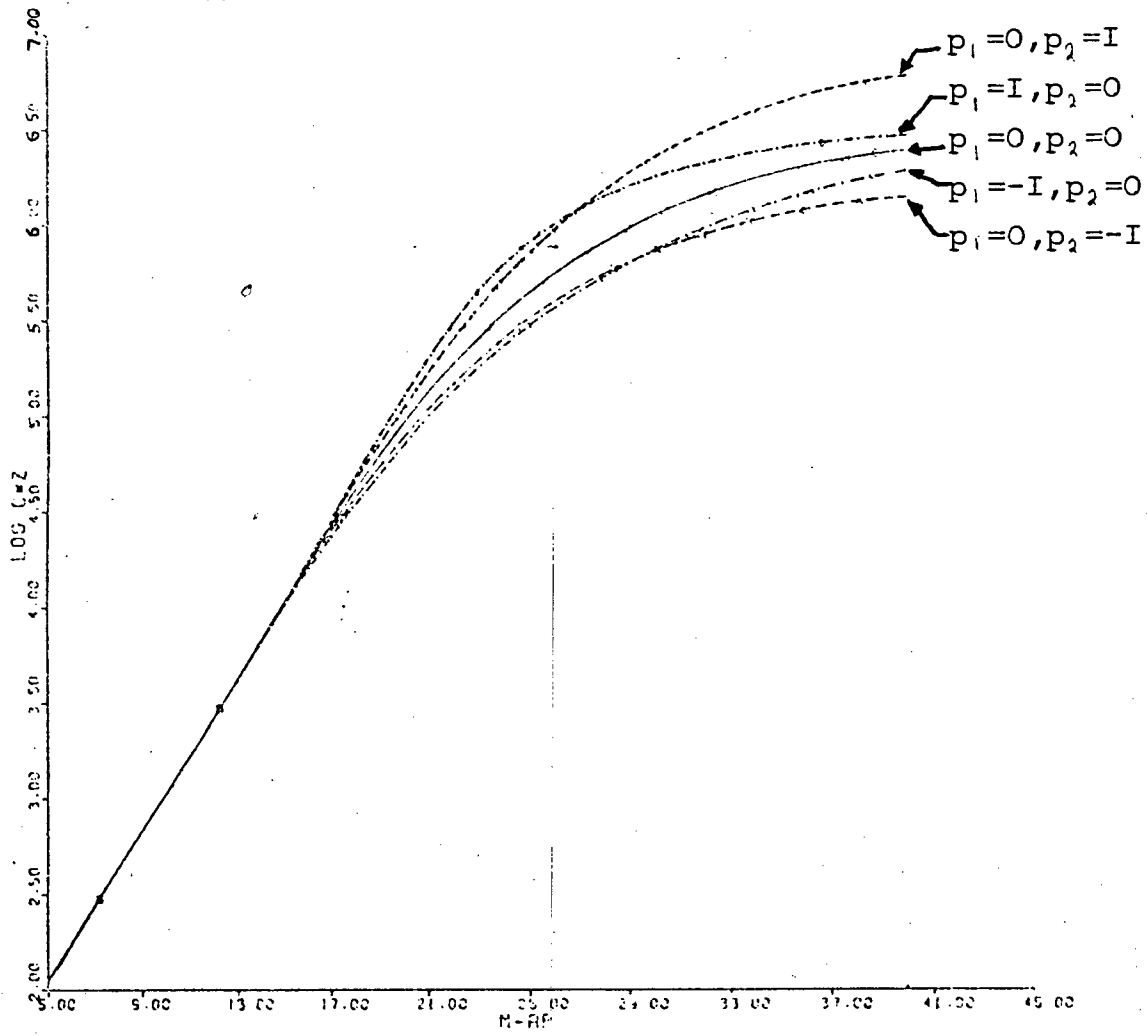


Figure 9

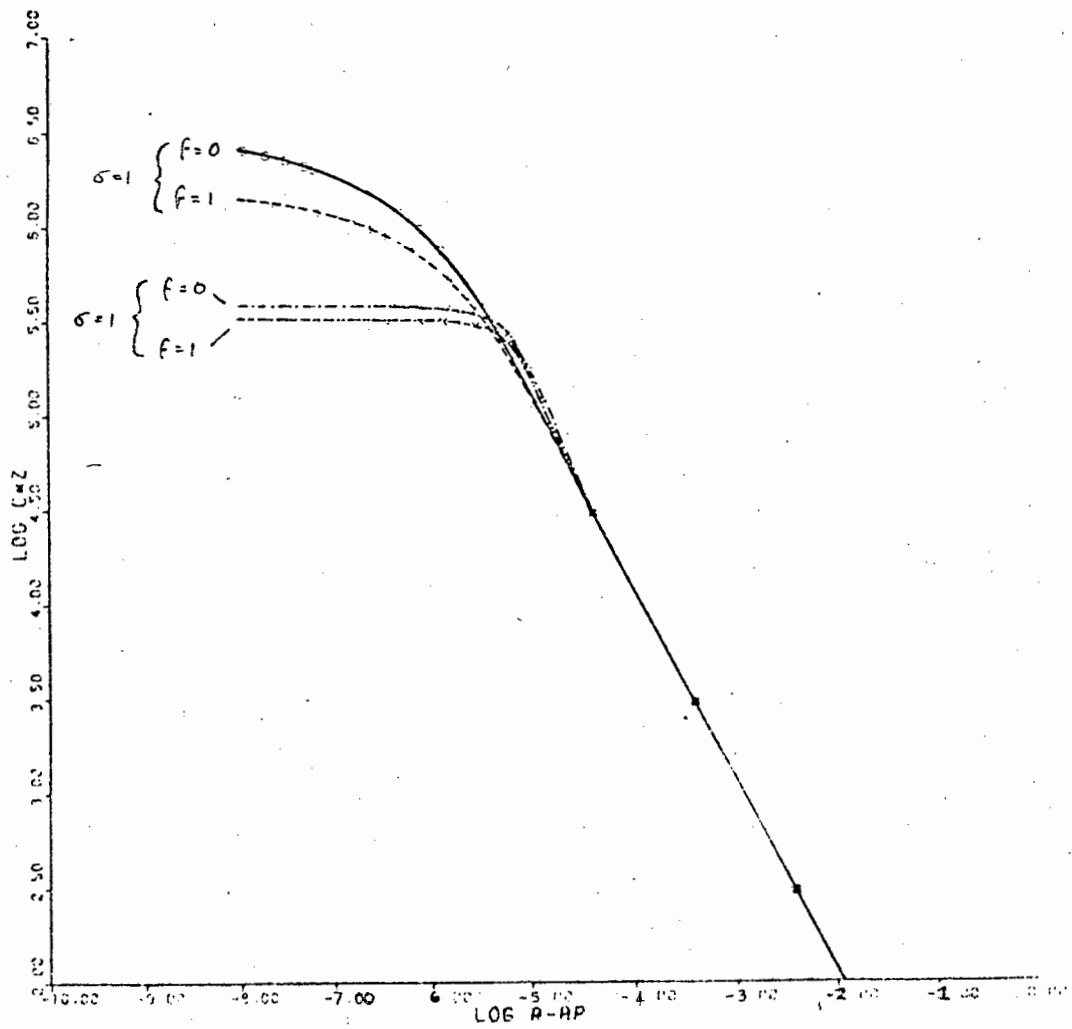
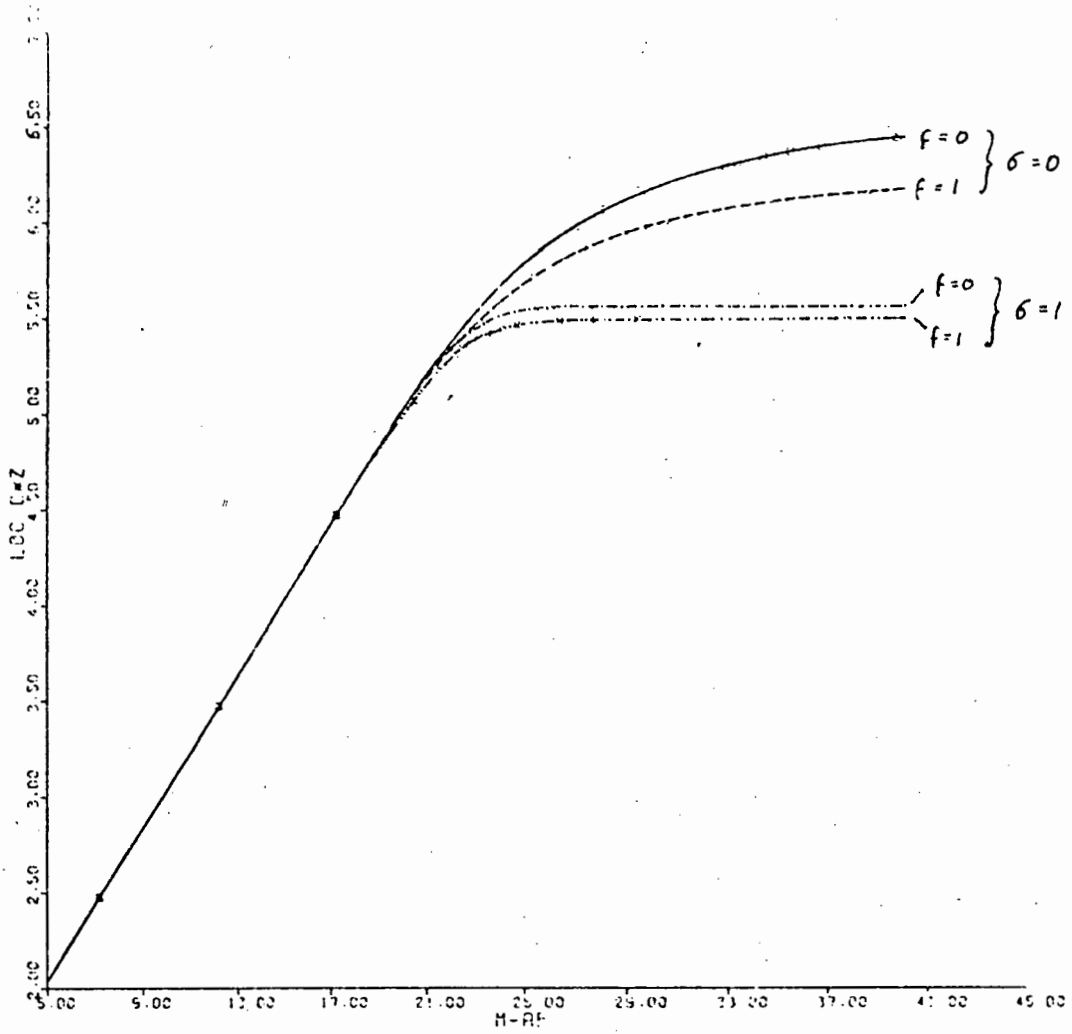


Figure 10

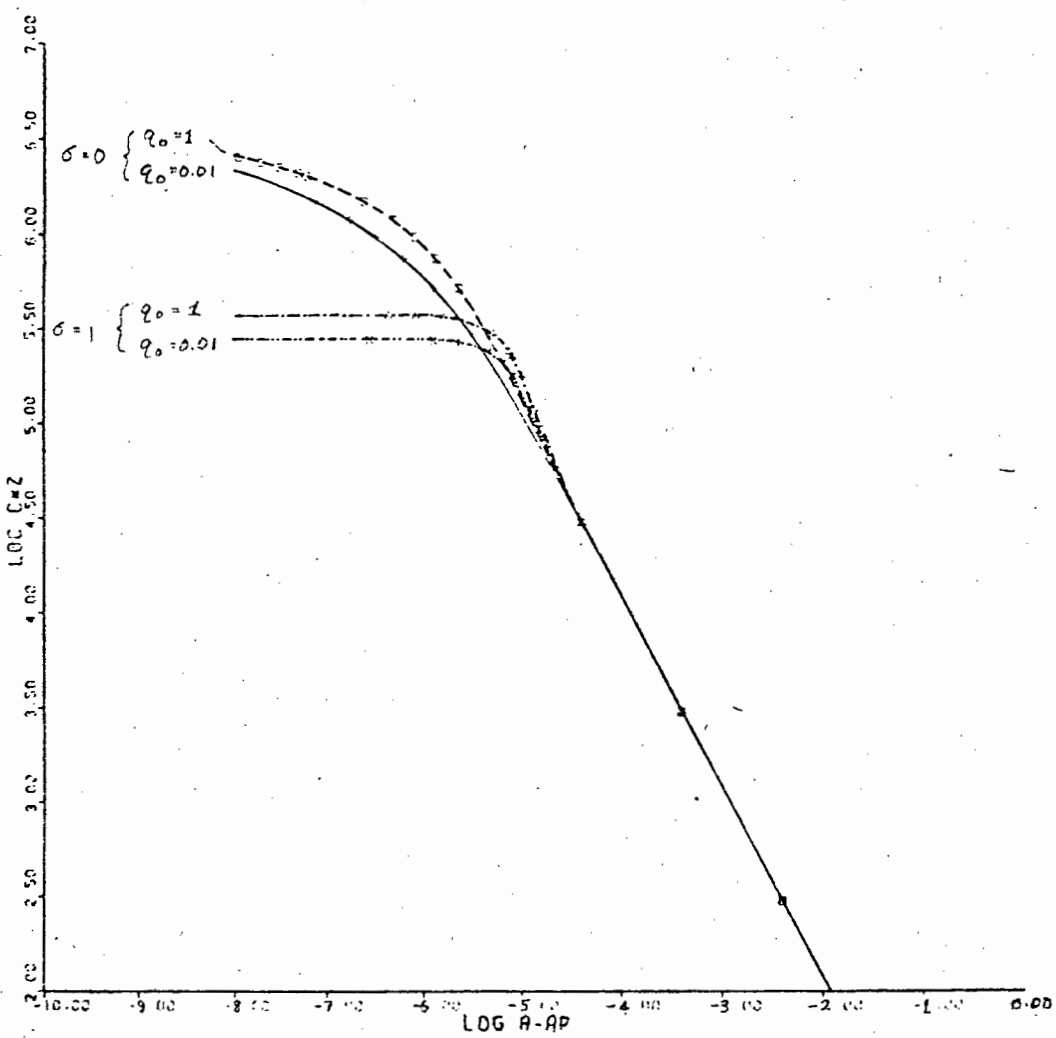
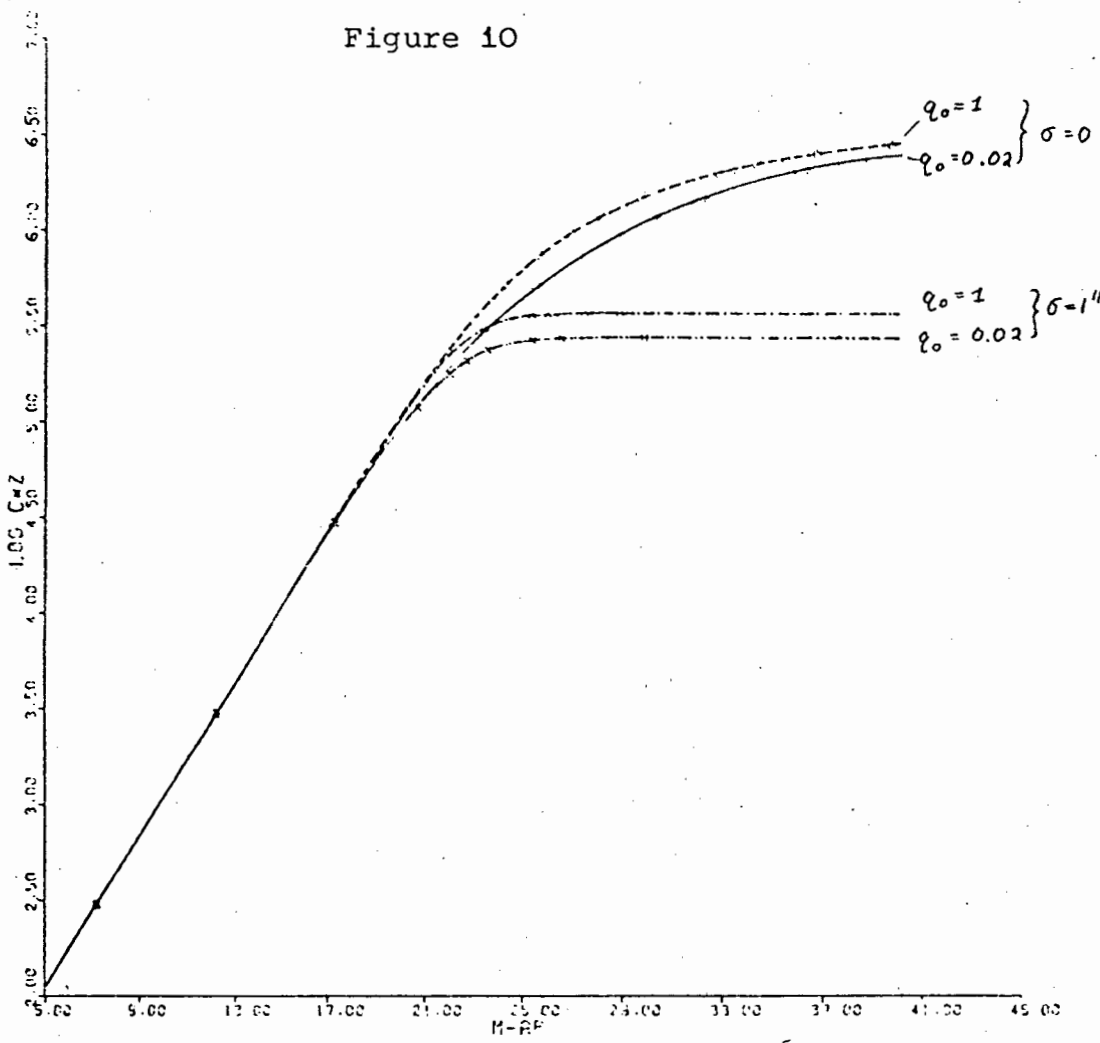


Figure 11

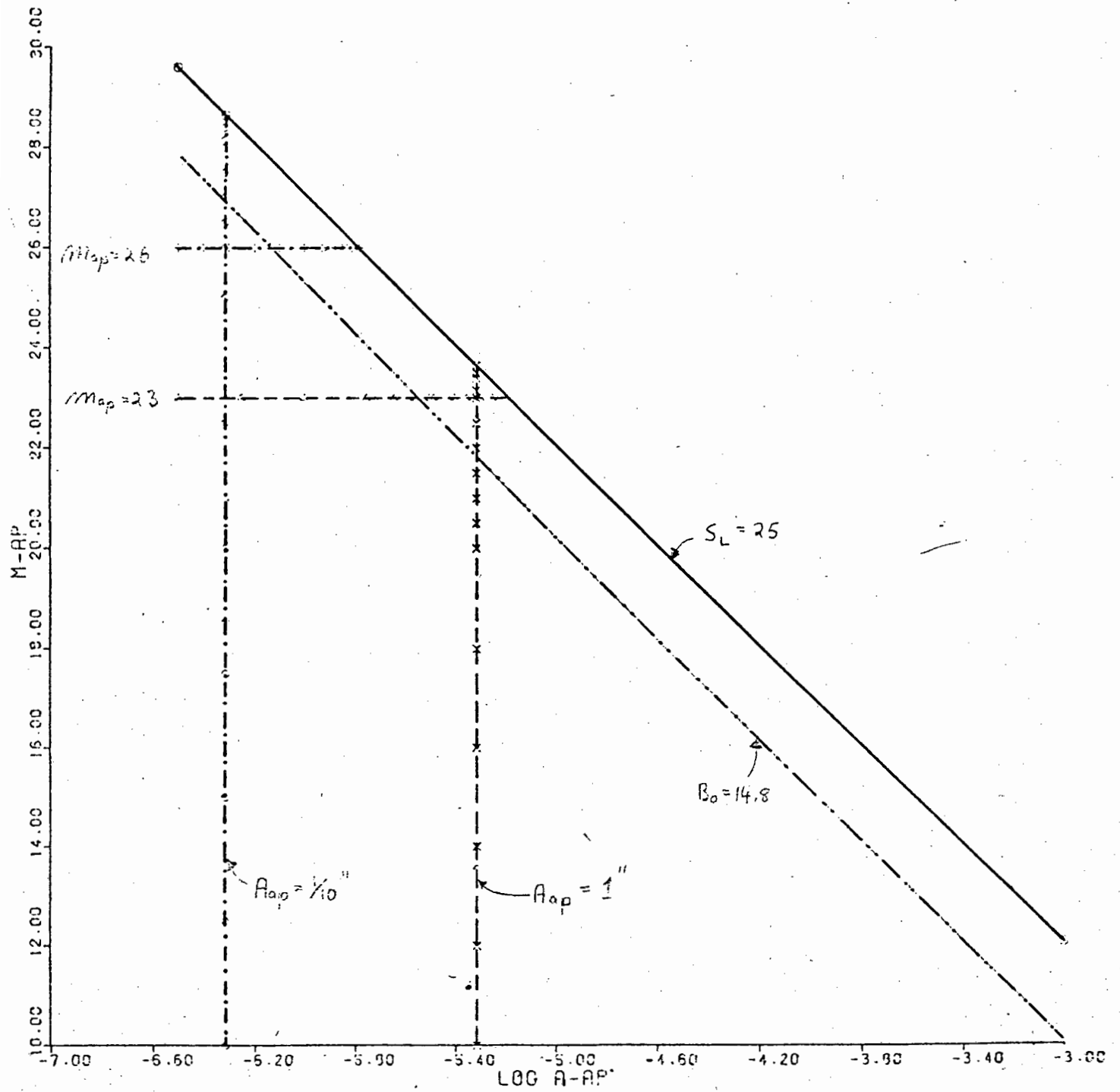


Figure 12

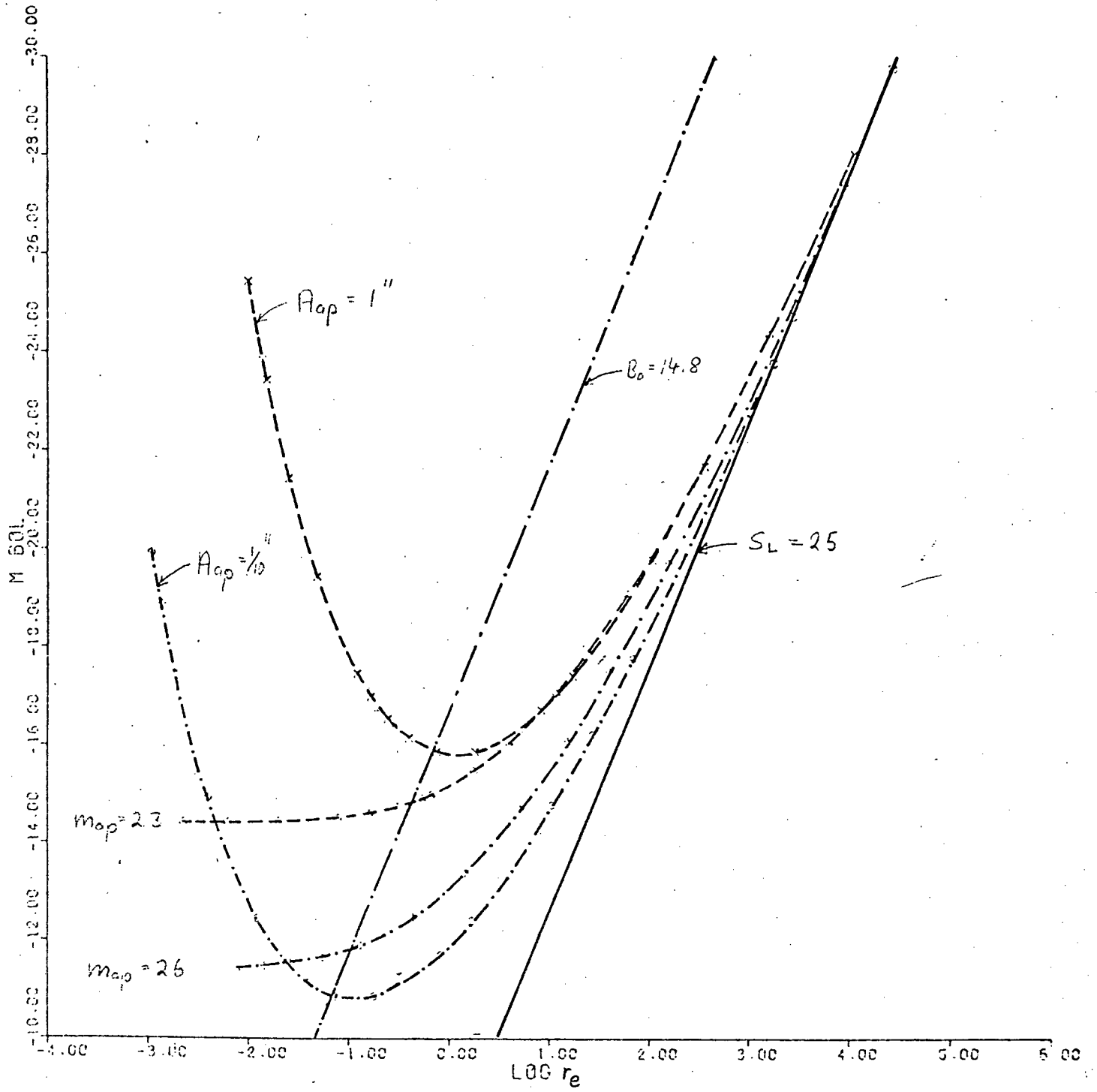


Figure 13

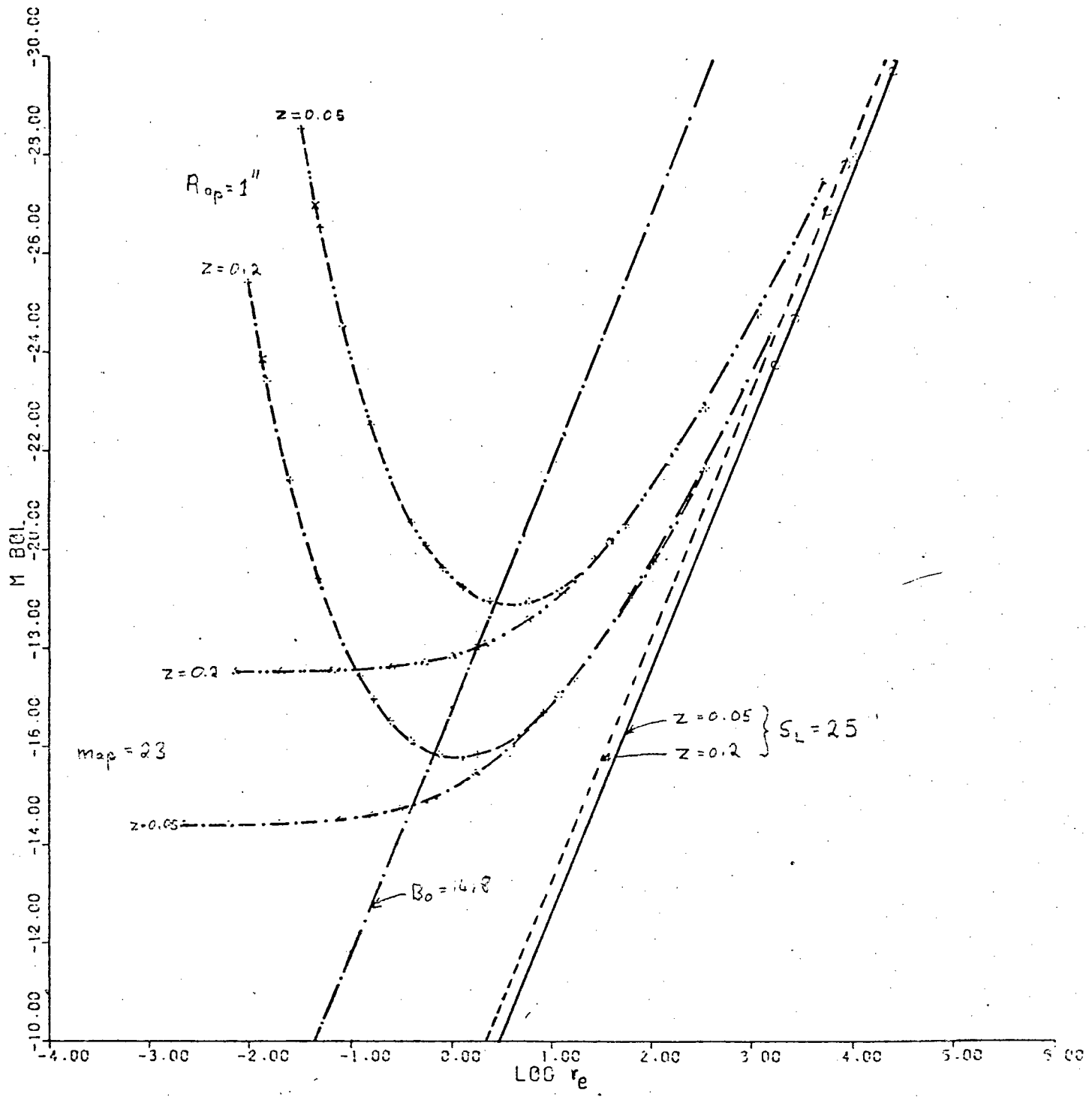
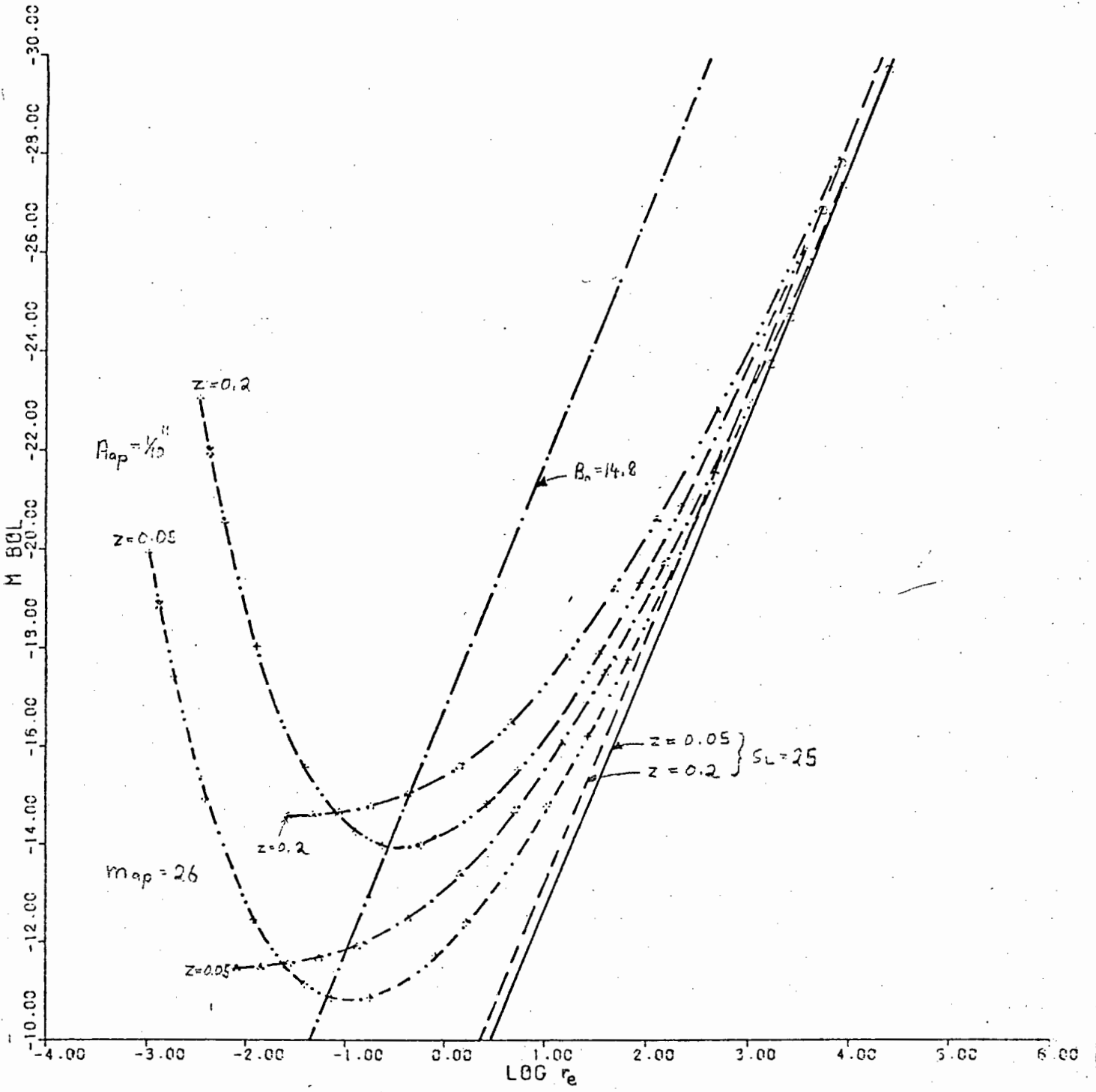


Figure 14



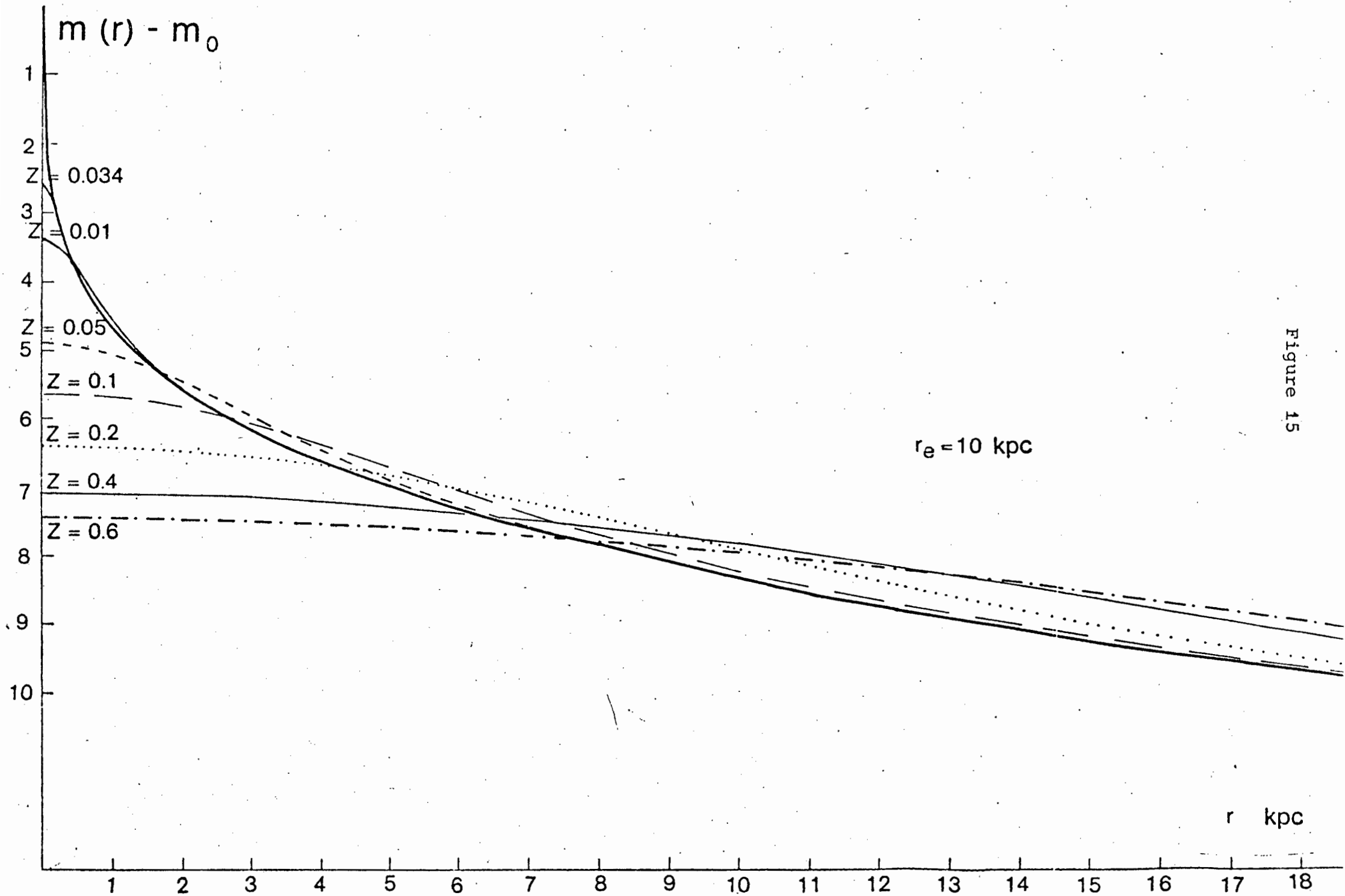


Figure 15

## 5. Conclusion

A simplified theory of observation has been given. The main purpose is to demonstrate an approach to analysing galactic observations without the use of 'corrections' and to showing qualitatively the effect of change of various cosmological and astrophysical quantities on the observational map. For comparison with actual observations the observational method may be changed to include a wider class of objects and a more complex map. Several suggestions can be made:

1) The objects are considered to be spherical. When ELLIPTICITY is significant we can carry out an analysis similar to that in section 1.2. with  $r = [x^2/a^2 + y^2/b^2]^{1/2}$  instead of  $r = (x^2 + y^2)^{1/2}$  where  $a$  is the major and  $b$  the minor axes of the image [see Ellis and Perry 1979].

2) In order to provide for a colour gradient in the source one could write e.g.

$$B_\nu(r, z) = B_{\nu(z)}^a g^a(\nu, z) f^a(r/a_\nu(z)) + B_{\nu(z)}^b g^b(\nu, z) f^b(r/a_\nu(z))$$

for a galaxy model with two different populations of stars.

3) More detailed brightness profiles including profiles for SO and spiral galaxies can be used to model a more realistic galaxy population. Does the function  $f$  evolve with increasing redshift  $z$ ?

4) A more detailed point-spread function may be used. E.g. F.Schweizer gives in his paper: "Effects of Seeing on the Light Distribution in the Cores of Elliptical Galaxies" [Schweizer 1979]:

$$s(r) \begin{cases} = s_0 e^{-(r^2/2\sigma^2)} & \text{for } 0 \leq r \leq 2.25\sigma \\ = s_1 e^{-(\beta r)} & \text{for } 2.25\sigma \leq r \leq 10\sigma \\ = 0 & \text{for } r > 10\sigma \end{cases}$$

This point-spread function accounts for the exponential wings in a star profile. In this paper Schweizer also points out that the seeing convolved profile is not very sensitive to the exponential wings.

5) The calculation of the magnitude correction (K-correction and bolometric correction) is only provisional: Galaxies do not have a power-law spectrum in the visible region of the spectrum, and the spectral response function is seldom close to a step function. For more accurate calculations tables of K-corrections could be used given by Oke and Sandage (1968); Oke (1971) or Pence (1976).

6) Different functional forms for the observer area distance to test the predictions of different cosmological models may be included.

This analysis is developed for observations in the visible light made by e.g. photographic plates. Does the same analysis hold for other wavelengths in the electromagnetic spectrum? Certainly the spectrum and the brightness profile differ for radio galaxies as well as the point-spread function. In different parts of the spectrum the detection limits may differ. In the radiospectrum the angular limit may be of little importance and the most important limits are the surface brightness limit and the magnitude limit.

It would be more realistic to give the detection limits as a probability function, which may include the effects of clustering.

There are many extensions <sup>of</sup> ~~to~~ the observational method given in this thesis, <sup>through which</sup> ~~nevertheless~~ important qualitative results may be obtained. In particular the effect of seeing has not been investigated in e.g. the analysis of number counts or magnitude-redshift diagrams, these will be applications of the observational map.

## 6. Appendix

## A) Short Manual for the Program

A.W.SIEVERS APPLIED MATHEMATICS 26 OCT 1981

```
*****
*
*   USERS MANUAL FOR GALAXY-MAP   *
*
*****
```

FORWARD AND INVERSE MAP WITH AND WITHOUT POINT-SPREAD

NOTE: THE INVERSE MAP WITH POINT-SPREAD IS NOT RELIABLE  
IF THE IMAGE IS JUST ABOVE DETECTION LIMIT

## INTRODUCTION:

-----

AN OBSERVATIONAL MAP OF GALAXYS FROM THE OBJECT-PLANE TO THE IMAGE-PLANE (OR ITS INVERSE) IS CALCULATED. THE OBJECT-PLANE IS LABELED (LOG A OR A,M-BOL) AND THE IMAGE-PLANE (LOG A-AP OR A-AP,M-AP), WHERE:

A = SCALING RADIUS OF THE BRIGHTNESS-PROFILE IN KPC  
M-BOL = BOLOMETRIC ABSOLUTE MAGNITUDE  
A-AP = APPARENT ANGLE OF IMAGE IN SEC OF ARC  
(MEASURED FROM CENTRE OF IMAGE : IF LOG A-AP  
THEN A-AP IN RADIANS)  
M-AP = APPARENT MAGNITUDE

## EFFECTS THAT ARE CONSIDERED ARE:

- A) VALUE OF  $H_0, Q_0$  IN A FRW-UNIVERSE
- B) VALUE OF DETECTION LIMIT FOR SURFACE BRIGHTNESS SL
- C) SCALE AND BRIGHTNESS EVOLUTION
- D) INTERGALACTIC ABSORPTION
- E) TWO DIFFERENT PROFILES
- F) ATMOSPHERIC BLURRING REPRESENTED BY A POINT-SPREAD FUNCTION OF THE GAUSSIAN TYPE

## DETAILS

-----

THE PARAMETERS USED IN THE MAP ARE INITIALISED TO A GALAXY LIKE M 87 AND A MAP WITHOUT POINT-SPREAD(PS), EVOLUTION OR ABSORPTION IS DONE IF NO PARAMETER IS CHANGED. THE INITIALISATION IS PRINTED AT THE BEGINNING OF A RUN. THE PROGRAM THEN PROMPTS FOR AN INSTRUCTION WHICH HAS TO BE TYPED STARTING FROM COLUMN ONE. IT DETERMINES WHICH TASK HAS TO BE DONE (WHICH PART OF THE MAIN PROGRAM IS TO BE EXECUTED) IF REQUIRED THE PROGRAM PROMPTS FOR DATA INPUT. DATA IS TYPED IN FREE FORMAT (ITEMS SEPARATED BY BLANKS OR COMMAS)

## LIST OF INSTRUCTIONS:

-----

SETPR1  
\*\*\*\*\*

H0 Q0 P1 P2 FRAC X10 X20 IN GRAD  
H0 = HUBBLE CONSTANT IN KM/SEC/MPC

Q0 = DEACCELERATION(DECCELERATION) PARAMETER  
 P1 = RADIAL EVOLUTION  
 P2 = BRIGHTNESS EVOLUTION  
 FRAC = FRACTION OF INTERGALACTIC GAS IONISED  
 X10 = SCALING OF A (SEE NOTE 1)  
 X20IN = CORRECTION IN MAGNITUDE DUE TO A FINITE SPECTRAL  
 WINDOW AND INSTRUMENTAL EFFECTS

SETPR2

\*\*\*\*\*

IF SL SIGMA IIN

IF = 1 FOR DE VAUCOULEURS PROFILE FOR ELLIPTICALS

IF = 2 FOR THE ABELL MIHALAS PROFILE

SL = DETECTION LIMIT ON THE SURFACE BRIGHTNESS IN MAG.  
 PER SQUARE ARC.SEC.

SIGMA = DISPERSION IN GAUSSIAN POINT-SPREAD FUNCTION IN SEC OF ARC  
 1 ARC.SEC. = 4.85E-6 RAD

INN = 0 X1=LOG10 A , Y1 = LOG10 A-AP (FORWARD MAP)

IIN = 1 X1= A , Y1 = A-AP ( " )

FOR THE INVERSE MAP X1,X2 AND Y1,Y2 ARE INTERCHANGED

ACURAT

\*\*\*\*\*

XAPMAX EPS IX IY IZ IXD IYD

XAPMAX = MAXIMUM VALUE FOR XAP(R/W) FOR WHICH POINT-SPREAD IS  
 IMPORTANT

EPS = CONVERGENCE CHECK IN SECANT AND SECA

IX,IY,IZ = NO.OF SUBINTERVALS ON THE X-,Y-AND Z-AXIS IN TRIPLE

IXD,IYD = NO.OF SUBINTERVALS ON THE X- AND Y-AXIS IN DOUBLE

INPUT

\*\*\*\*\*

X1 X2 Z NX1 NX2 NZ X1INC X2INC ZINC

X1 = A(OR A-AP) FOR IIN = 1 (INITIAL VALUES FOR X1)  
 = LOG10(A OR A-AP) FOR IIN = 0

X2 = M-BOL OR M-AP

Z = INITIAL VALUE FOR THE REDSHIFT

NX1 = NO OF X1 VALUES TO BE MAPPED (LIMITED TO 98)

NX2 = SAME FOR X2

NZ = SAME FOR Z

X1INC = INCREMENT IN X1

X2INC = " IN X2

ZINC = " IN Z

MAP FORWARD MAP IS DONE (SEE NOTE 2)

\*\*\*

IMAP INVERSE MAP IS DONE ( " )

\*\*\*\*

TABLE TABLE OF RESULTS IS PRINTED

\*\*\*\*\*

NEWARR COUNTER N1 SET TO ZERO (SEE NOTE 2)

\*\*\*\*\*

STDATA N1 ELEMENTS OF OUTPUT ARRAYS AND VALUES OF PARAMETERS

\*\*\*\*\*

WRITTEN TO FILE (UNIT 11) (SEE NOTE 4)

RDATA

SAME BUT ITEMS READ FROM FILE

\*\*\*\*\*

## PSTART

\*\*\*\*\*

TITLE FOR X-AXIS

TITLE FOR Y-AXIS

TITLE FOR GRAPH

NXTI NYTI NTI FIX LAX FIY LAY FACT

NXTI, NYTI, NTI = NO OF CHARACTERS IN TITLES FOR X-, Y- AND GRAPH

FIX, FIY = VALUE AT FIRST TICK ON X-, Y-AXIS

LAX, LAY = VALUE AT LAST TICK ON X-, Y-AXIS

FACT = RATIO OF DESIRED PLOT TO NORMAL PLOT SIZE

NOTE: TO DO MORE THEN ONE GRAPH CALL PSTART AGAIN.

## PLOT

\*\*\*\*

LTYP INTEQ J

LTYP DETERMINES TYP OF LINE DRAWN

LTYP .GT. 0 POINTS ARE CONNECTED WITH STRAIGHT LINES, FOR EVERY LTYP'TH POINT A SYMBOL IS DRAWN

LTYP .EQ. 0 SAME BUT NO SYMBOL IS DRAWN

LTYP .LT. 0 ONLY SYMBOL DRAWN AT EVERY LTYP'TH POINT, POINTS NOT CONNECTED

INTEQ = INTEGER EQUIVALENT OF PLOTTING SYMBOL DRAWN (SEE CALCOMP OR GDP INSTRUCTIONS)

J DETERMINES WHICH ARRAYS ARE PLOTTED

J = 1 ARRAYS (Y1, Y2) (SEE NOTE 2+3)

J = 2 ARRAYS (Y1, Z) "

J = 3 ARRAYS (Y2, Z) "

J = 4 ARRAYS (X1, X2) (INPUT ARRAYS)

PROJECT (LOG A-AP OR A-AP, LOG C\*Z) AND (M-AP, LOG C\*Z) ARRAYS

\*\*\*\*\*

ARE PRINTED (NOTE 3)

STOP OR A BLANK LINE PROGRAM TERMINATES

\*\*\*\*

## NOTE 1

-----

THE SCALING RADIUS A IN THE BRIGHTNESS PROFILE IS SCALED BY X10. THE RELATION IS  $A' = X10 * A$ . IF  $X10 = 1$  THE SCALING RADIUS IS THE ONE IN THE PROFILE  $B/B0$  WHERE  $B0 =$  CENTRL SURFACE BRIGHTNESS AND  $B =$  SURFACE BRIGHTNESS AT DISTANCE R FROM CENTRE. X10 IS INITIALISED TO  $X10 = 3459$  SO THAT THE SCALING RADIUS IS THE RADIUS THAT CONTAINS 1/2 OF THE LIGHT OF THE DE VAUCOULEURS MODLE.

## NOTE 2

-----

THE PROGRAM SETS UP ARRAYS X1, X2 AND Z AND STORES THE OUTPUT IN ARRAYS Y1 AND Y2. A COUNTER N1 COUNTS THE NUMBER OF POINTS MAPPED. IT IS INITIALISED TO ZERO AND IS ONLY SET IF ONE OF THE INSTRUCTIONS NEWARR OR RDATA ARE GIVEN. THE OBSERVER-AREA-DISTANCE  $R0(Z)$  AND THE COLOUR-CORRECTION ARE PRINTED FOR EVERY REDSHIFT.

FORWARD MAP:

X1 = LOG A (IIN=0) OR A (IIN=1) A IN KPC

X2 = M-BOL IN MAGNITUDES

Z = Z THE REDSHIFT

Y1 = LOG A-AP(IIN=0,A-AP IN RAD) OR A-AP (IIN=1,IN ARC SEC)  
 Y2 = M-AP IN MAGNITUDES  
 INVERSE MAP: X AND Y ARE INTERCHANGED

## NOTE 3

-----  
 THE REDSHIFT IN ARRAY Z IS REPLACED BY LOG10 C\*Z ,  
 C = SPEED OF LIGHT IN KM PER SECOND

## NOTE 4

-----  
 A DATAFILE HAS TO BE ASSIGNED TO THE RUN. THE PROGRAM CAN  
 READ AND WRITE TO THIS FILE ON UNIT 11. DATA IS WRITTEN TO OR  
 READ FROM AS FOLLOWS:

N1	INVERS			
HQ	Q0	P1	P2	
FRAC	SIGMA	X10	X20IN	
SL	GRAD	IF	IIN	
X1(1)	X2(1)	Z(1)	Y1(1)	Y2(1)
X1(2)	X2(2)	Z(2)	Y1(2)	Y2(2)
*	*	*		

X1(N1) X2(N1) Z(N1) Y1(N1) Y2(N1)  
 RDATA CAN ONLY BE USED IF A DATAFILE IN THIS FORMAT IS ASSIGNED  
 TO THE RUN. N1(AND ALL OTHER PARAMETERS GIVEN ABOVE) IS SET EACH  
 TIME RDATA IS USED.

\*\*\*\*\*

## B) The Program

```

C
C
C          MAIN PROGRAM FOR GALAXY MAP
C          *****
C
C          THIS PROGRAM CALCULATES AN OBSERVATIONAL MAP OF
C          GALAXIES FROM THE "OBJECT-" TO "IMAGE-PLANE"
C          OR THE INVERSE
C          PROGRAM WRITTEN IN FORTRAN(ASCII) LEVEL 9R1
C          AT MOST 98 POINTS CAN BE MAPPED AT ONCE
C          OUTPUT CAN BE PLOTTED ON CALCOMP PLOTTER
C          THE GRAPHICS DISPLAY PACKAGE AT UCT
C          IS USED FOR PLOTTING
C          -----
C
C          DISCRIPTION OF VARIABLES USED:
C
C          H0=HUBBLE PARAMETER IN (KM/SEC/MPC)
C          Q0=DEACCELERATION PARAMETER IN A FRIEDMANN UNIVERSE
C          OBJECT PLANE (X1,X2):
C             X1=A=(SCALING RADIUS) IF IIN=1 , A IN KPC
C             X1=A*LOG10(A)           IF IIN=0 , A IN KPC
C             X2=ABSOLUTE BOLOMETRIC MAGNITUDE=M-BOL
C          IMAGE PLANE (Y1,Y2)
C             Y1=A-AP=APPARENT ANGLE IF IIN=1 , A-AP IN ARC SEC
C             Y1=A*LOG10(A-AP)       IF IIN=0 , A-AP IN RADIANS
C             Y2=M-AP=APPARENT MAGNITUDE
C          P1= RADIAL EVOLUTION INDEX
C          P2= BRIGHTNESS EVOLUTION INDEX
C          FRAC= FRACTION OF INTERSTELLAR GAS IONISED
C          GRAD= SPECTRAL GRADIENT IN POWER LAW SPECTRUM
C          X10= RESCALING OF A
C          X20IN= INSTRUMENTAL PART OF BOLOMETRIC CORRECTION X20
C          SIGMA= DISPERSION IN GAUSSIAN POINT-SPREAD FUNCTION IN ARC-SEC
C          SIGMAD= SIGMA IN RADIANS (1 ARC SEC = 4.8481E-6 RAD)
C          Z= REDSHIFT IN A FRIEDMANN UNIVERSE
C          SL= DETECTION LIMIT ON SURFACE BRIGHTNESS IN (MAG/(ARC SEC)**2)
C          IF= 1 FOR DE VAUCOULEURS PROFILE FOR ELLIPTICALS
C          IF= 2 FOR ABELL MIHALAS PROFILE
C          GINF= PROFILE INTEGRATED UP TO INFINITY
C          NX1,X1INC = NO OF X1-VALUES,INCREMENT IN X1
C          NX2,X2INC = NO OF X2-VALUES,INCREMENT IN X2
C          NZ ,ZINC  = NO OF Z-VALUES,INCREMENT IN Z
C          EPS = ACURACY WITH WHICH ROOT IS FOUND IN SECANT AND SECA
C          IXD,IYD  = NO OF SUBINTERVALS USED IN DOUBLE
C          IX,IY,IZ = NO OF SUBINTERVALS USED IN TRIPEL
C          INVERS = .TRUE.(INVERSE MAP) = .FALSE.(FORWARD MAP)
C          XAPMAX = IS THE MAXIMUM VALUE FOR XAP = R/W FOR WHICH
C                   POINT-SPREAD IS IMPORTANT
C                   R = APPARENT RADIUS IN KPC
C                   W = HALF WIDTH OF POINT-SPREAD DISK IN KPC
C          PLDONE =.TRUE.(PLOTTING IS DONE) =.FALSE.(NO PLOTTING)
C          N1 = GIVES NO. OF POINTS IN OUTPUT ARRAYS
C
C          PROGRAM WRITTEN BY A.W.SIEVERS DEPARTMENT OF APPLIED MATHS
C          JULY 1981

```

```

C
REAL GINF(3),HO,QO,X1,X2,Z,P1,P2,FRAC,GRAD,SIGMAD,X10,X20IN,
+ X1INC,X2INC,ZINC,EPS,XAPMAX,SIGMA
INTEGER I,IF,IIN,NX1,NX2,NZ,IX,IY,IZ,IXD,IYD,N1
CHARACTER INSTR*6,ARRAY*6(20)
LOGICAL INVERS,PLDONE

C
C   VARIABLES INITIALISED
C   COMMON BLOCKS DEFINED
C
COMMON /CGINF/GINF/CPAR1/HO,QO,FRAC,GRAD,X20IN/CCPAR1/P1,P2,X10
+ /CIF/IF/CFLAG/IIN,INVERS/CPAR2/SL,SIGMAD
+ /CACURA/IX,IY,IZ/CACURB/XAPMAX,EPS,IXD,IYD
+ /CINP/X1,X2,Z,NX1,NX2,NZ,X1INC,X2INC,ZINC
+ /CMAP2/N1
DATA HO,QO,P1,P2,FRAC,SIGMA,X10,X20IN,X1,X2,Z,IF,IIN/50.0,0.01,
+ 4*0.0,3.459E3,0.0,7.3,-21.64,0.34E-2,1,1/,
+ X1INC,X2INC,ZINC,NX1,NX2,NZ/3*0.0,3*1/,
+ GINF/126669.0,2*19.64/,
+ EPS,IX,IY,IZ/1E-4,2,2,2/,
+ SL,GRAD/24.0,0.7/,IXD,IYD/2,2/,INVERS/.FALSE./,XAPMAX/15./,
+ N1/0/
SIGMAD = 4.8481E-6 * SIGMA

C
C   USER MAY CHOOSE AMONG FOLLOWING COMMANDS
C
ARRAY(1)=6HSETPR1
ARRAY(2)=6HSETPR2
ARRAY(3)=6HACURAT
ARRAY(4)=6HINPUT
ARRAY(5)=6HMAP
ARRAY(6)=6HIMAP
ARRAY(7)=6HTABLE
ARRAY(8)=6HNEWARR
ARRAY(9)=6HPSTART
ARRAY(10)=6HPLOT
ARRAY(11)=6H
ARRAY(12)=6H
ARRAY(13)=6HSTDATA
ARRAY(14)=6HRDATA
ARRAY(15)=6HPRJECT
ARRAY(16)=6H
ARRAY(17)=6H
ARRAY(18)=6H
ARRAY(19)=6H
ARRAY(20)=6HSTOP
PLDONE = .FALSE.
WRITE(5,2000)
2000 FORMAT(1H1,10X,'INITIALISATION OF GALAXY MAP'/
+ 1H ,10X,28(1H*))

C
C   INITIALISATION IS PRINTED
C
PRINT *, 'X1=',X1, 'X2=',X2, 'Z=',Z
PRINT *, 'HO=',HO, 'QO=',QO, 'P1=',P1, 'P2=',P2
PRINT *, 'FRAC=',FRAC, 'SIGMA=',SIGMA, 'X10=',X10
PRINT *, 'SL=',SL, 'GRAD=',GRAD, 'X20IN=',X20IN
PRINT *, 'IF=',IF, 'IIN=',IIN, 'EPS=',EPS
PRINT *, 'IX=',IX, 'IY=',IY, 'IZ=',IZ, 'IXD=',IXD

```

```

PRINT *, 'IYD=', IYD, 'XAPMAX=', XAPMAX
WRITE(5,2005)
2005 FORMAT(1H0, 'TYPE INSTRUCTION STARTING IN COLUMN 1')
10 WRITE(5,2010)
2010 FORMAT(1H, 'INSTRUCTION?')
READ(8,1000)INSTR
1000 FORMAT(A6)
WRITE(5,2015)INSTR
2015 FORMAT(1H, A6)
DO 20 I=1,20
  IF(INSTR.EQ.ARRAY(I)) GO TO 5
20 CONTINUE
PRINT *, 'DID YOU SPELL THE INSTRUCTION CORRECTLY?', INSTR
GO TO 10
5 GO TO (101,102,103,104,105,106,107,108,109,110,
+       120,120,113,114,115,120,120,120,120) I
C
C       DATA INPUT FOR H0,Q0,P1,P2,FRAC,X10,X20IN,GRAD
C
101 CALL PARAL
GO TO 10
C
C       DATA INPUT FOR IF,SL,SIGMA,IIN
C
102 CALL PARA2
GO TO 10
C
C       DATA INPUT FOR XAPMAX, EPS, IX, IY, IZ, IXD, IYD
C
103 CALL ACURAT
GO TO 10
C
C       DATA INPUT FOR X1,X2,Z,NX1,NX2,NZ,X1INC,X2INC,ZINC
C
104 CALL INPUT
GO TO 10
C
C       FORWARD MAP FOR POINTS READ BY INPUT
C
105 INVERS = .FALSE.
CALL MAP
GO TO 10
C
C       INVERSE MAP FOR POINTS READ BY INPUT
C
106 INVERS = .TRUE.
CALL MAP
GO TO 10
C
C       TABLE OF RESULTS PRINTED
C
107 CALL TABLE
GO TO 10
C
C       COUNTER OF OUTPUT ARRAYS RESET
C
108 N1 = 0
GO TO 10
C

```

```

C          PLOT INITIALISED
C
109 CALL PSTART
    PLDONE = .TRUE.
    GO TO 10
C
C          PLOTTING OF OUTPUT ARRAYS
C
110 CALL GRAPH
    GO TO 10
C
C          DATA STORED IN A FILE (UNIT 11)
C
113 CALL STDATA
    PRINT *, 'DATA WRITTEN TO FILE:N1 =',N1
    GO TO 10
C
C          DATA READ FROM A FILE
C          UNIT 11
C
114 CALL RDATA
    PRINT *, 'DATA READ FROM FILE:N1 =',N1
    GO TO 10
C
C          PROJECTIONS PRINTED
C
115 CALL PRJECT
    GO TO 10
C
C          PROGRAM TERMINATES
C
120 PRINT *, 'PROGRAM TERMINATES'
    IF(PLDONE) THEN
        PRINT *, 'END OF PLOT'
        CALL PENDE
    END IF
    STOP 9999
    END
    SUBROUTINE PARAL
    *****
C
C          DATA INPUT FOR H0,Q0,P1,P2,FRAC,X10,X20IN,GRAD
C          -----
C          DATA IS READ IN FREE FORMAT
C          ITEMS SEPARATED BY BLANKS OR COMMAS
C
    REAL H0,Q0,FRAC,GRAD,P1,P2,X10,X20IN
    COMMON/CPAR1/H0,Q0,FRAC,GRAD,X20IN
    +      /CCPAR1/P1,P2,X10
    WRITE(5,2000)
2000 FORMAT(1H0,'DATA INPUT : H0,Q0,P1,P2,FRAC,X10,X20IN,GRAD?')
    READ(8,2001)H0,Q0,P1,P2,FRAC,X10,X20IN,GRAD
2001 FORMAT(
    PRINT *, 'H0=',H0, 'Q0=',Q0, 'P1=',P1, 'P2=',P2
    PRINT *, 'FRAC=',FRAC, 'X10=',X10, 'X20IN=',X20IN, 'GRAD=',GRAD
    RETURN
    END

```





SUBROUTINE RDATA  
\*\*\*\*\*

READS DATA FROM DATA-FILE(WRITTEN TO BY STDATA)

UNIT 11

N1 POINTS READ INTO X1,X2,Z,Y1,Y2

N1 APPEARS ON FIRST RECORD

REAL X1(100),X2(100),Z(100),Y1(100),Y2(100)

LOGICAL INVERS

COMMON /CMAP2/N1,X1,X2,Z,Y1,Y2

+ /CPAR1/H0,Q0,FRAC,GRAD,X20IN/CCPAR1/P1,P2,X10

+ /CIF/IF/CFLAG/IIN,INVERS/CPAR2/SL,SIGMAD

READ(11,\*) N1,INVERS

READ(11,\*)H0,Q0,P1,P2

READ(11,\*)FRAC,SIGMA,X10,X20IN

READ(11,\*)SL,GRAD,IF,IIN

DO 10 I=1,N1

READ(11,\*) X1(I),X2(I),Z(I),Y1(I),Y2(I)

10 CONTINUE

SIGMAD = 4.8481E-6 \* SIGMA

RETURN

END

SUBROUTINE PROJECT

\*\*\*\*\*

(LOG A-AP,LOC C\*Z) AND (M-AP,LOG C\*Z) CURVES  
ARE COMPUTED AND PRINTED

-----  
C = SPEED OF LIGHT IN KM/SEC

REAL X1(100),X2(100),Z(100),Y1(100),Y2(100),C

COMMON /CMAP2/N1,X1,X2,Z,Y1,Y2

C = 299792.5

DO 10 I=1,N1

Z(I) = ALOG10(C\*Z(I))

10 CONTINUE

WRITE(5,2000) (Y1(J),Z(J),Y2(J),J=1,N1)

2000 FORMAT(1H0,4X,'LOG(A-AP)',4X,'LOG(C\*Z)',5X,'MAP' /

+ (1H0,3X,F8.3,5X,F8.3,4X,F8.3))

RETURN

END

REAL FUNCTION F(X)

\*\*\*\*\*

BRIGHTNESS PROFILES CALCULATED

-----  
IF DETERMINES WHICH PROFILE IS EVALUATED

REAL X,U

INTEGER IF

COMMON /CIF/IF

PROFILE IS SELECTED

GO TO (10,20,20) IF

DE VAUC PROFILE

```

C
10 U = X**.25
   F = EXP(-U)
   RETURN

C
C       ABELL MIHALAS PROFILE
C
20 XP1 = X+1.
   IF (X.LE.21.4) THEN
     F = 1./(XP1*XP1)
   ELSE
     F = 22.4/(XP1*XP1*XP1)
   END IF
   RETURN
   END
   REAL FUNCTION FINV(X)
   *****

C
C       INVERSE OF BRIGHTNESS PROFILES EVALUATED
C       -----
C       FOR DIFFERENT IF
C
REAL X
INTEGER IF
COMMON /CIF/IF

C
C       INVERSE IS SELECTED
C
GO TO (10,20,20) IF

C
C       DE VAU PROFILE
C
10 FINV = (-ALOG(X))**4
   RETURN

C
C       ABELL MIHALAS PROFILE
C
20 IF (X.GE.1.99298E-3) THEN
   FINV = 1./SQRT(X) - 1.
ELSE
   FINV = (22.4/X)**0.33333333 - 1.
END IF
RETURN
END
REAL FUNCTION R0(Z)
*****

C
C       OBSERVER AREA DISTANCE IN MPC
C       -----
C       FRIEDMANN UNIVERSE : C = SPEED OF LIGHT
C       HO = HUBBLE CONSTANT : Q0 = DEACCELERATION PARAMETER
C       Z = REDSHIFT
C
REAL Z,HO,Q0,C,K1,K2
COMMON /CPAR1/HO,Q0
C = 299792.5
K1 = Z*C / (HO * (1.+Z)**2)
K2 = SQRT(1. + 2.*Q0*Z) + 1.+Q0*Z
R0 = K1*(1. + Z*(1.-Q0)/K2)

```

RETURN

END

REAL FUNCTION MAGCOR(Z)

\*\*\*\*\*

BOLOMETRIC CORRECTION

-----  
ASSUMPTIONS

1. POWER LAW SPECTRUM : SPECTRAL GRADIENT GRAD

2. ABSORPTION BY ELECTRON SCATTERING

FRAC = FRACTION OF HYDROGEN IONISED

3. FRIEDMANN UNIVERSE : TAU = OPTICAL DEPTH \* 2.5\*ALOG10(E)

E = BASE OF NATURAL LOGARITHM ; Q0 > 0

4. SQUARE SPECTRAL WINDOW, CORRECTION WINDOW

REAL H0, Q0, FRAC, GRAD, WINDOW, K1, K2, K3, TAU

COMMON /CPAR1/H0, Q0, FRAC, GRAD, WINDOW

IF (FRAC .GT. 0.0) THEN

K1 = 3.\*Q0 - 1.

K2 = Q0\*Z

K3 = (K1+K2)\*SQRT(1. + K2+K2) - K1

TAU = 4.7049\*FRAC\*K3/(Q0\*H0)

ELSE

TAU = 0.0

END IF

MAGCOR = 2.5\*GRAD\*ALOG10(1.+Z) + TAU + WINDOW

RETURN

END

REAL FUNCTION BOUND(X0, A)

\*\*\*\*\*

THE INTEGRATION BOUND YB FOR DOUBLE AND TRIPLE

-----  
IS CALCULATED

SIGN GIVES THE SIGN OF THE FIRST DERIVATIVE OF  
THE INTEGRAND

COMMON /CIF/IF

PROFILE SELECTED

GO TO (10,20) IF

DE VAUC PROFILE

10 B1 = X0 + 3.

B2 = 40000./A

SIGN = (X0-B2)\*B2 - .25\*(B2\*A)\*\*.25 + 1.

IF(SIGN.LT.0.0 .AND. B2.LT.B1) THEN

BOUND = B2

ELSE

BOUND = B1

END IF

RETURN

ABELL MIHALAS PROFILE

20 B1 = X0 + 3.

B2 = 400./A



```

X20=MAGCOR(Z)
PRINT *, 'R0 = ', ROZ, 'MPC' COLOUR CORRECTION= ', X20, 'MAG'
C
C
C
X1-LOOP BEGINS
DO 20 I2=1, NX1
  STOX1 = X1
C
C
C
  X1 CONVERTED TO LINEAR SCALE
  IF (IIN.EQ.0) X1=10**X1
C
C
C
  X1 IS CONVERTED TO RADIANS : ONLY FOR LIN.INVERSE MAP
  IF (IIN.EQ.1 .AND. INVERS) X1=X1/ASEC
C
C
C
  X2-LOOP BEGINS
  DO 30 I3=1, NX2
C
C
C
    OUTPUT ARRAYS X1ARR,X2ARR,ZARR SET UP
    N1 = N1 + 1
    X1ARR(N1)=STOX1
    X2ARR(N1)=X2
    ZARR(N1)=Z
C
    IF(INVERS) THEN
C
C
C
      INVERSE MAP IS DONE WITH INVMAP
      CALL INVMAP(X1,X2,Z,Y1ARR(N1),Y2ARR(N1),FLAG)
C
    ELSE
C
C
C
      FORWARD MAP IS DONE WITH PSMAP
      CALL PSMAP(X1,X2,Z,Y1ARR(N1),Y2ARR(N1),FLAG)
C
    END IF
C
    GALAXY COULD NOT BE MAPPED
C
    IF(.NOT.FLAG) THEN
      Y1ARR(N1) = 0.0
      Y2ARR(N1) = 0.0
    END IF
C
    IF OUTPUT IS ON LOG SCALE
    IF(IIN.EQ.0.AND.FLAG) Y1ARR(N1) = ALOG10(Y1ARR(N1))
C
    CONVERT TO SEC OF ARC (FORWARD MAP AND LIN SCALE ONLY)
    IF(IIN.EQ.1.AND..NOT.INVERS) Y1ARR(N1) = ASEC*Y1ARR(N1)
    X2=X2+X2INC
30 CONTINUE
X2 = X2I
X1=STOX1+X1INC

```

```

20    CONTINUE
      X1 = X1I
      Z = Z + ZINC
10    CONTINUE
      RETURN
      END
      SUBROUTINE PSMAP(X1I,X2I,Z,Y1,Y2,FLAG)
C      *****
C      FORWARD MAP
C      -----
C      X1=A(SCALING RADIUS IN KPC) : X2=M-BOL(BOLOMETRIC MAGNITUDE)
C      Y1=A-AP(APPARANT ANGLE IN RAD) : Y2=M-AP(APPARANT MAGNITUDE)
C      FOR REDSHIFT Z
C
      REAL X1,X2,Z,Y1,Y2,GINF(3),SL,SIGMAD,EPS,Q1,ALFA,XAP,RO,
+      X20,K1,AQ1,BAP,AAP,XAPMAX,
+      P1,P2,X10
      INTEGER IF
      LOGICAL TEST,FLAG
      EXTERNAL PROFIL
      COMMON /CPAR2/SL,SIGMAD/CGINF/GINF/CACURB/XAPMAX,EPS
+      /CPSMAP/Q1,ALFA,XAP/CMAP1/RO,X20/CIF/IF
+      /CCPAR1/P1,P2,X10
      FLAG = .FALSE.
      PI = 3.141593
      ZLOG = ALOG10(1.+ Z)
      K1 = SL-X20-7.5*ZLOG - 37.82
      X1 = X1I/X10*(1.+ Z)**PI
      X2 = X2I - 2.5*P2*ZLOG - 5.*PI*ZLOG
      AQ1=0.4*(X2-K1)
      Q1=(GINF(IF)/PI)*X1*X1*10**AQ1
      ALFA=SIGMAD*RO*1000./X1
C
C      TEST:DOES IMAGE EXIST (NO POINT-SPREAD)
C
      IF (Q1.GT.1.) THEN
2000  FORMAT(1H0,'GALAXY BELOW DETECTION LIMIT (NO POINT-SPREAD)')
      RETURN
      ELSE
C
C      BETA-APPARENT (BAP) AND A-AP COMPUTED FOR NO POINT-SPREAD
C
      BAP=FINV(Q1)
      AAP=.001*BAP*X1/RO
C
      IF (SIGMAD.GT.0.0) THEN
C
C      POINT-SPREAD ON
C
C      INITIAL GUESS FOR XAP
C
      XAP=AAP/SIGMAD
C
C      MAP IS COMPLETED WITHOUT POINT-SPREAD IF XAP.GE.XAPMAX
C
      IF (XAP.GE.XAPMAX) GO TO 10
C
C      TEST: DOES IMAGE EXIST WHITH POINT-SPREAD ON ?

```



```

+      /CACURB/XAPMAX, EPS
DATA BD/41.87515, -450.9787, -873.3407, 2816.3958, 7315.3342, 4282.6471
+      , -.7032808, 21.785877, -111.2023, 3521.4592, 7626.6401, 4330.0641/
+      , BA/-28.999653, -225.19037, -684.14948, -1009.9881, -715.31806,
+      -188.83001, -2.671145, 15.395485, -9.5759662, -14.92826,
+      42.047339, 36.346761/,
+      PI/3.1415927/
GB = SL-X2-5.*ALOG10(X1)-27.82-2.5*ALOG10(GINF(IF)/PI)

C
C      B-AP IS APPROXIMATED BY A POLYNOMIAL
C
C      GO TO (10,20) IF
C
C      DE VAUCOULEURS PROFILE
C
10 IF(GB.LT.-11.5138) THEN
C
C      NO INVERSE POSSIBLE
C
C      FLAG = .FALSE.
C      PRINT *, 'GALAXY BELOW DETECTION (INVERSE MAP)'
C      RETURN
C      END IF
C      IF (GB.GT.2.113) THEN
C      FLAG = .FALSE.
C      PRINT *, 'APPROXIMATION FOR B-AP BREAKS DOWN'
C      PRINT *, 'B-AP.GT.200 (DE VAUCOULEURS PROFILE)'
C      RETURN
C      END IF
C      IF (GB.LT.-11.37) THEN
C
C      ANALYTIC APPROXIMATION FOR BAP < 1.7
C
C      BAP = (SQRT(3628800.*10**(.4*GB) - 65.) - 5.)*4
C      GO TO 30
C      END IF
C      GA = GB + 10.
C      IF(GB.LT.-10.4) THEN
C
C      BAP(BETA APPARENT) APPROXIMATED BY POLYNOMIAL
C
C      BAP=BD(6)+GA*(BD(5)+GA*(BD(4)+GA*(BD(3)+GA*(BD(2)+GA*BD(1))))
C      ELSE
C      BAP=BD(12)+GA*(BD(11)+GA*(BD(10)+GA*
+      (BD(9)+GA*(BD(8)+GA*BD(7))))
C      END IF
C      GO TO 30
C
C      ABELL MIHALAS PROFILE
C
20 IF(GB.LT.-1.991918) THEN
C      FLAG = .FALSE.
C      PRINT *, 'GALAXY BELOW DETECTION (INVERSE MAP)'
C      RETURN
C      END IF
C      IF (GB.GT.4.0) THEN
C      FLAG = .FALSE.
C      PRINT *, 'APPROXIMATION FOR B-AP BREAKS DOWN'
C      PRINT *, 'B-AP.GT.895 (ABELL MIHALAS PROFILE)'

```

```

RETURN
END IF
IF (GB.LT.-.8897) THEN
  BAP=BA(6)+GB*(BA(5)+GB*(BA(4)+GB*
+      (BA(3)+GB*(BA(2)+GB*BA(1))))
ELSE
  BAP=BA(12)+GB*(BA(11)+GB*(BA(10)+GB
+      *(BA(9)+GB*(BA(8)+GB*BA(7))))
END IF

C
C
C      A BETTER APPROXIMATION FOR BAP FOUND IN SECA
C
30 IF (SIGMAD.EQ.0.0) THEN
C
C      INVERSE WITHOUT POINT-SPREAD
C
CALL SECA(GBAP,BAP,EPS,TEST)
IF (TEST) THEN
C
C      INVERSE MAP WITHOUT POINT-SPREAD IF TEST =.TRUE.
C
Y1 = X1*1000.*R0*X10/(BAP*(1.+ Z)**P1)
Y2 = X2 - X20 + 2.5*ALOG10(G(BAP,0.0)/((R0*R0*(1.+ Z)**3))
+      + 2.5*P2*ALOG10(1.+ Z) + 5.*P1*ALOG10(1.+ Z) - 25.
FLAG = .TRUE.
ELSE
  PRINT *, 'NO BAP FOUND IN SECA:BAP=',BAP, 'A-AP=',X1, 'MAP=',X2
  FLAG = .FALSE.
END IF
ELSE
C
C      INVERSE WITH POINT-SPREAD
C
XAP = X1/SIGMAD
S = SIGMAD
IF (XAP.GT.XAPMAX) THEN
C
C      INVERSE COMPLETED WHITHOUT POINT-SPREAD
C
SIGMAD = 0.0
GO TO 50
END IF
C
C      NO INVERSE DONE IF B-AP IS SMALLER BY A FACTOR MORE THAN 100
C
GBMIN = GBAP(BAP/100)
IF (GBMIN.GT.0.0) THEN
  FLAG = .FALSE.
  PRINT *, 'GALAXY BELOW DETECTION WITH POINT-SPREAD'
  RETURN
END IF
50 CALL SECA(GBAP,BAP,EPS,TEST)
IF (TEST) THEN
C
C      INVERSE MAP WITH POINT-SPREAD IF TEST =.TRUE.
C
Y1 = X1*1000.*R0*X10/(BAP*(1.+ Z)**P1)
Y2 = X2 - X20 + 2.5*ALOG10(G(BAP,SIGMAD)/((R0*R0*(1.+ Z)**3))
+      + 2.5*P2*ALOG10(1.+ Z) + 5.*P1*ALOG10(1.+ Z) - 25.

```

```

        FLAG = .TRUE.
        SIGMAD = S
    ELSE
        PRINT *, 'NO BAP FOUND IN SECA:BAP=',BAP, 'A-AP=',X1, 'MAP=',X2
        FLAG = .FALSE.
    END IF
END IF
RETURN
END

```

```

SUBROUTINE SECA(F,ROOT,EPS,TEST)
*****

```

```

    THE SECANT METHOD IS USED TO FIND A POS.ROOT OF
    THE FUNCTION F (MONOTONIC INCREASING)

```

```

LOGICAL TEST

```

```

TEST = .FALSE.

```

```

X1 = ROOT

```

```

F1 = F(X1)

```

```

IF (F1.GT.0.0)THEN

```

```

    X2 = ROOT/2.

```

```

ELSE

```

```

    X2 = ROOT + ROOT/2.

```

```

END IF

```

```

F2 = F(X2)

```

```

IF (ABS(F2).LT.1E-32) GO TO 10

```

```

DO 100 J1 = 1,20

```

```

    IF (F2.EQ.F1) RETURN

```

```

    DIRF = (F2-F1)/(X2-X1)

```

```

    X3 = X2-F2/DIRF

```

```

    IF(X3.LE.0.0) X3 = X2 + X2/4.

```

```

    F3 = F(X3)

```

```

    X1 = X2

```

```

    X2 = X3

```

```

    F1 = F2

```

```

    F2 = F3

```

```

    IF(ABS(X2/X1-1.).LE.EPS.OR.ABS(F3).LT.1E-32)GO TO 20

```

```

100 CONTINUE

```

```

    RETURN

```

```

10 ROOT = X2

```

```

    TEST = .TRUE.

```

```

    RETURN

```

```

20 ROOT = X3

```

```

    TEST = .TRUE.

```

```

    RETURN

```

```

END

```

```

REAL FUNCTION GBAP(B)

```

```

*****

```

```

COMMON /CINV/GB/CPAR2/SL,SIGMAD

```

```

IF (SIGMAD.EQ.0.0) THEN

```

```

    GBAP = -2.5*ALOG10(B*B*F(B)/G(B,0.0)) - GB

```

```

ELSE

```

```

    GBAP = -2.5*ALOG10(B*B*PSPROF(B)/G(B,SIGMAD)) - GB

```

```

END IF

```

```

RETURN

```

```

END

```

SUBROUTINE SECANT(F,ROOT,EPS,TEST)  
 \*\*\*\*\*

C  
C  
C  
C  
C

THE SECANT METHOD IS USED TO FIND A POS.ROOT OF  
 THE FUNCTION F

LOGICAL TEST

TEST = .FALSE.

X1 = ROOT

F1 = F(X1)

IF (F1.LT.0.0)THEN

X2 = ROOT/2.

ELSE

X2 = ROOT + ROOT/2.

END IF

F2 = F(X2)

IF (ABS(F2).LT.1E-32) GO TO 10

DO 100 J1 = 1,20

IF (F2.EQ.F1) RETURN

DIRF = (F2-F1)/(X2-X1)

X3 = X2-F2/DIRF

IF(X3.LE.0.0) X3 = X2/4.

F3 = F(X3)

X1 = X2

X2 = X3

F1 = F2

F2 = F3

IF(ABS(X2/X1-1.).LE.EPS.OR.ABS(F3).LT.1E-32)GO TO 20

100 CONTINUE

RETURN

10 ROOT = X2

TEST = .TRUE.

RETURN

20 ROOT = X3

TEST = .TRUE.

RETURN

END

REAL FUNCTION PROFIL(Z)

\*\*\*\*\*

C  
C  
C  
C  
C

ZERO OF PROFIL IS FOUND IN BISECA  
 TO INVERT POINT-SPREAD PROFILE

REAL Z,X0,Q1,BOUND,PI

INTEGER IX,IY

COMMON /CPROF/X0/CACURB/X,E,IX,IY/CPSMAP/Q1,ALFA

EXTERNAL DOUBIN

C  
C  
C  
C

THE ARGUMENT OF PROFIL IS SAVED SO THAT DOUBIN  
 CAN BE EVALUATED

X0 = Z

C  
C  
C

BOUND FOR Y-INTEGRATION CALCULATED

B = BOUND(X0,ALFA)

PI = 3.141593

C  
C

DOUBLE INTEGRATION ROUTINE DOUBLE IS USED

```

C          RESULT OF INTEGRATION = V
C
CALL DOUBLE(DOUBIN,V,0.0,PI,0.0,B,IX,IY)
PROFIL = V/PI - Q1
RETURN
END
REAL FUNCTION PSPROF(B)
*****

C          POINT-SPREAD PROFILE AS FUNCTION OF B=XAP*ALFA
C          FOR INVERSE MAP WITH POINT-SPREAD
C
REAL B,X0,BOUND,PI,ALFA,XAP,BO,V
INTEGER IX,IY
COMMON /CPROF/X0/CACURB/X,E,IX,IY/CPSMAP/Q1,ALFA,XAP
EXTERNAL DOUBIN

C          ALFA,X0 CALCULATED SO THAT DOUBIN
C          CAN BE EVALUATED
C
X0 = XAP
ALFA = B/XAP

C          BOUND FOR Y-INTEGRATION CALCULATED
C
BO = BOUND(X0,ALFA)
PI = 3.141593

C          DOUBLE INTEGRATION ROUTINE DOUBLE IS USED
C          RESULT OF INTEGRATION = V
C
CALL DOUBLE(DOUBIN,V,0.0,PI,0.0,BO,IX,IY)
PSPROF = V/PI
RETURN
END
SUBROUTINE DOUBLE(F,SUM,XA,XB,YA,YB,INX,INY)
*****

C          DOUBLE-INTEGRATION ROUTINE
C          -----
C          A GAUSSIAN 16-POINT QUADRATURE IS DONE
C          ON EVERY SUBINTERVAL
C          F = FUNCTION TO BE INTEGRATED
C          SUM = RESULT OF INTEGRATION
C          XA,XB = INTERVAL ON X-AXIS
C          YA,YB = " " " Y- "
C          INX,INY = NO OF SUBINTERVALS ON THE X-,Y-AXIS
C
REAL NI,NJ
DIMENSION A(16),T(16)
DATA (T(I),I=1,16)/9.501250984E-2,-9.501250984E-2,2.816035508E-1,
+   -2.816035508E-1,4.580167777E-1,-4.580167777E-1,6.178762444E-1,
+   -6.178762444E-1,7.554044084E-1,-7.554044084E-1,8.656312024E-1,
+   -8.656312024E-1,9.445750231E-1,-9.445750231E-1,9.894009350E-1,
+   -9.894009350E-1/,
+   (A(I),I=1,16)/2*1.894506105E-1,2*1.826034150E-1,
+   2*1.691565194E-1,2*1.495959888E-1,2*1.246289713E-1,
+   2*9.515851168E-2,2*6.225352394E-2,2*2.715245941E-2/

```

```

C      INTEGRATION FROM YA TO YB
C
C      XC = (XBI-XAI)/2 : I STANDING FOR I-TH SUBINTERVAL
C      XD = (XBI+XAI)/2
C      SIMILAR FOR Y
C
SUM = 0.0
S1 = 0.0
S2 = 0.0
XN = FLOAT(INX)
YN = FLOAT(INY)
XC = (XB-XA)/(2.*XN)
YC = (YB-YA)/(2.*YN)
DO 20 I=1, INX
  NI = FLOAT(I)
  XD' = XA + 2.*XC*(NI-.5)
  DO 30 J=1, INY
    NJ = FLOAT(J)
    YD = YA + 2.*YC*(NJ-.5)
    DO 40 K=1, 16
      XIK = XC*T(K) + XD
      DO 50 L=1, 16
        YJL = YC*T(L) + YD
        S1 = S1 + A(L)*F(XIK, YJL)
50      CONTINUE
        S2 = S2 + S1*A(K)
        S1 = 0.0
40      CONTINUE
30      CONTINUE
20      CONTINUE
C
C      INTERMEDIATE SUM
C
SUM = SUM + XC*YC*S2
C
C      INTEGRATION FROM YB TO INFINITY
C
S2 = 0.0
XC = (XB-XA)/2.
XD = (XB+XA)/2.
DO 60 K=1, 16
  XIK = XC*T(K) + XD
  DO 70 L=1, 16
    TL = T(L) + 1.
    YJL = 2./TL + YB - 1.
    S1 = S1 + A(L)/(TL*TL)*F(XIK, YJL)
70      CONTINUE
    S2 = S2 + S1*A(K)
    S1 = 0.0
60      CONTINUE
C
C      FINAL RESULT
C
SUM = SUM + S2*XC*2.
RETURN
END

```

```

REAL FUNCTION DOUBIN(X,Y)
*****

FUNCTION INTEGRATED IN DOUBLE
-----
TO COMPUTE A POINT ON THE POINT-SPREAD PROFILE

REAL X,Y,ALFA,Q1,X0,U,B,F,A1,B1
INTEGER IF
COMMON /CIF/IF/CPROF/X0
+      /CPSMAP/Q1,ALFA
B = Y*ALFA

PROFILE SELECTED

GO TO (10,20,20) IF

DE VAU PROFILE
10 U = B**.25
   F = EXP(-U)
   GO TO 100

ABELL MIHALAS PROFILE
20 B1 = B + 1.
   IF (B .LE. 21.4) THEN
     F = 1.0/(B1*B1)
   ELSE
     F = 22.4/(B1*B1*B1)
   END IF

INTEGRANT COMPUTED

100 A1 = X0*Y*COS(X) - Y*Y/2. - X0*X0/2.
    DOUBIN = Y*EXP(A1)*F
    RETURN
END
REAL FUNCTION G(B,SIGMAD)
*****

G(BETA,SIGMAD)/G-INFINITY
-----
G(B,SIGMAD) = INTEGRAL OF 2*PI*PROFILE FROM 0 TO B

REAL GINF(3),B,U,G1,RESULT,XAP,BOUND,SIGMAD,PI,BCRIT,GINFIN
INTEGER IF,IX,IY,IZ
COMMON /CPSMAP/Q1,ALFA,XAP/CACURA/IX,IY,IZ
+      /CGINF/GINF/CIF/IF
EXTERNAL TRIPIN
PI = 3.1415927
BCRIT = 21.4
IF (SIGMAD .GT. 0.0) THEN

POINT SPREAD ON

YB = BOUND(XAP,ALFA)
CALL TRIPLE(TRIPIN,RESULT,0.0,PI,0.0,YB,0.0,XAP,IX,IY,IZ)
G = RESULT * ((B/XAP)**2) * 2.0/GINF(IF)

```

RETURN  
ELSE

POINT SPREAD OFF  
CHOICE BETWEEN DIFFERENT PROFILES MADE

GO TO (10,20,20) IF

DE VAU PROFILE

10 U = B\*\*0.25  
IF (U .LE. 0.8) THEN  
G1 = U\*\*8/40320 \* (1. + U/9.\*(1. + U/10.\*(1. + U/11.)))  
G = G1\*EXP(-U)  
ELSE  
G1 = 1.+U\*(1.+U/2.\*(1.+U/3.\*(1.+U/4.\*(1.+U/5.\*(1.+U/6.\*  
+ (1. + U/7.))))))  
G = 1. - EXP(-U) \* G1  
END IF  
RETURN

ABELL MIHALAS PROFILE

20 GINFIN = ALOG(1.+BCRIT) + 1./((1.+BCRIT)\*\*2.)  
IF (B .LE. BCRIT) THEN  
G = (ALOG(1.+ B) + 1./(1.+ B) - 1.)/GINFIN  
ELSE  
G = (GINFIN - (1.+ BCRIT)\*(1./(1.+ B) - 1./((2.\*(1.+ B)\*\*2))))  
+ /GINFIN  
END IF  
ENDIF

NOTE GINFIN = GINF/2.\*PI

RETURN  
END

SUBROUTINE TRIPLE(F,ANS,XA,XB,YA,YB,ZA,ZB,NX,NY,NZ)  
\*\*\*\*\*

TRIPLE-INTEGRATION ROUTINE

-----  
A GAUSSIAN 16-POINT QUADRATURE IS DONE ON  
EVERY SUBINTERVAL

F = FUNCTION TO BE INTEGRATED  
ANS = RESULT OF INTEGRATION  
XA,XB = INTEVAL ON X-AXIS  
YA,YB = " " Y- "  
ZA,ZB = " " Z- "

NOTE:INTEGRATION FROM YA TO YB TO INFINITY  
NX,NY,NZ = NO OF SUBINTERVALS ON X-,Y-,Z-AXIS  
IN THE FIRST 3 DO-LOOPS A SUBINTERVAL IS  
SELECTED AND SOME QUANTITIES EVALUATED  
RELATED TO THIS INTERVAL  
IN THE INNER THREE DO-LOOPS THE SUM IS DONE  
OVER THIS SUBINTERVAL  
NO CONVERGENCE CHECK IS DONE

DIMENSION A(16),T(16)  
DATA (T(I),I=1,16)/9.501250984E-2,-9.501250984E-2,2.816035508E-1,



```

XD = (XB+XA)/2.
ZD = (ZB+ZA)/2.
DO 70 K=1,16
  XIK = XC*T(K) + XD
  DO 80 L=1,16
    TL = T(L) + 1.
    YIK = 2./TL + YB - 1.
    DO 90 M=1,16
      ZIK = ZC*T(M) + ZD
      S1 = S1 + A(M)*F(XIK,YIK,ZIK)
90    CONTINUE
      S2 = S2 + A(L)/(TL*TL)*S1
      S1 = 0.0
80    CONTINUE
      S3 = S3 + A(K)*S2
      S2 = 0.0
70 CONTINUE

```

```

C
C
C      FINAL ANSWER

```

```

ANS = ANS + 2.*XC*ZC*S3
RETURN
END
REAL FUNCTION TRIPIN(X,Y,Z)
*****

```

```

C
C
C      FUNCTION INTEGRATED IN TRIPLE
C
C      -----
C

```

```

C      TO CALCULATE G(BETA) FOR SIGMAD > 0
C

```

```

REAL X,Y,Z,ALFA,U,F,A1,B,B1
INTEGER IF
COMMON /CIF/IF/CPSMAP/Q1,ALFA
B = Y*ALFA

```

```

C
C
C      PROFILE SELECTED

```

```

C      GO TO (10,20,20) IF

```

```

C      DE VAUCOULEURS PROFILE
C

```

```

10 U = B**.25
F = EXP(-U)
GO TO 100

```

```

C
C
C      ABELL MIHALAS PROFILE

```

```

20 B1 = 1.+ B
IF (B .LE. 21.4) THEN
  F = 1.0/(B1*B1)
ELSE
  F = 22.4/(B1*B1*B1)
END IF

```

```

C
C
C      INTEGRAND COMPUTED

```

```

100 A1 = Z*Y*COS(X) - Y*Y/2. - Z*Z/2.
TRIPIN = Y*Z*EXP(A1)*F
RETURN

```

END

SUBROUTINE PSTART

\*\*\*\*\*

PLOT IS INITIALISED

-----  
ORIGIN IS DEFINED

AXES AND TITLE ARE DRAWN

XTI,NXTI(.LE.40) = TITLE,NO OF CHARACTERS IN TITLE FOR X-AXIS

YTI,NYTI(.LE.12) = SAME FOR Y-AXIS

TITLE,NTI(.LE.40) = SAME FOR GRAPH TITLE

FIX,FIY = VALUE FOR X,Y AT FIRST TICK OF AXES

LAX,LAY = VALUE FOR X,Y AT LAST TICK OF AXES

DELX,DELY = NO.OF DATA UNITS PER CM

FACT = RATIO OF PLOT TO NORMAL PLOT SIZE

REAL FIX,FIY,LAX,LAY,DELX,DELY,FACT,SIZEX,SIZEY,TITX,TITY

INTEGER NXTI,NYTI,NTI

CHARACTER XTI\*40,YTI\*12,TITLE\*40

COMMON /CPSTA/FIX,DELX,FIY,DELY

PRINT \*, 'INPUT FOR : TITLE FOR X-,Y-AXIS AND GRAPH'

PRINT \*, ' ON SEPERATE RECORDS'

READ(8,1000) XTI,YTI,TITLE

1000 FORMAT(A40/A12/A40)

PRINT \*, 'INPUT FOR : NO OF CHAR.IN TITLE FOR X-,Y-AXIS AND GRAPH'

PRINT \*, ' FIX,LAX,FIY,LAY,FACT'

READ(8,1001) NXTI,NYTI,NTI,FIX,LAX,FIY,LAY,FACT

1001 FORMAT()

DELX = FACT\*(LAX-FIX)/20.

DELY = FACT\*(LAY-FIY)/20.

PLOT IS INITIATED,NEW PLOT-PAGE OPENED

CALL NEWPAG

NEW ORIGIN DEFINED

CALL PLOT(1.5,1.5,-3)

AXES DRAWN

FACT GIVES RATIO OF NEW PLOT TO OLD PLOT

CALL FACTOR(FACT)

SIZEX = 20./FACT

SIZEY = 20./FACT

NXTI = -NXTI

CALL AXIS(0.0,0.0,XTI,NXTI,SIZEX,0.0,FIX,DELX)

CALL AXIS(0.0,0.0,YTI,NYTI,SIZEY,90.,FIY,DELY)

TITLE FOR PLOT DRAWN

TITX = 6./FACT

TITY = 21./FACT

CALL SYMBOL(TITX,TITY,.25,TITLE,0.0,NTI)

RETURN

END

## SUBROUTINE GRAPH

\*\*\*\*\*

PLOTS N1 POINTS FROM ARRAYS Y1 Y2 Z

-----  
LTYP DETERMINES TYP OF LINE DRAWN

LTYP.GT.0 POINTS CONECTED BY STRAIGHT LINES,AT EVERY

LTYP, SYMBOL IS PLOTTED

= 0 SAME BUT NO SYMBOLS PLOTTED

.LT.0 SYMBOLS PLOTTED BUT POINTS NOT CONNECTED

INTEQ = INTEGER EQUIVALENT OF SYMBOL

J DETERMINES WITCH ARRAYS ARE PLOTTED

J = 1 ARRAYS (Y1,Y2)

J = 2 ARRAYS (Y1,Z)

J = 3 ARRAYS (Y2,Z)

J = 4 ARRAYS (X1,X2)

NOT MORE THAN 98 POINTS CAN BE PLOTTED

REAL X1(100),X2(100),Z(100),Y1(100),Y2(100)

INTEGER N1,LTYP,INTEQ

COMMON /CPSTA/FIRSTX,DELTAX,FIRSTY,DELTAY

+ /CMAP2/N1,X1,X2,Z,Y1,Y2

PRINT \*, 'DATA INPUT FOR : LTYP,INTEQ,J'

PRINT \*, 'J=1 FOR (Y1,Y2):J=2 FOR (Y1,Z):J=3 FOR (Y2,Z):J=4 FOR (X1

+,X2)'  
READ(8,1001) LTYP,INTEQ,J

1001 FORMAT()

PRINT \*, 'LTYP=',LTYP,' INTEQ=',INTEQ,' J=',J

GO TO (10,20,30,40) J

10 Y1(N1+1) = FIRSTX

Y1(N1+2) = DELTAX

Y2(N1+1) = FIRSTY

Y2(N1+2) = DELTAY

CALL LINE(Y1,Y2,N1,1,LTYP,INTEQ)

GO TO 50

20 Y1(N1+1) = FIRSTX

Y1(N1+2) = DELTAX

Z(N1+1) = FIRSTY

Z(N1+2) = DELTAY

CALL LINE(Y1,Z,N1,1,LTYP,INTEQ)

GO TO 50

30 Y2(N1+1) = FIRSTX

Y2(N1+2) = DELTAX

Z(N1+1) = FIRSTY

Z(N1+2) = DELTAY

CALL LINE(Y2,Z,N1,1,LTYP,INTEQ)

GO TO 50

40 X1(N1+1) = FIRSTX

X1(N1+2) = DELTAX

X2(N1+1) = FIRSTY

X2(N1+2) = DELTAY

CALL LINE(X1,X2,N1,1,LTYP,INTEQ)

50 RETURN

END

SUBROUTINE PENDE

\*\*\*\*\*

PLOT IS TERMINATED

CALL ENDPLT

RETURN

END

## 7. References

- 1) Voigt, H.H., 1974. "Outline of Astronomy", vol.1, Noordhoff International Publishing Leyden.
- 2) Swihart, T.L., 1968. "Astrophysics and Stellar Astronomy", Wiley Science Text Series.
- 3) Mihalas, D., 1978. "Stellar Atmospheres" 2nd ed., Freeman, San Francisco.
- 4) Chandrasekhar, S., 1960. "Radiative Transfer", Dover.
- 5) Scheffler, H. and Elsaesser, H., 1974. "Physik der Sterne und der Sonne", B. I. Wissenschaftsverlag.
- 6) Aller, L.H., 1963. "The Atmospheres of the Sun and Stars", The Ronald Press Company New York.
- 7) Abell, G.O. and Mihalas, D.M., 1966. Astr. J., 71, 635.
- 8) Allen, C.W., 1973. "Astrophysical Quantities" 3rd ed., University of London. The Athlone Press.
- 9) Arp, H., 1965. Astrophys. J., 142, 402.
- 10) Bahcall, J. and May, R.M., 1968. Astrophys. J., 152, 37.
- 11) Bahcall, J. and Salpeter, E., 1965. Astrophys. J., 142, 1677.
- 12) Conte, S.D., 1965. "Elementary Numerical Analysis", McGraw-Hill.
- 13) Disney, M., 1976. Nature, 263, 573.
- 14) Ellis, G.F.R., 1971. Proc. Int. School of Physics, 'Enrico Fermi', XLVII, General Relativity and Cosmology, p.104, ed. Sachs, R.K., Academic Press, New York.
- 15) Ellis, G.F.R. and Perry J.J., 1979. Mon. Not. R. astr. Soc., 187, 357.
- 16) Ellis, G.F.R., 1980. Ann. N. Y. Acad. Sci., 336, 130.
- 17) Ellis, R.S., Fong, R. and Phillips, S., 1977. Mon. Not. R. astr. Soc., 181, 163.
- 18) Gunn, J.E. and Peterson, B.A., 1965. Astrophys. J., 142, 1633.
- 19) Hildebrand, F.B., 1974. "Introduction to Numerical Analysis" 2nd. ed., McGraw-Hill.

- 20) King, I.R., 1971. Pub. A. S. P., 83, 199.
- 21) King, I.R., 1978. Astrophys. J., 222, 1.
- 22) Kormendy, J., 1973. Astr. J., 78, 255.
- 23) Kormendy, J., 1977. Astrophys. J., 218, 333.
- 24) Lighthill, M.J., 1960. "Fourier Analysis and Generalised Functions", Cambridge University Press.
- 25) Longair, M.S., 1979. Q. J. R. astr. Soc., 20, 5.
- 26) Oke, J.B. and Sandage, A., 1968. Astrophys. J., 154, 21.
- 27) Oke, J.B., 1971. Astrophys. J., 170, 193.
- 28) Pence, W., 1976. Astrophys. J., 203, 39.
- 29) Sandage, A., 1961. Astrophys. J., 133, 355.
- 30) Schweizer, F., 1979. Astrophys. J., 233, 23.
- 31) Stock, J. and Williams, A.D., 1962. "Photographic Photometry", Stars and Stellar Systems II, ed. Hiltner, W.A.
- 32) Vaucouleurs, G. de, 1959. "General Physical Properties of External Galaxies", Handbuch der Physik, vol. LIII, p.311, Springer Verlag.
- 33) Vaucouleurs, G. de, 1977. "Topics in Extragalactic Astronomy", Occasional Reports of the Royal Observatory, Edinburgh.
- 34) Vaucouleurs, G. de and Capaccioli, M., 1979. Astrophys. J. Suppl. Series, 40, 699.
- 35) Weaver, H., 1962. "Photographic Photometry", Handbuch der Physik, vol LIV, p.131, Springer Verlag.
- 36) Weinberg, S., 1972. "Gravitation and Cosmology", Wiley.